

**The Central Sulawesi, Indonesia Earthquake and Tsunami of 28th
September 2018 – A Field Report by EEFIT-TDMRC**



01/11/2019

The Central Sulawesi, Indonesia Earthquake and Tsunami of 28th September 2018 – A Field Report by EEFIT-TDMRC

Prof Tiziana Rossetto, EPICentre, University College London

Prof Alison Raby, Plymouth University

Dr Andrew Brennan, University of Dundee

Richard Lagesse, Ove Arup & Partners Singapore Ltd

Dr David Robinson, University College London – CEGE EPICentre

Rohit Kumar Adhikari, University College London – CEGE EPICentre

Muhammad Rezki-Hr, Newcastle University

Dr Ella Meilianda, TDMRC, Syiah Kuala University

Dr Yunita Idris, TDMRC, Syiah Kuala University

Ibnu Rusydy, TDMRC, Syiah Kuala University

Intan Dewi Kumala, TDMRC, Syiah Kuala University

Report reviewed by

Matthew Free, Ove Arup & Partners, London, UK

Antonios Pomonis, World Bank

Joshua Macabuag, World Bank

Date

1st November 2019

Table of Contents

Table of Contents	3
List of Figures	5
List of Tables	12
1.0 Introduction	13
1.1 Reconnaissance Mission Objectives	13
1.2 The EEFIT-TDMRC Team	14
1.3 Itinerary	15
2.0 The 2018 Central Sulawesi Earthquake and Tsunami (Lagesse, R.)	17
2.1 Geological and Tectonic Setting	17
2.2 Seismicity and Seismotectonics	20
2.3 Overview of the 28 th September 2018 Sulawesi Event	24
3.0 Fault Surface Rupture Investigation (Lagesse, R., Brennan, A.; Rusydy, I.)	26
4.0 Landslide Investigation (Lagesse, R., Brennan, A.; Rusydy, I.)	32
4.1 Balaroa	32
4.2 Petobo	34
4.3 Jono Oge	40
4.4 Summary	41
5.0 Liquefaction and Ground Subsidence Investigation (Brennan, A.; Lagesse, R.; Rusydy, I.)	43
5.1 Local Liquefaction	43
5.1.1 Palu City	44
5.1.2 Sigi	49
5.1.3 Donggala Dolphin Park	53
5.2 Seafront Loss Due to Liquefaction	55
5.2.1 Loli Tasiburi	55
5.2.2 Donggala Town	57
5.2.3 Lero	58
5.3 Summary	61
6.0 Tsunami Investigation (Raby, A.; Robinson, D.; Rossetto, T.)	62
6.1 Tsunami terminology	62
6.2 Past tsunami in the Palu Bay area	62
6.2 The 28 th September 2018 Tsunami and its characteristics	64
6.2.1 Cause of tsunami in Palu Bay	64
6.2.2 International tsunami surveys	64
6.2.3 Tsunami characteristics	66

6.3 General tsunami observations obtained through interviews and video footage by TDMRC-EEFIT Team	69
6.3.1 General tsunami observations from Wani	70
6.3.2 General tsunami observations from Kampung Muara near Tasiburi	72
6.3.3 General tsunami observations from Mambooro	74
6.4 Tsunami Inundation Observations	75
6.4.1 Tsunami inundation inland	75
6.4.2. Tsunami inundation along Palu river	78
6.4.3 Sheltering effects	79
6.5 Tsunami warning and evacuation	81
6.6 Summary	83
7.0 Observation of Impact on Buildings and Infrastructure (Rossetto, T.; Adhikari, R.; Idriss, Y.; Raby, A).....	84
7.1 Damage Scale and Survey Sheet	84
7.2 Observations on the characteristics and performance of typical low-rise houses.....	89
7.2.1 Timber “stilt” houses.....	89
7.2.2 Timber frame houses with infills	90
7.2.3 Confined masonry housing	92
7.2.4 Guidance for low-rise housing construction in seismic areas in Indonesia	93
7.3 Observations on the performance of educational facilities	97
7.3.1 Tadulako University Campus	97
7.3.2 Schools	100
7.4 Healthcare Facilities	111
7.4.1 Tadulako University Hospital.....	111
7.4.2 Anutapura Hospital	113
7.5 Hotel Buildings.....	114
7.5.1 Grand Duta Hotel	115
7.5.2 Mercure Hotel.....	117
7.5.3 Swiss Belhotel	119
7.6 Palu Airport.....	120
7.7 Ponulele Bridge	122
7.8 Damage to coastal defences	123
7.8.1 Rudimentary seawall	123
7.8.2 Mambooro seawall.....	124
7.8.3 Revetment, south of Mambooro	124
7.8.4 Masonry seawall	125
7.9 Quay walls.....	125

7.10 Port Structures	126
7.10.1 Donggala Port structures	126
7.10.2 Wani Port structures	126
7.11 River walls.....	128
7.12 Vessels	128
7.12 Summary	129
8.0 Palu Contingency Plan (Meilianda, E.; Rezki-Hr, M.; Kumala, D.I.)	131
8.1 Number of affected people	132
8.2 Healthcare facilities	133
8.3 Ports	133
8.4 Electricity Generators	133
8.5 Institutional Arrangements	133
8.6 Summary	134
9.0 Conclusions	135
10.0 Acknowledgements.....	138
11.0 References	138

List of Figures

Figure 1.1 - The EEFIT-TDMRC Team.....	15
Figure 1.2 - A map showing the main survey area, key survey routes (red lines) and main locations visited during the field mission. The area inside the black rectangle is the ‘base survey area’ in the Palu city.....	16
Figure 2.1 – Tectonic setting in Southeast Asia and Indonesia (Metcalf, 2009).....	17
Figure 2.2 – Summary geology map of Sulawesi showing mega-tectonic provinces after Moss and Wilson, (1998).	19
Figure 2.3 – Published geology map of the Palu area (Geological Research and Development Centre, 1973).....	20
Figure 2.4 – Distribution of seismicity in Indonesia after Zare et al. (2018).....	21
Figure 2.5 – Hazard levels (from left to right) for peak ground acceleration (PGA), 0.2s and 1.0s period spectral acceleration for return periods of 500 years (top) and 2,500 years (bottom) after Cipta et al. (2016).	21
Figure 2.6 – Distribution and depth of major historical earthquakes in Sulawesi during the period 1967 to 2012 after Supartoyo (2014).	22
Figure 2.7 – ‘Multiple strand’ model of fault dislocation in Palu area proposed by Socquet et al. (2006) showing measured relative GPS velocities.	23
Figure 2.8 – Overview map of the Palu-Koro Fault in the Palu area and the major events in the earthquake sequence, drawn by the EEFIT-TDMRC Team. Earthquake epicentres are shown by the blue circles (with magnitude, depth and time)	25

Figure 3.1 – Co-seismic assessment of fault rupture displacement after Valkaniotis et al. (2018). The left image is west to east displacement and right image is north to south displacement. 26

Figure 3.2 – Normal fault scarp displaying vertical displacement of approximately 4m in the south of Palu valley..... 27

Figure 3.3 – Triangular facets on the western side of Palu valley..... 27

Figure 3.4 – Offset road due to strike-slip fault displacement. 28

Figure 3.5 – Fault surface rupture through rice paddy field..... 28

Figure 3.6 – Displacement of approximately 5m along fault surface rupture shown due to offset rice paddy terraces. 29

Figure 3.7 – Normal faulting observed North of Labua on the East side of Palu Bay. Photo taken facing North East 29

Figure 3.8 – Damage to water channel on North side of large rupture at Labua indicates observed total displacement may be only partly due to 28th September event 30

Figure 3.9 – Overview of Palu valley showing the Palu-Koro Fault, major landslides, Bendung Irigasi Gumbasa irrigation channel and the major natural drainage courses. 31

Figure 4.1 – Overview of the Petobo landslide area showing zones of depletion and accumulation as well as damaged buildings and the Palu-Koro Fault surface rupture. 33

Figure 4.2 – Geological profile exposed in Balaroa Landslide head scarp..... 33

Figure 4.3 – Overview of the Petobo landslide area showing zones of depletion and accumulation as well as damaged buildings and the location of the Bendung Irigasi Gumbasa irrigation channel. 34

Figure 4.4 – Deposited debris thickness in the accumulation zone of the Petobo Landslide..... 35

Figure 4.5 – Swampland adjacent to the toe of the Petobo Landslide..... 35

Figure 4.6 – Historical map of the Palu valley area in the 1930’s (Kruyt, 1938)..... 36

Figure 4.7 – Geological profile exposed in Petobo Landslide head scarp. 37

Figure 4.8 – Particle size distribution of samples taken from Petobo head scarp 38

Figure 4.9 – Difference in vegetation growth due to groundwater conditions on either side of the Bendung Irigasi Gumbasa.in the Petobo area. Green vegetation growth (left) indicates wetter ground conditions as opposed to brown land with lack of vegetation growth (right) indicating mostly dry ground..... 39

Figure 4.10 – Far northern end of the Bendung Irigasi Gumbasa irrigation channel above the head of the Petobo Landslide before (left) and after (right) the earthquake..... 40

Figure 4.11 – Upper part of the Jono Oge Landslide with the main scarp and minor scarps indicated. 41

Figure 5.1 - Map of sites observed by the EEFIT-TDMRC Team to be affected by localised liquefaction (map: Google). 44

Figure 5.2.- Liquefaction ejecta in a field at Gelanggang Mahasiswa, Kabonena. Observe the vertical offset in front of the pavilion where the field has settled relative to nearby intact ground..... 45

Figure 5.3.- Liquefaction ejecta in a field at Gelanggang Mahasiswa, Kabonena. The ejecta, is seen to follow the path of the fault across the field, although the soil on both sides appears to have settled by a similar distance..... 45

Figure 5.4 - Particle size distribution of ejecta collected at Kabonena..... 46

Figure 5.5. - Damage to a one-storey building in Lasoso due to differential settlement induced by liquefaction. Sandy ejecta in garden.....	46
Figure 5.6 – Left: Front of Masjid Iqra. Right: Masjid Iqra in Lasoso. Severe liquefaction-induced damage and tilting of minaret due to liquefaction beneath base.	47
Figure 5.7 -. Masjid Iqra. Failure of garden paving above sandy soil, and ejecta in background.	47
Figure 5.9 – Microtremor data for urban Palu reported by Thein et al. (2014) a) survey locations: LSS is Lasoso, MSQ is not the Masjid Iqra but rather the Great Mosque Darassalam Palu b) shear wave velocity measurements along Line B, redrawn for near surface soils following Thein et al. (2014) ...	48
Figure 5.10 - Relationship between shear wave velocity and cyclic resistance ratio for sands, Andrus & Stokoe (2000).....	49
Figure 5.11 - Settlement and spreading cracks outside the town of Sigi	50
Figure 5.12 - Differential settlement and ground disturbance in Sigi. Pipework in foreground appears to be new rather than uplifted.	50
Figure 5.13 - Large settlements with sandy ejecta adjacent to relatively unaffected soil in Sigi.	51
Figure 5.14 - Ejecta at Sigi. Uniform sand, in damp condition.....	51
Figure 5.15 -. Data for Line C (see Figure 5.9a) for point SGI in Sigi. redrawn after Thein et al. (2014)	52
Figure 5.16 - View across dolphin enclosure to sea road. Slight damage to bridge abutments consistent with soil displacements, though bridge remains operational.	53
Figure 5.17 - Cracks parallel to coastline, consistent with lateral spreading of the ground.....	54
Figure 5.18 - Failure of piled sea wall at Donggala Koto Wisata	54
Figure 5.19.- Soil layers exposed by lateral spreading at Donggala Koto Wisata.	55
Figure 5.20 - Waterfront at Loli Tasiburi. Note the headland in the background which locals had indicated is now far shorter than before.....	56
Figure 5.21 - Particle size distribution for surface soils at Loli Tasiburi.....	56
Figure 5.22 - Aerial photograph of post-earthquake Donggala port, overlain by prior road map showing missing land around the estuary mouth.	57
Figure 5.23.- Photographs of Donggala Port, looking a) South East across the estuary towards the partially collapsed metal rooved storage houses b) detail beneath the concrete structure seen tilted on the South edge of the bay, showing evidence of soil having been displaced from beneath the structure.	57
Figure 5.24 – Settlement in the road with sandy soil ejected through cracks.	58
Figure 5.25 – Differential settlement of School in Lero, with liquefaction ejecta in the yard.....	58
Figure 5.26 – Lero: View down towards the sea. The seafront had previously been the site of seven homes and a road.....	59
Figure 5.27 – Lero: Cracks observed parallel to shoreline consistent with lateral spreading.	60
Figure 5.28 – Further cracks, and submerged land and palm trees, in Lero.	60
Figure 5.29 – More ground cracks at Lero, and view across the estuary towards a now submerged restaurant.....	61
Figure 6.3 - Epicentres of the tsunamigenic earthquakes of 20 th century in the region around Palu Bay (Pelinovsky et al., 1997).	63

Figure 6.4 - Measurements of tsunami inundation heights and runup (see definition in Figure 6.2) measured by International survey teams as of 16 November 2018 (ERCC, 2018). 65

Figure 6.5 - Tsunami inundation at Jalan Taman Ria, Balaroa (0° 53'1.58" S 119° 50' 53.42" E). 66

Figure 6.6 - Badan Informasi Geospasial Contour map of Palu Bay before the earthquake, Retrieved from <https://cloud.big.go.id>. Accessed 30 Oct 2018. 67

Figure 6.7 - Tide gauge data from Pantoloan Port (Valkaniotis et al., 2018) 68

Figure 6.8 - Frames of YouTube video recorded from the Palu Grand Mall car park (https://www.youtube.com/watch?v=rCQ_hPZFibM). The earthquake occurred at 18:02:45 (UTC+8) and several waves were seen to arrive from multiple directions between 18:08:15 and 18:10:49, Takagi et al (2019). 69

Figure 6.9 - Location of the observations presented 70

Figure 6.10 - Wani village on the east coast of Palu bay which experienced considerable damage 71

Figure 6.11 - Video frames at 18:03:01, 18:06:29, 18:06:30, 18:06:36 and during the EEFIT mission. Notice the mopeds have fallen over, following by the bore-like tsunami about 3 minutes later. This short arrival time supports the argument, discussed in Section 6.2.1, for a secondary tsunami source within Palu Bay. 71

Figure 6.12 - Location (left) and photograph (right) of the house where the man in the car ended up at around 50 m inland from the sea 72

Figure 6.13 - Photos of TDMRC-EEFIT Team Interviewing locals and recording a piece for the mission video blog. 72

Figure 6.14 - Youtube video frame indicating wave rundown and the sharp change in bathymetry following a submarine landslide. 73

Figure 6.15 - List of dead and missing at Kampung Muara..... 73

Figure 6.16 - Damage in Labuhan Bajo..... 74

Figure 6.17 - Interview being conduct with the tropical fisherman who was swimming in the sea when the earthquake occurred..... 75

Figure 6.18 - Locations 1, 2 and 3 where inundation was observed and described below 75

Figure 6.19 - Evidence of inundation and the respective effects: (Left column) Pre-earthquake/tsunami images from Google Streetview (Right column) EEFIT observations at same locations Descriptions of each location are provided in the paragraph above. 77

Figure 6.20 - Concrete river wall near entrance to the Palu river 78

Figure 6.21 - Submerged bridge deck of the Palu Bridge IV which may have acted as a submerged breakwater to the tsunami waves, preventing them travelling up the river 79

Figure 6.22 - (top) Poor quality 1960s housing in Labuan Bajo that has been sheltered by a large area of mangroves at the shoreline. (below) A map showing the position of the building within the port, behind the large green area of mangroves 80

Figure 6.23 - Mangrove plantations to the west of Palu bay: (Top row) Newly established mangrove plantation (Bottom row) Tourist park dedicated to mangroves. 81

Figure 6.24 - Tide gauges installed in Indonesia by German, US and Indonesian organisations (Lauterjung and Letz, 2017) 82

Figure 6.25 - EEFIT member indicating a typical evacuation route inland from the main road through Loli Tasiburi Banawa. 82

Figure 7.1 - The earthquake and tsunami building rapid visual assessment survey forms-Page 1 87

Figure 7.2 - The earthquake and tsunami building rapid visual assessment survey forms-Page 2 88

Figure 7.3 –Picture of coconut lumber. 89

Figure 7.4 - Performance of timber stilt houses in Palu and Donggala, Central Sulawesi: Left – The palace of the Princes of Palu. This structure was affected by ground shaking but not tsunami inundation and was undamaged. Right - The remaining concrete foundations of the timber stilt houses in the Labuan Bajo Fisherman Village, shown in red circle. Collapsed stilt houses can be seen in the background. . 90

Figure 7.5 - Detail of individual concrete foundation for stilt house (Umpak). (Base image source: Pedoman Teknis Rumah dan Bangunan Gedung Tahan Gempa, Kementrian Pekerjaan Umum dan Perumahan Rakyat, Indonesia, 2006). 90

Figure 7.6 - Examples of infilled timber frame construction in Labuan Bajo. Left - Timber framed house with wire-reinforced mortar. Right - Two storey timber framed house with mortar infill. 91

Figure 7.7 - Examples of infilled timber frame construction. Left - Timber framed warehouse with masonry infill in Labuan Bajo (left). Right - Elementary school at Wani, timber frame construction with mortar infill. 91

Figure 7.8 - Typical earthquake damage observed in infilled timber frame construction. Left - Out-of-plane failure of infill panels. Right - Separation of infill from frame due to differential settlement of foundations..... 91

Figure 7.9 - Comparison of construction characteristics and seismic behaviour of a) RC frames with masonry infills and b) confined masonry construction: construction sequence (top); relative size of confining elements (middle), and the seismic response (bottom) (Source: EERI, 2011). 92

Figure 7.10 – Heavily damaged CM houses in Palu bay area along the Jl. Rajamoili road, about 100m from coastline. The walls of this house were directly hit by the tsunami inundation..... 93

Figure 7.11 – Undamaged CM houses in Palu bay area along the Jl. Rajamoili road. These houses were sheltered from the tsunami inundation by other houses-buildings. 93

Figure 7.12 - Recommended detailing for “stilt” type timber frame construction from Technical guidelines of earthquake resistant houses and buildings construction published by the Indonesian Ministry of Public Works and Houses (Pedoman Teknis Rumah dan Bangunan Gedung Tahan Gempa, Kementrian Pekerjaan Umum dan Perumahan Rakyat, Indonesia)..... 94

.Figure 7.13 - Detailing for beam – to – column connections recommended in “stilt” type timber frames, from the Technical guidelines of earthquake resistant houses and buildings construction published by the Indonesian Ministry of Public Works and Houses (Pedoman Teknis Rumah dan Bangunan Gedung Tahan Gempa, Kementrian Pekerjaan Umum dan Perumahan Rakyat, Indonesia, 2006)..... 95

Figure 7.14 - Design of masonry infilled timber framed buildings, as recommended in Technical guidelines of earthquake resistant houses and buildings construction that published by the Indonesian ministry of public works and houses (Pedoman Teknis Rumah dan Bangunan Gedung Tahan Gempa, Kementrian Pekerjaan Umum dan Perumahan Rakyat, Indonesia, 2006). 95

Figure 7.15 - Design of foundations and of the connection between the infill and timber frame in masonry infilled timber framed housing, recommended by the Technical guidelines of earthquake resistant houses and buildings construction published by the Indonesian Ministry of Public Works and Houses (Pedoman Teknis Rumah dan Bangunan Gedung Tahan Gempa, Kementrian Pekerjaan Umum dan Perumahan Rakyat, Indonesia). 96

Figure 7.16 - Design of confined masonry buildings, as recommended in the Technical guidelines of earthquake resistant houses and buildings construction that published by the Indonesian ministry of public works and houses (Pedoman Teknis Rumah dan Bangunan Gedung Tahan Gempa, Kementrian Pekerjaan Umum dan Perumahan Rakyat, Indonesia)..... 96

Figure 7.17 - Design of foundations, and confining reinforced concrete elements in confined masonry buildings, as recommended by the Technical guidelines of earthquake resistant houses and buildings

construction that published by the Indonesian ministry of public works and houses (Pedoman Teknis Rumah dan Bangunan Gedung Tahan Gempa, Kementerian Pekerjaan Umum dan Perumahan Rakyat, Indonesia, 2006). 97

Figure 7.18 - Map of the Tadulako University Campus showing the damage states and location of the buildings surveyed by the EEFIT-TDMRC Team. 98

Figure 7.19 - Tadulako University Rektorat (DET2): exterior view (left); damage to internal infill panels (right)..... 98

Figure 7.20 - Tadulako University collapsed 3-storey building of the Faculty of Social and Political Sciences. Left – front view. Right – back view..... 99

Figure 7.21 - Tadulako University collapsed 3-storey building of the Faculty of Social and Political Sciences. Left – Side view of the building. Right – Failed external joint..... 99

Figure 7.22 - Locations of schools visited in Palu, Sigi and Donggala Regency during the EEFIT-TDMRC mission. 100

Figure 7.23 - Typical layout and construction details of a representative CM school building in Palu. 101

Figure 7.24 – Damage observed in buildings at three school complexes. 102

(a) SMP Negeri 1 Biromaru School in Sigi. Building A is a 2 storey RC infilled frame structure, whilst all other buildings are one-storey CM construction). Building B was reduced to rubble, whilst most of the other CM buildings suffered range of damage states – from slight (DET2), very heavy (DET3) to partial collapse of their shorter walls (DET4). 102

(b) SD Inpres 1 Talise School in North Palu. Affected only by shaking (not ground failure) from the earthquake. All three buildings are single-storey CM buildings. All suffered unrepairable damage (DET3). Main damage mechanisms are separation of walls and gable failure, due to poor quality materials and ineffective confinement. 102

(c) SD Negeri Pengawu School in Palu. Two small-plan single-storey CM buildings (B and C) suffered minor, repairable damage. The large plan CM single-storey building D suffered heavy damage to collapse of some walls (DET4) due to differential ground movement. Building E is CM but was under construction at time of earthquake. Building A is a 2-storey RC infilled frame structure..... 102

Figure 7.25 - Collapse of a CM school building in SMP Negeri 1 Biromaru School, Sigi. 103

Figure 7.26 - Heavy damage sustained by CM school buildings at SMP Negeri 1 Biromaru School. (a) Out-of-plane collapse of the shorter wall in Building C (see Fig. 7.24). All the other cross walls either collapsed or are on the verge of collapse. (b) In-plane flexural and shear cracks through the spandrels. (c) In-plane flexural and shear cracks through the tie-columns. 104

Figure 7.27 - Typical failure mechanisms observed in CM school buildings. Picture shows damage in building A at SD Inpres 1 Talise school. 105

Figure 7.28 - Confined masonry school building (E in Fig. 7.24) in SD Negeri Pengawu school in Palu that was under construction at the time of the earthquake. Note the offset of the middle tie-column at the tie-beam level. 105

Figure 1.29 - Extensive damaged in CM building (building D in Fig. 7.24c) in SD Negeri Pengawu school due to differential settlement.(a) differential movement of ground across a ground crack passing under the building caused failure of the floor. (b), (c) and (d) show crack opening induced by differential ground movement..... 106

Figure 7.30 - A small plan box-type CM school building that suffered no damage (building B in Fig. 7.24c) in SD Negeri Pengawu school. 107

Figure 7.31 - Construction details of a well-designed CM school building from El Salvador (Credit: Rohit Kumar Adhikari, World Bank, 2019)..... 108

Figure 7.32 - MTS Alkhairaat Pusa Palu School. Left – 3-storey RC frame building that sustained minor damage to infill panels. Right – Typical sizes of beams and columns in RC frame schools. 109

Figure 7.33 - SD Negeri Pengawu School in Palu (Building A in Fig. 7.24c). Left – 2-storey RC school building that sustained moderate damage to infill panels. Right – Damage to the infill walls 109

Figure 7.34 - SMP Negeri 1 Biromaru School, Building A in Fig. 7.24a. Left – front entrance to the building. Right – the rear of the building showing columns that support the balcony sited on a 1m high “slab” of made ground covered in concrete screed. 110

Figure 7.35. - TLCs established in the school compounds by the government and NGOs. 111

Figure 7.36 - Tadulako University Hospital Building A. Left – Front view. Right – rear view, showing damage to gable..... 112

Figure 7.37 - Tadulako University Hospital Building A. Left – Beam reinforcement detailing. Right – damage to brick masonry infills. 112

Figure 7.38 - Tadulako University Hospital Building B. Left – Side view of Building B, showing out of plane failure of infill wall at second floor (n.b. plane of infill wall is E-W). Right – location of damage due to pounding between Buildings A and B..... 113

Figure 7.39 - Tadulako University Hospital Buildings: Left - Building A out-of-plane failure of infill walls (plane of walls is E-W). Middle - Damage to entrance and interior fittings of Building A. Right – Detail of damage due to pounding between Buildings A and B. 113

Figure 7.40 - Damage at Anutapura Hospital a) soft story collapse of four story RC frame structure; b) RC frame of remaining structure visible following removal of collapsed debris; c) column=beam joint reinforcement exposed in collapsed structure; d) low-rise hospital structures were relatively undamaged and remained operational. 114

Figure 7.41 - Locations of hotels surveyed in Palu bay area during the EEFIT-TDMRC mission... 115

Figure 7.42 – Grand Duta Hotel, Palu Beach..... 116

Figure 7.43 – Grand Duta Hotel, Left – image of intact column at ground floor. Right – Image of staircase inside the ground floor of the hotel. The staircase railing was damaged when it was hit by a large desk moved by the tsunami inundation. 116

Figure 7.44 – Three –storey RC building near the Grand Duta Hotel. This structure was inundated by the tsunami at its ground floor, but sustained no structural damage, just non-structural damage to sea front windows and to back walls and to fittings at ground-floor level. 117

Figure 7.45 – Mercure Hotel, which suffered soft-storey failure of ground floor. Top – Image of the hotel before the earthquake, Source: Tripadvisor.com. Bottom – Pictures of the Hotel after the earthquake, showing the soft-storey failure of the ground storey of the structure. 118

Figure 7.46 – Mercure Hotel – Images of cover spalling in RC frame joints in the second storey of the structure 118

Figure 7.47 – Mercure Hotel – Detail of a joint within the first floor of the building (now at ground level following soft-storey collapse of ground floor). 119

Figure 7.48 - Swiss Belhotel (Left) Undamaged front facade facing away from the bay (Right) Loss of confined masonry one-storey buildings to the shoreward side of the hotel 120

Figure 7.49 - Swiss Belhotel - damage to internal fittings at the ground storey of the shoreward side of the hotel. No structural damage observed in the main RC structure. 120

Figure 7.50 - View of Palu Airport passenger building from the runway. Damage to the infill walls at the ground floor is observed. A stack of fallen ceiling cladding can be seen in upper storey window. 121

Figure 7.51 - Picture of missing ceiling cladding and damaged fixtures, inside Palu Airport passenger building..... 121

Figure 7.52 - Images of Ponulele bridge before the earthquake and tsunami. The location of the liquefaction jet seen by the EEFIT-TDMRC Team is indicated by the red arrow in the picture on the right. Source for photos: Shutterstock.com..... 122

Figure 7.53 - Picture of Ponulele bridge showing the failed deck. Source: Tripadvisor. 123

Figure 7.54 - Rudimentary seawall. Left - Sketch of layout and section. Right - Damaged sections with tree trunks closing the gap. 123

Figure 7.55 - Mamboro seawall showing loss of the crest of the structure..... 124

Figure 7.56 - Stepped revetment South of Mamboro missing its crest..... 124

Figure 7.57 - Damaged masonry seawall just to the south of Tasiburi..... 125

Figure 7.58 - Collapse of quay wall at ‘Dolphin Park’ at Donggala Koto Wisata. 125

Figure 7.59 - Damage to old port of Donggela 126

Figure 7.60 - Sketch of section through undamaged jetty at Wani port 126

Figure 7.61 - Jetty structure and revetment at Wani port. Top – Jetty. Middle - Armoured revetment neighbouring the jetty. Bottom - Displaced armour units c. 0.8 m side lengths. 127

Figure 7.62 - River wall and surroundings at Lero. Top left - Schematic layout of site. Top right - River mouth. Bottom left - Landward side of river wall. Bottom right - Sheared face of river wall..... 128

Figure 7.63 - Grounded vessels at Watusanpu Naval Base 129

Figure 8.1 - Disaster Risk Management (DRM) Cycle in Indonesia and the Associated Plan. Modified from BNPB (2011). 131

Figure 8.2 - Palu Disaster Management Phases 131

List of Tables

Table 6.1 - Details of earthquakes and subsequent tsunamis in central Sulawesi (Pelinovsky et al., 1997) 63

Table 7.1 - The adopted new Earthquake and Tsunami damage scale 85

Table 8.1: Comparison between numbers of affected people estimated in the Contingency Plan (CP) for Palu versus those actually affected in the earthquake and tsunami. 132

Table 8.2 - Damaged Health Facilities 133

1.0 Introduction

On the 28th September 2018 at 18:02 local time, an earthquake of moment magnitude 7.5 (USGS) hit Indonesia, with epicentre located 78km north of the city of Palu, capital of the Central Sulawesi province on Sulawesi Island. The consequent earthquake ground shaking caused significant damage to buildings and infrastructure and triggered extensive ground failures in areas of Palu and Sigi regencies. The earthquake was followed by a tsunami, that caused devastation along the Palu bay's shores including Palu City and the port facilities in Pantoloan and Wani II. According to Pusat Krisis Kesehatan Kementerian Kesehatan, (2018), the tally of the event's casualties as of the 7th November 2019 was 4,340 fatalities (including 2,096 unidentified bodies), with 1,373 further people missing and 83,122 injured. According to the Central Sulawesi Administration (as reported in the Response Update Brief, 2019), on 30 January 2019, 42,864 buildings were damaged or destroyed (of which 3,673 were destroyed and 9,181 were severely damaged). This has caused 173,552 people to be displaced from their homes (Pusat Krisis Kesehatan Kementerian Kesehatan, 2018).

Around 6,900 of the damaged buildings were in the areas affected by four liquefaction triggered debris flows. Damage to non-residential buildings was extensive affecting at least 450 buildings including hospitals, hotels, shopping malls, other commercial facilities, office and public administration buildings. In addition, 327 worship places were damaged or destroyed. Furthermore, in the education sector according to data from the Ministry of Education (released on October 31st) 1247 school units were damaged or destroyed, containing 6051 classrooms. In addition, there was significant damage to the tertiary education sector in Palu city including facilities of Tadulako University. Significant damage also occurred in the Palu city airport, while the Ponulele bridge, at the mouth of Palu river, collapsed. There was also extensive damage to road and other infrastructure (incl. the electricity supply and telecom networks). These effects on key infrastructure seriously hampered the emergency response efforts.

Immediately after an earthquake and/or tsunami, there is a unique opportunity to gather information on the performance of buildings and infrastructure and on the impact of the disaster on local communities. This report presents field observations made during a reconnaissance of areas affected by the 28th September 2018 Central Sulawesi event. The reconnaissance took place between the 17th and 23rd November 2018 and was conducted jointly by the United Kingdom Earthquake Engineering Field Investigation team (EEFIT) and the Tsunami and Disaster Mitigation Research Centre (TDMRC) at the Syiah Kuala University in Banda Aceh, Sumatra, Indonesia.

1.1 Reconnaissance Mission Objectives

The detailed objectives of the reconnaissance are grouped into three categories; (1) Field Investigation, (2) Dissemination and (3) Future Capacity Building.

Objectives 1 – Field Investigation:

- To carry out technical evaluations of the performance of structures, foundations, civil engineering works and industrial plant affected by the earthquake ground shaking, liquefaction and tsunami.
- Particular focus on the evaluation of damage to schools and critical infrastructure such as hospitals.
- To investigate the characteristics of the earthquake and of the associated liquefaction and tsunami, identifying areas affected.
- To assess the effectiveness of earthquake protection methods, including repair and retrofit, and to make comparisons of the actual performance of structures with the expectations of designers.
- To test different field data collection methods for informing the development of EEFIT's new reconnaissance data management system.

Objectives 2 – Dissemination:

- To disseminate mission findings through a joint EEFIT-TDMRC report and a technical publication, both to be made available online as open access.
- To disseminate field mission observations with the International Tsunami Survey Team (ITST) – Palu and members of UNESCO’s Intergovernmental Oceanographic Commission, through reporting and avenues specified by ITST.
- To disseminate mission findings to academics, practicing engineers, NGOs and the general public through lectures and talks in the UK.
- To train new researchers in the techniques of earthquake investigation and data analysis (1 academic and 3 researchers with no previous experience of post-disaster field reconnaissance took part in the mission).
- To introduce EEFIT methods in the techniques of earthquake, tsunami and liquefaction investigation and data analysis to the TDMRC research partner.

Objectives 3 – Future Capacity Building:

- To support TDMRC in initiating the effort to establish a research centre for disaster mitigation (similar to TDMRC) in the University of Tadulako in Palu.
- To support TDMRC in needs assessment and the capacity building of the local University for disaster mitigation research.

1.2 The EEFIT-TDMRC Team

The members of the EEFIT-TDMRC Team were:

- Professor Tiziana Rossetto, (EEFIT Team Lead), Professor in Earthquake and Tsunami Engineering, University College London.
- Professor Alison Raby, Professor of Environmental Fluid Mechanics, Plymouth University.
- Dr Andrew Brennan, Senior Lecturer in Geotechnical Engineering, University of Dundee.
- Richard Lagesse, Engineering Geologist, Ove Arup & Partners Singapore Ltd.
- Dr David Robinson, Research Associate in Tsunami Modelling, University College London.
- Rohit Kumar Adhikari, PhD Student on seismic assessment of schools, University College London.
- Muhammad Rezki-Hr, PhD student on transport infrastructure resilience, Newcastle University.
- Dr Ella Meilianda, (TDMRC Team Leader) Assistant Professor in Coastal Morphology at TDMRC Syiah Kuala University.
- Dr Yunita Idris, Researcher in Structural Engineering at TDMRC Syiah Kuala University.
- Ibnu Rusydy, Researcher in Geological Engineering at TDMRC Syiah Kuala University.
- Intan Dewi Kumala, Psychologist at TDMRC Syiah Kuala University.

A photo of the team can be seen in Figure 1.1.



Figure 1.1 - The EEFIT-TDMRC Team

The team was aided in the field by a number of people, who provided logistical information, information on the events, helped with data collection and field surveys. These are highly thanked and include:

- Syarifuddin, Senior Engineering Officer in Public Work Department of Palu Municipality.
- Andrew Powell and Indra Purnana Putra, Save the Children.
- Dave Hodgkin, International Federation of Red Cross (IFRC) Shelter Adviser to the Indonesian National Shelter Sub-Cluster.
- Cecilia Schmoelzer, Global Shelter Cluster Focal Point for Technical Coordination, IFRC-Shelter Research Unit.
- Prof. Dra. Mery Napitupulu, Vice rector of Cooperation and Development Affairs, Tadulako University, Palu, Indonesia.
- Prof. Dr. Ir. Amar Akbar Ali, Dean of Engineering Faculty and: Vice rector of Cooperation and Development Affairs, Tadulako University, Palu, Indonesia.
- Dr Sukiman Nurdin, Department of Civil Engineering, Tadulako University, Palu, Indonesia.
- Dr Suki Manudin, University of Tadulako
- Dr Leo Sembiring, Head of Experimental Station for Coastal Engineering, Research Centre for Water Resources, Research and Development Agency, Ministry of Public Works and Public Housing. Ali Hamsal and ST Suriyenni, Energy and Mineral Resources Services of Central Sulawesi Province
- Tahir and Hamrik, BMKG Institute of Geophysics and Meteorology, Palu, Indonesia.

1.3 Itinerary

The joint EEFIT-TDMRC team arrived in Central Sulawesi on the 17th November 2018 and left on the 23rd November 2018. During this time, the team visited areas of Palu affected by the earthquake and tsunami. They also conducted surveys in Donggala and Sigi regions. The key locations visited by the team are shown in Figure 1.2. Detailed map of each survey location (e.g. school, hotel etc.) are provided in the relevant chapters.

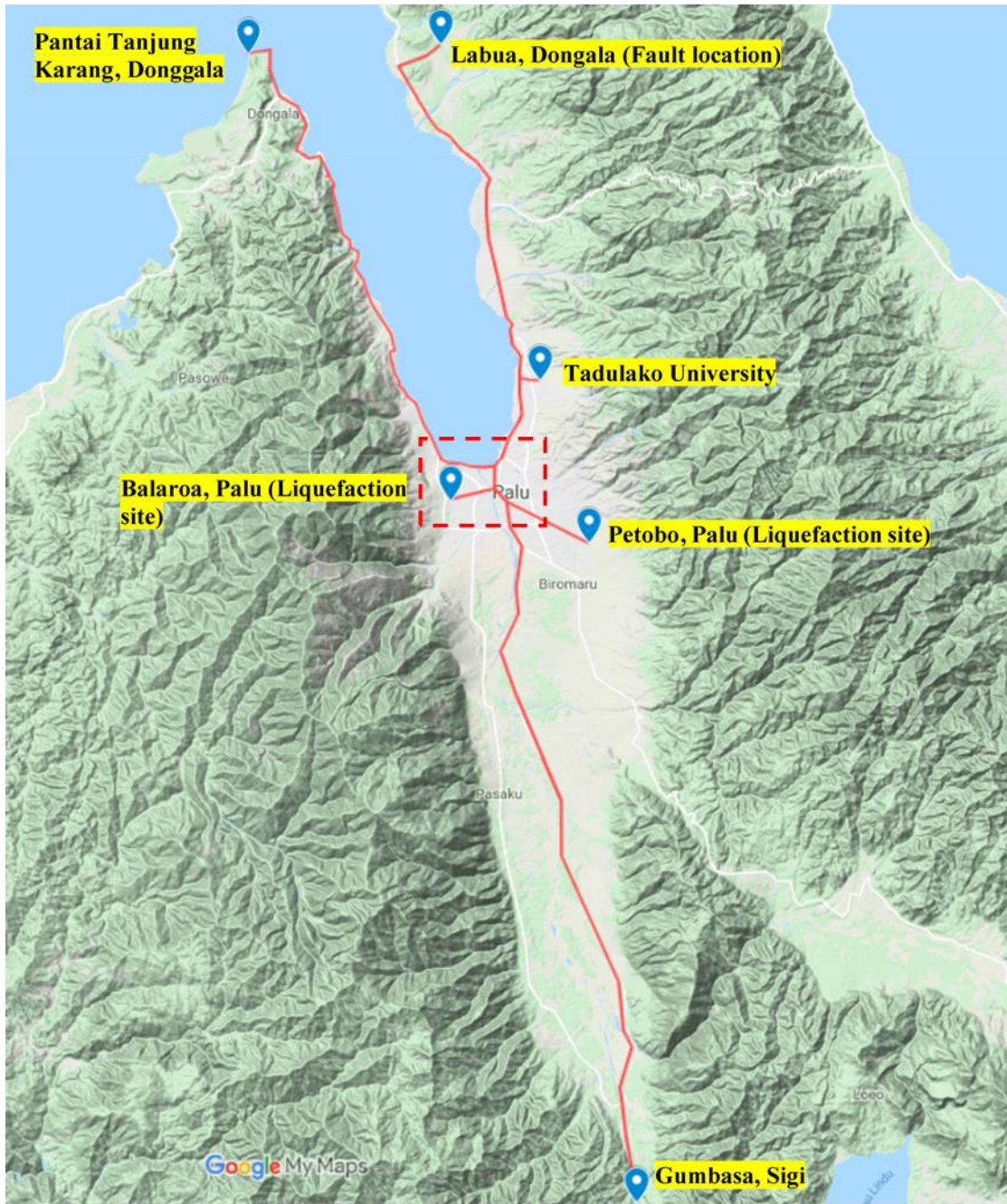


Figure 1.2 - A map showing the main survey area, key survey routes (red lines) and main locations visited during the field mission. The area inside the black rectangle is the 'base survey area' in the Palu city

2.0 The 2018 Central Sulawesi Earthquake and Tsunami (Lagesse, R.)

2.1 Geological and Tectonic Setting

The island of Sulawesi is situated in a complex tectonic environment at the triple junction of three major plates: Sunda Plate, Australian Plate and Philippine Sea Plate. Active interaction of these plates since the Cretaceous time period has formed a complex assemblage of minor tectonic components including micro-continental fragments, accretionary complexes, melange-terrane, island arcs and ophiolites as a result of significant subduction, collision and localised extension (Satyana et al., 2011).

Studies of current plate motions suggest the Australian Plate and Philippine Sea Plate are converging and subducting beneath the relatively stable Sunda Plate in an NNE (~75mm/yr) and WNW (~90mm/yr) direction, respectively. The Sunda Plate is typically considered part of the Eurasian Plate, however, GPS velocities measured by Socquet et al. (2006) reveal that the Sunda Plate is in fact detached and has an easterly motion of 10mm/yr relative to the Eurasian Plate. Due to the complex tectonics interactions, significant rotational movements have been imparted on the crustal blocks in the Sulawesi region.

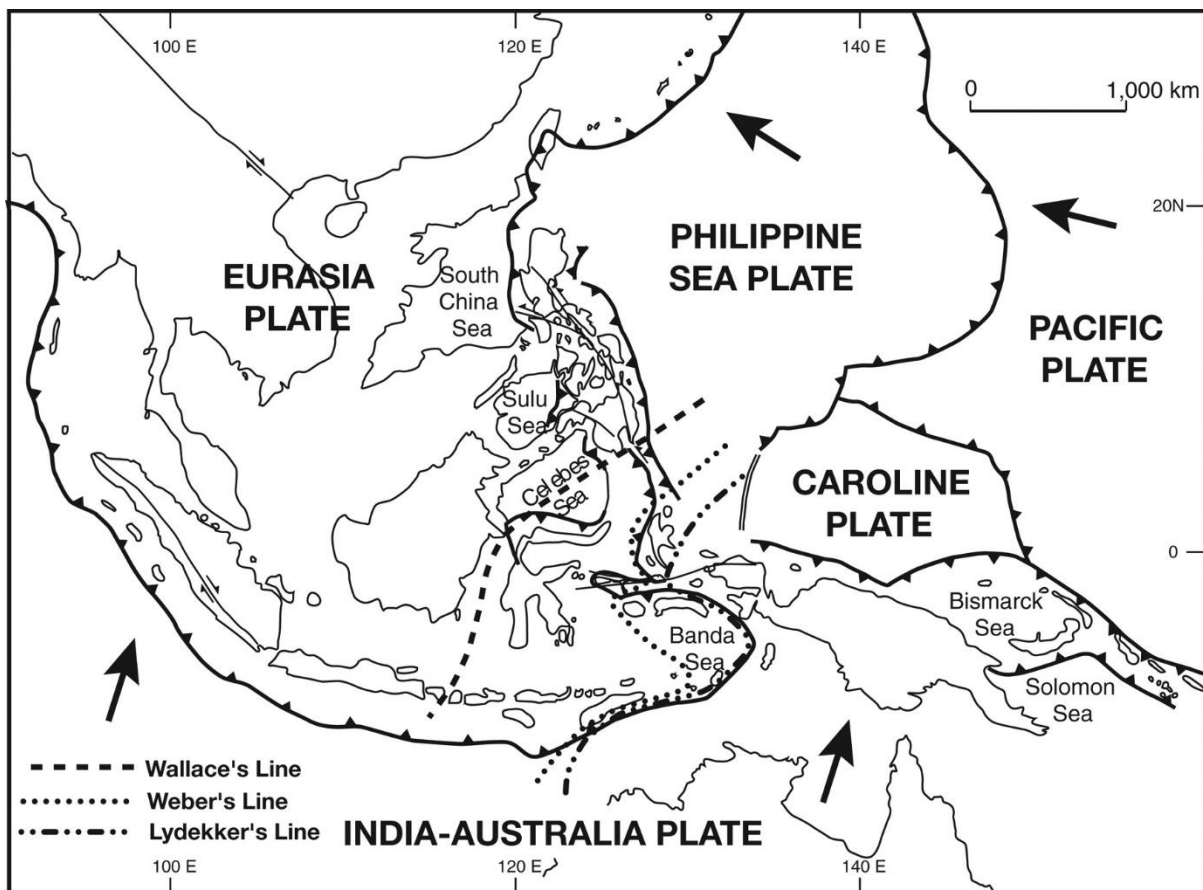


Figure 2.1 – Tectonic setting in Southeast Asia and Indonesia (Metcalf, 2009)

The major tectonic features and provinces in Sulawesi have been governed by the interactions between the biogeographical region of Sundaland and the Australian continent. It lies in the intermediate region known as ‘Wallace’ named after the British naturalist, Alfred Russel Wallace who characterised this region by the boundary between Asian and Australian megafauna (Satyana et al., 2011). The defined boundary, demarcated by the ‘Wallace Line’ (Figure 2.1), is delineated by a deep-water channel over which a land bridge is never thought to have existed during the ice ages (Bird et al., 2005); the Makassar Strait between western Sulawesi and Borneo forms part of this channel.

Sulawesi is considered to comprise four distinct north-south trending mega-tectonic provinces (Sukamto, 1975; Bergman et al., 1996; Moss & Wilson, 1998), as presented in Figure 2.2 and listed below:

- West and North Sulawesi Pluto-Volcanic Arc;
- Central Sulawesi Metamorphic Belt;
- East Sulawesi Ophiolite Belt (ESO); and
- Banggai-Sula and Tukang Besi Micro-continent.

These tectonic components are thought to have been sequentially accreted onto Sundaland during the Cretaceous time period (150-60 Mya) and are characterised by their geology and structure. The West and North Sulawesi Pluto-Volcanic Arc which forms the northern and southern arms of Sulawesi is comprised of thick Cenozoic sedimentary and volcanic sequences overlying Mesozoic tectonically intercalated metamorphic, ultrabasic igneous and marine sedimentary rocks (Leeuwen, 1981). The Central Sulawesi Metamorphic Belt which also forms part of the south-eastern arm comprises sheared metamorphic rocks and an eastern highly tectonised melange complex (Hamilton, 1979).

The eastern side of south Sulawesi as well as parts of the south-eastern arm comprise tectonically intercalated sedimentary and mafic-ultramafic igneous rocks of the East Sulawesi Ophiolite Belt (Sukamto, 1975; Parkinson, 1991; Bergman et al., 1996). The islands of Buton-Tukang Besi and Banggai-Sula in the east of Sulawesi are considered by some authors (Fortuin et al., 1990; Davidson, 1991) to represent a separate micro-continental block with continental-origin metamorphic and igneous lithologies underlying Palaeozoic and Mesozoic sediments, although not all agree (Smith & Silver, 1991).

Palu is located in the West and North Sulawesi Pluto-Volcanic Arc tectonic province at the southern end of the isthmus that connects Central Sulawesi with North Sulawesi. The Cretaceous basement metamorphic and igneous rocks form the mountainous region forming the eastern side of the valley where the city is situated. These rocks predominantly comprise amphibolitic schist, mica schist, gneiss and marble. The schists are more abundant on the western side whereas the gneiss and marble are dominant on the eastern side.

Numerous unmapped intrusive igneous bodies, typically less than 50m across and of diorite to granodiorite composition, are also recorded intruding the metamorphic parent rock. Unconformably overlying the basement complex is a melange of sedimentary rocks, including some meta-sediments in close proximity to intrusions, of the Eocene-age (55-35 Mya) Tinombo Formation. This sequence is unconformably overlain by a Miocene (22-5 Mya) sedimentary succession typically derived from debris and detritus of underlying older formations; this stratigraphic unit accounts for the carbonate rocks forming the lower-lying land at the Donggala headland.

The valley floor and alluvial fans along the Gulf of Palu comprise Holocene-age fluvial and alluvial sediments. The published geological map for the Palu area is presented in Figure 2.3.

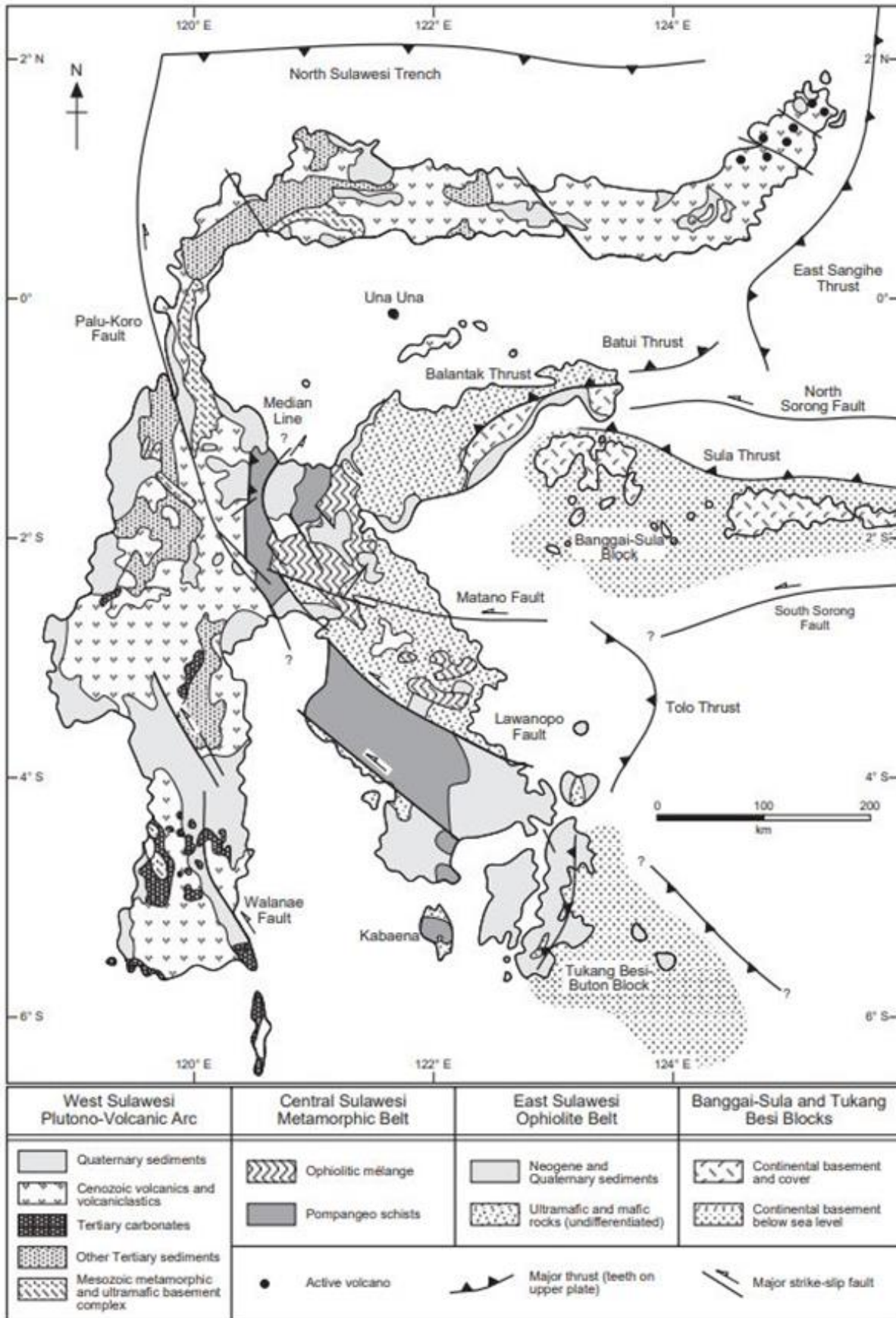


Figure 2.2 – Summary geology map of Sulawesi showing mega-tectonic provinces after Moss and Wilson, (1998).

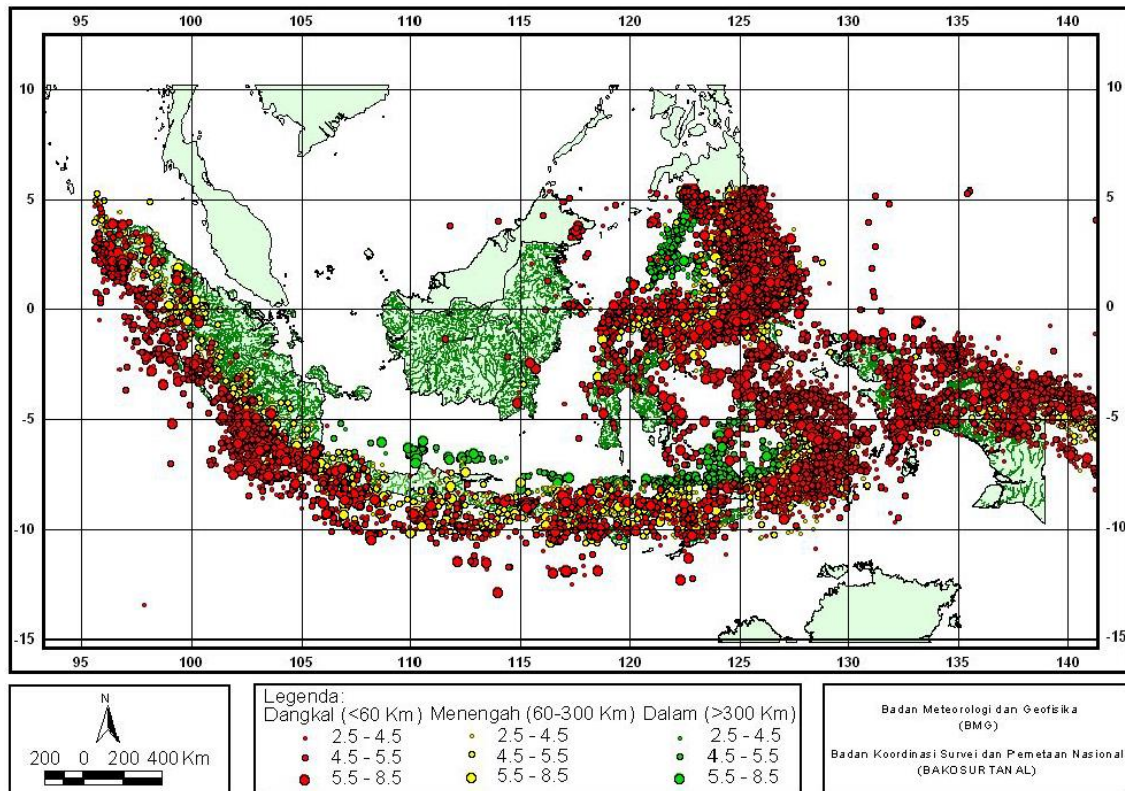


Figure 2.4 – Distribution of seismicity in Indonesia after Zare et al. (2018)

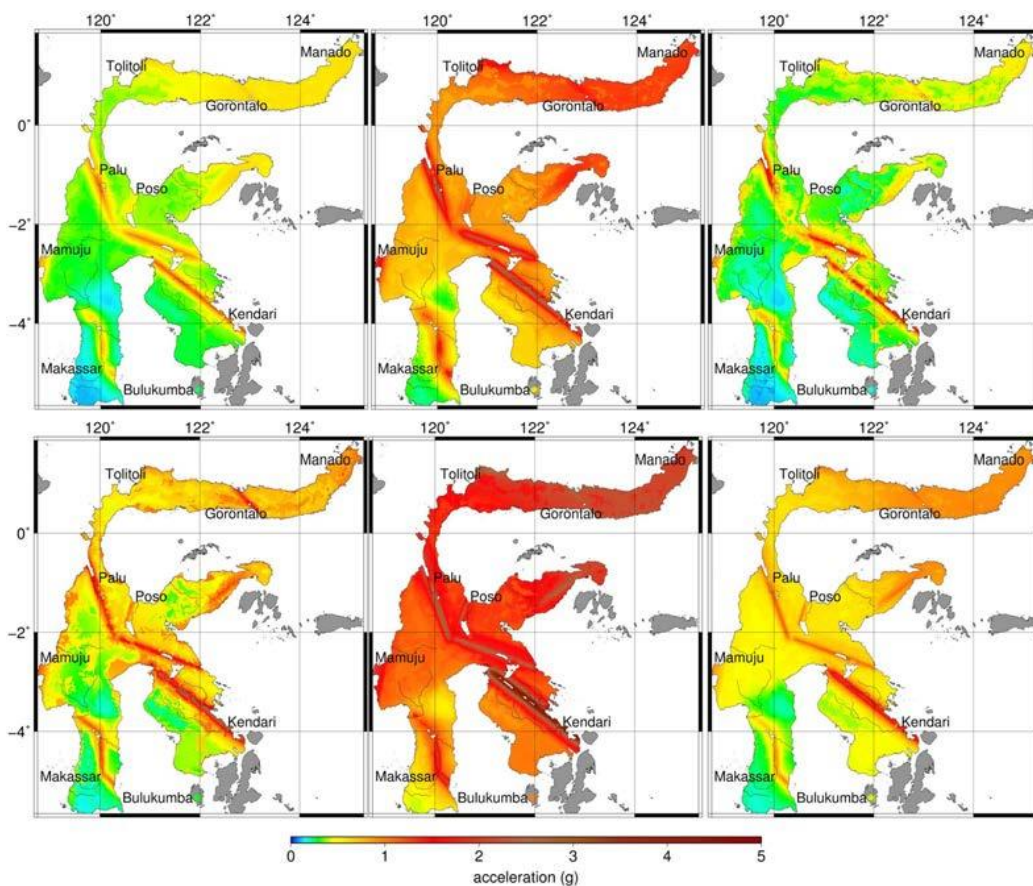


Figure 2.5 – Hazard levels (from left to right) for peak ground acceleration (PGA), 0.2s and 1.0s period spectral acceleration for return periods of 500 years (top) and 2,500 years (bottom) after Cipta et al. (2016).

The Central Sulawesi, Indonesia Earthquake and Tsunami of 28th September 2018

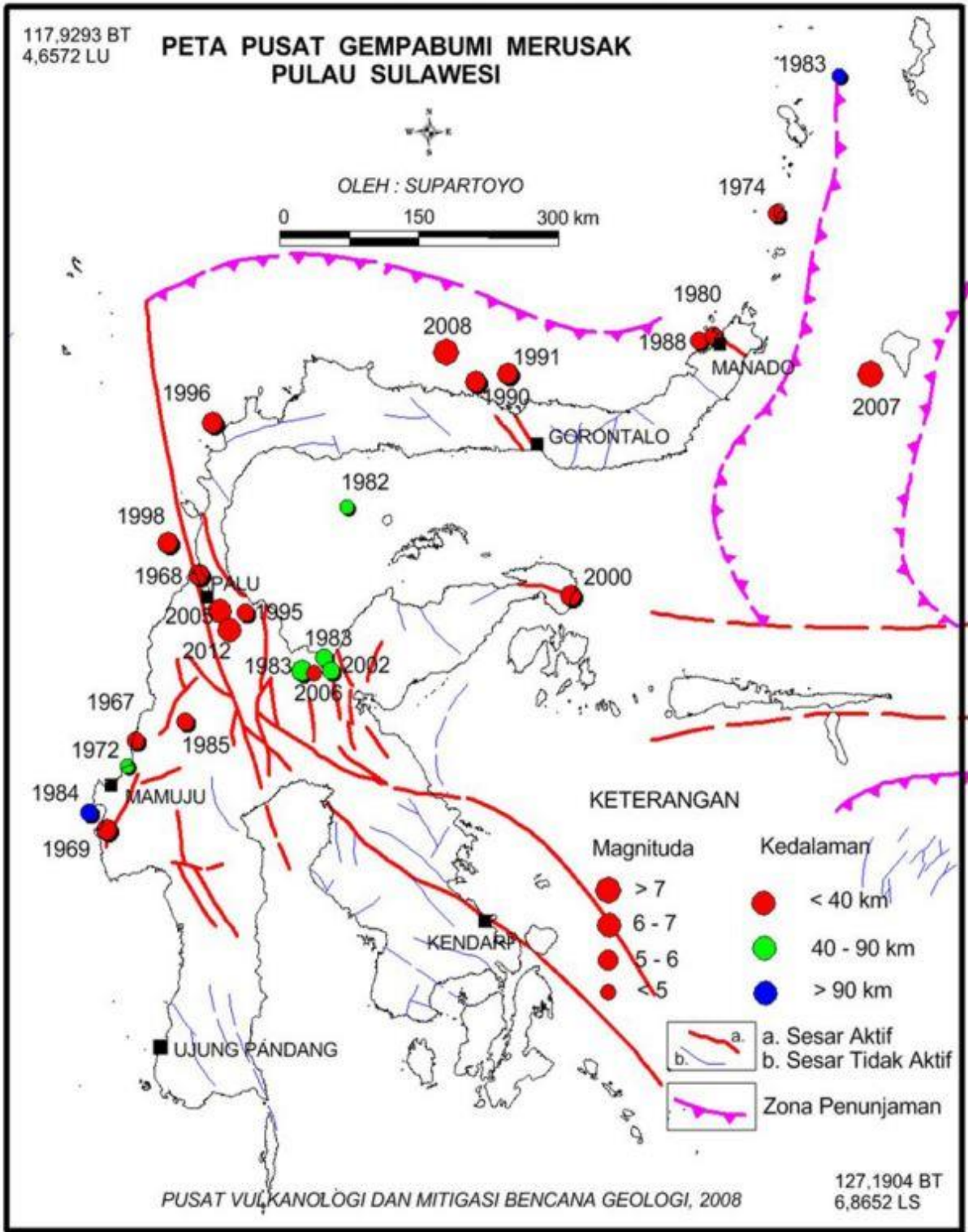


Figure 2.6 – Distribution and depth of major historical earthquakes in Sulawesi during the period 1967 to 2012 after Supartoyo (2014).

The island of Sulawesi is coincident with the triple junction between the tectonic plates and this has led to the development of a number of major fault systems bisecting the island. This includes the Palu-Koro Fault which bisects the interior of the Molucca Sea Plate (a sub-component of the Sunda Plate) and extends from the northwest of Sulawesi, at the western end of the Minahassa Subduction Zone, trending NNW-SSE across Central Sulawesi before transitioning into the Matano and Lawanopo Faults in the

The Central Sulawesi, Indonesia Earthquake and Tsunami of 28th September 2018

southeast of the island (Figure 2.2). The Palu-Koro fault accommodates 42mm/year of left-lateral strike-slip relative motion due to the differential movements of the crustal blocks (Socquet et al., 2006). While the overall fault motion is considered strike-slip, the fault system displays more complex transtensive behaviour which likely explains the presence of a pull-apart basin structures localised in the Palu area.

The fault structure and kinematics along the Palu-Koro Fault are not perfectly understood but if the estimated slip were to occur on one single locked fault at a depth of between 8-16km (Stevens et al., 1999; Walpersdorf et al., 1998c) then it should produce at least one magnitude (M_w) 7 earthquake every 100 years considering typical displacement versus magnitude correlations such as Wells & Coppersmith (1994) and assuming all displacement is released seismicity. However, fault trenching investigations carried out by Bellier et al. (2001) reveal that this frequency is not recorded in the ground by palaeoseismological investigations. Bellier et al. (2001) also found that three earthquakes with a magnitude of $6.8 < M_w < 8.0$ have occurred in the last 2,000 years along the main branch of the fault – the same branch that ruptured on 28th September – implying a cumulative slip of 30m with a slip rate of 15 mm/s (before the 2018 event).

In light of this, Socquet et al. (2006) proposes two models for the fault interactions in the pull-apart basin area around Palu. The first model suggests a single locked fault at depth, as mentioned above, with a separate fault in the vicinity of the Makassar Strait to account for the additional slip. The second model comprises multiple parallel dislocations locked at shallow depths which combine to accommodate the estimated slip (Figure 2.7). It is suggested that this ‘multiple strand’ model is closer to reality in terms of local kinematics and the fault system is divided into multiple active branches, over an approximately 50km wide zone near Palu, that could be regarded as surface splays of a strike-slip flower structure. While the local tectonic geomorphology fits this model, more detailed investigation is required to confirm this and the ‘single strand’ model is probably a reasonable approximation for larger-scale modelling.

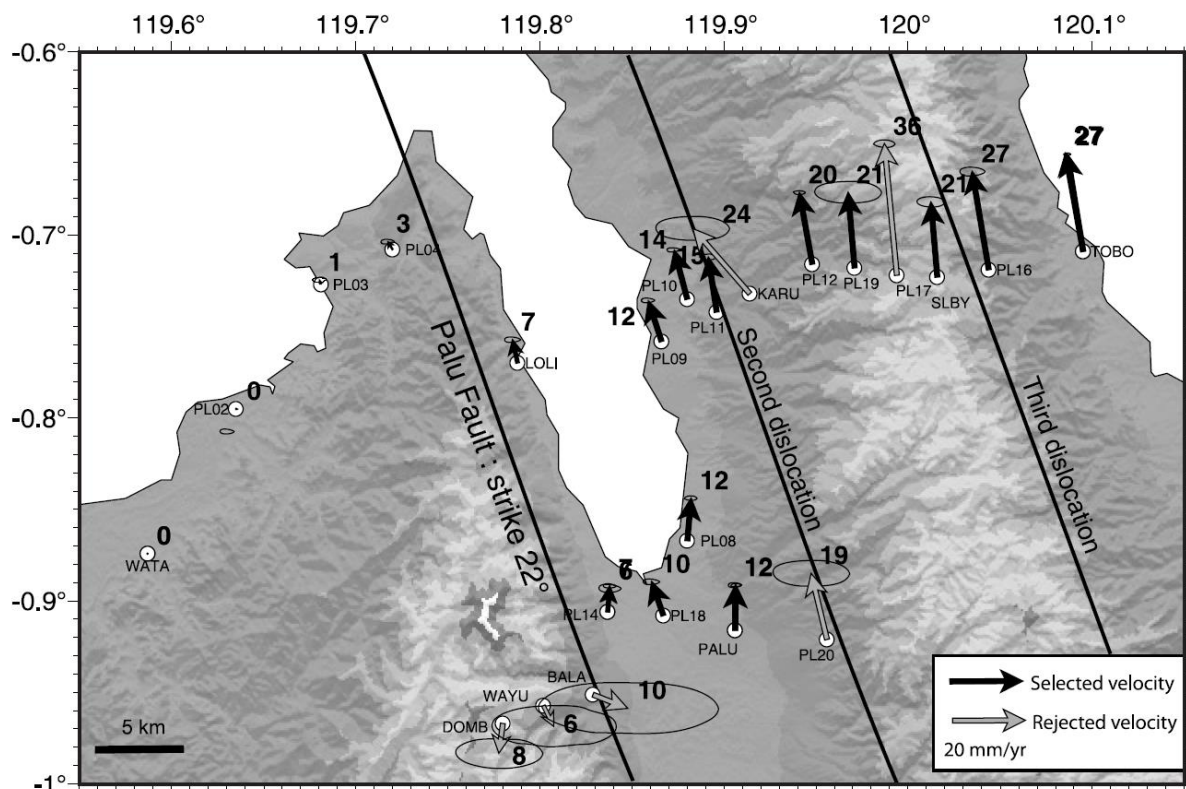


Figure 2.7 – ‘Multiple strand’ model of fault dislocation in Palu area proposed by Socquet et al. (2006) showing measured relative GPS velocities.

2.3 Overview of the 28th September 2018 Sulawesi Event

The main shock of the 28th September 2018 sequence of earthquakes occurred due to the rupturing of the Palu-Koro Fault with the epicentre located approximately 80km north of Palu city and an estimated hypocentral depth of approximately 10-15km (Valkaniotis et al., 2018; Figure 2.8). The earthquake occurred at 18:03 local time (10:03 UTC) and had a moment magnitude (M_w) of 7.5 with a total fault rupture length of more than 150km. From measurements in the field, the EEFIT-TDMRC Team estimate a fault mean displacement at the surface of 3 to 5m. The total calculated fault rupture area is approximately 150km by 30km with most of the rupture occurring to the south of the epicentre.

The main shock was preceded by a number of significant foreshocks including a magnitude 6.1 M_w three hour before at around 15:00 local time. An active aftershock sequence occurred including over 40 recorded events of magnitude 4.4 M_w or greater in the first five days following the mainshock with the largest magnitude 5.8 M_w event occurring at 18:25 local time (Valkniotis, 2018).

The earthquake caused significant damage to buildings and infrastructure due to the ground-shaking, but the additional losses occurred as a result of the secondary hazards including tsunami, landslides, fault surface rupture and liquefaction. These are discussed in greater detail in the following Sections of the report.

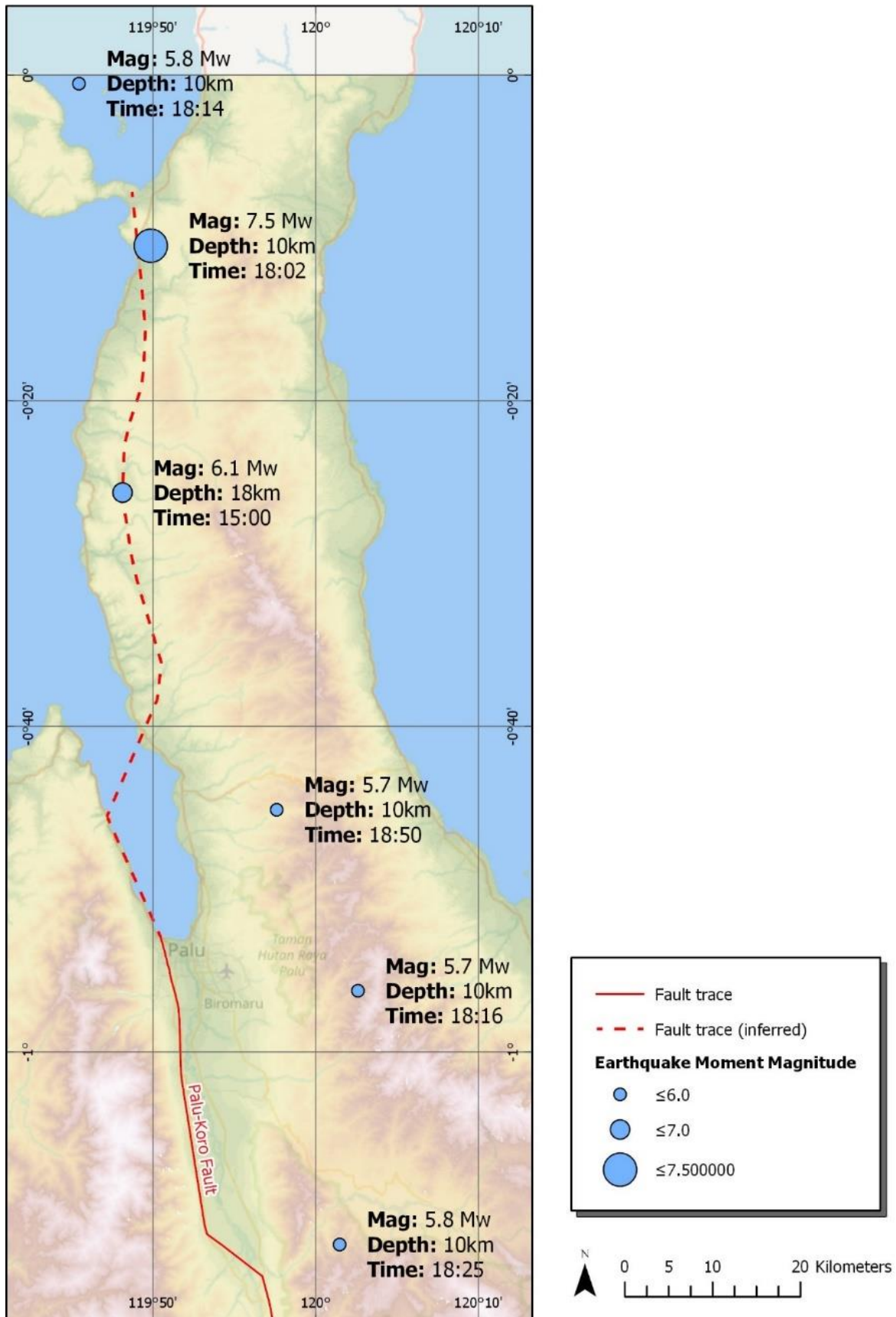


Figure 2.8 – Overview map of the Palu-Koro Fault in the Palu area and the major events in the earthquake sequence, drawn by the EEFIT-TDMRC Team. Earthquake epicentres are shown by the blue circles (with magnitude, depth and time)

3.0 Fault Surface Rupture Investigation (Lagesse, R., Brennan, A.; Rusydy, I.)

As mentioned previously, the epicentre of the earthquake was situated approximately 80km north of Palu city, and the total fault rupture length along the Palu-Koro Fault was more than 140km with a calculated mean displacement of 3-5m (Valkanotis et al., 2018). Pre-mission information suggested that surface rupture of the fault had occurred and, although the fault had been mapped using satellite imagery and co-seismic displacement analysis (Figure 3.1), part of the mission was focussed on ground-truthing the fault rupture at the surface.

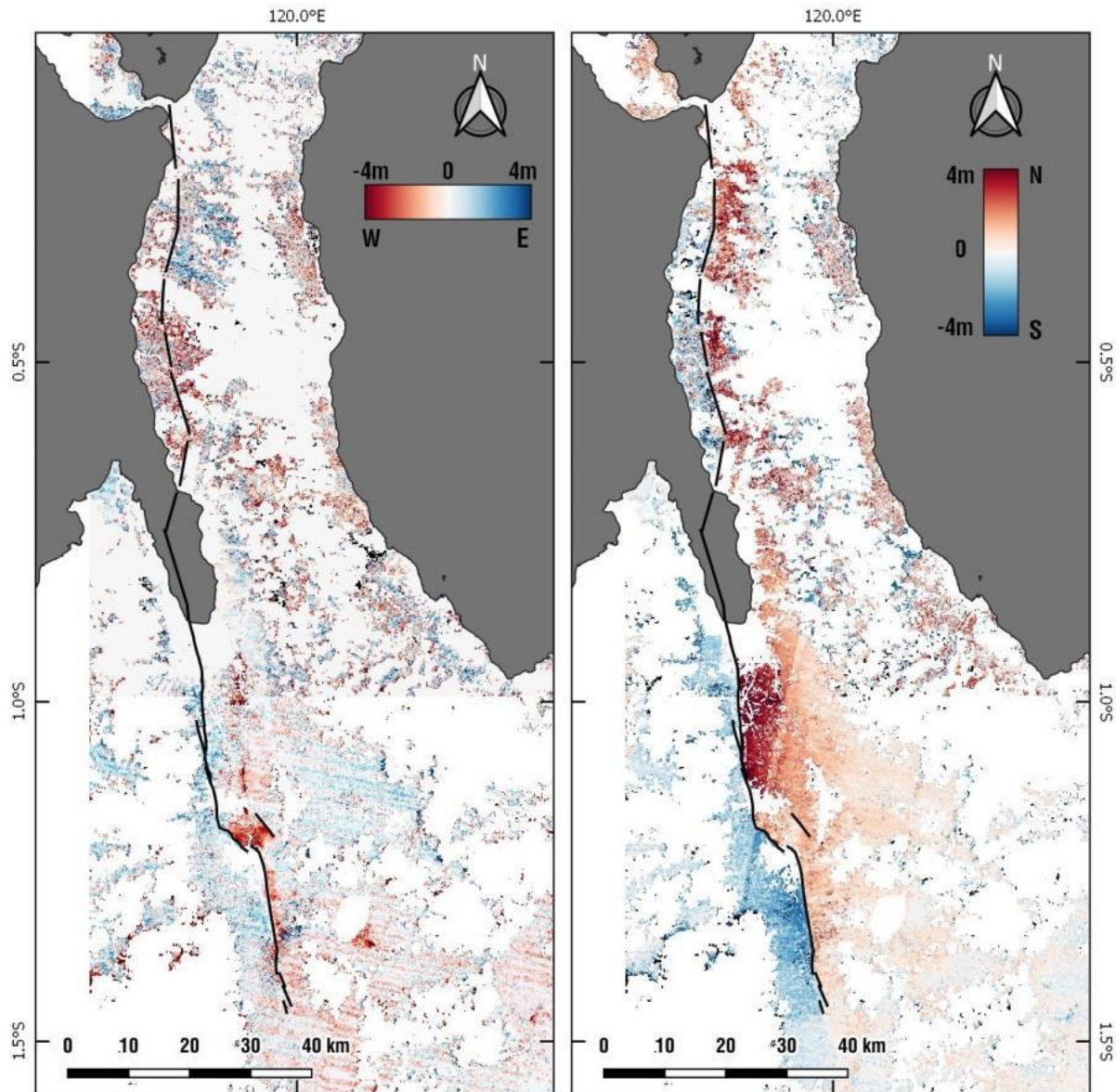


Figure 3.1 – Co-seismic assessment of fault rupture displacement after Valkanotis et al. (2018). The left image is west to east displacement and right image is north to south displacement.

South of the epicentre, where most of the rupture was expected to have occurred, the fault trends in a north-south direction inland from the coast towards Palu. At some point along the eastern side of the Gulf of Palu the fault is expected to cross-over to the western side of the bay before running south and intersecting land at the western end of the Palu bay-front area. The onshore expression of the fault runs south along the western side of the valley to the far southern end with a left-stepping oblique bend

approximately 30km south of Palu city. Significant fault displacement has not been measured in the field nor via remote sensing method. This is presumably related to the termination of the valley and greater relief restricting the surface expression of the fault. However, the fault is expected to extend further to the south where it eventually joins the major strike-slip Matano Fault.

The Gulf of Palu and the valley extending to the south of the city are thought to have formed due to fault interactions causing a pull-apart basin, of which the fault rupture seems to have occurred along the westernmost bounding fault. The fault demonstrates step-over faulting, (which is typical of pull-apart basins), in the south of the valley and likely underlying the gulf itself where it crosses over the bay. The step-over fault in the south of the valley represents an extensional bend and exhibits up to 4m of normal displacement in this area (Figure 3.2). Significant breaks of slope in the area of the oblique bend may represent relict fault scarps.

Conversely, it is possible that a step-over fault underlying the bay formed a contractional bend and resultant thrust faulting has led to uplift of the sea bed. This might be a possible cause of the tsunami but was not proven by any of the bathymetric survey data available to the EEFIT-TDMRC Team at the time of the mission.

Tectonic geomorphological features such as triangular facets, hanging valleys and offset drainage lines on the western side of the valley (Figure 3.3) suggest that this represents the main fault scarp of the fault system, as proposed by Socquet et al. (2006), demonstrating a history of both strike-slip and normal displacement.

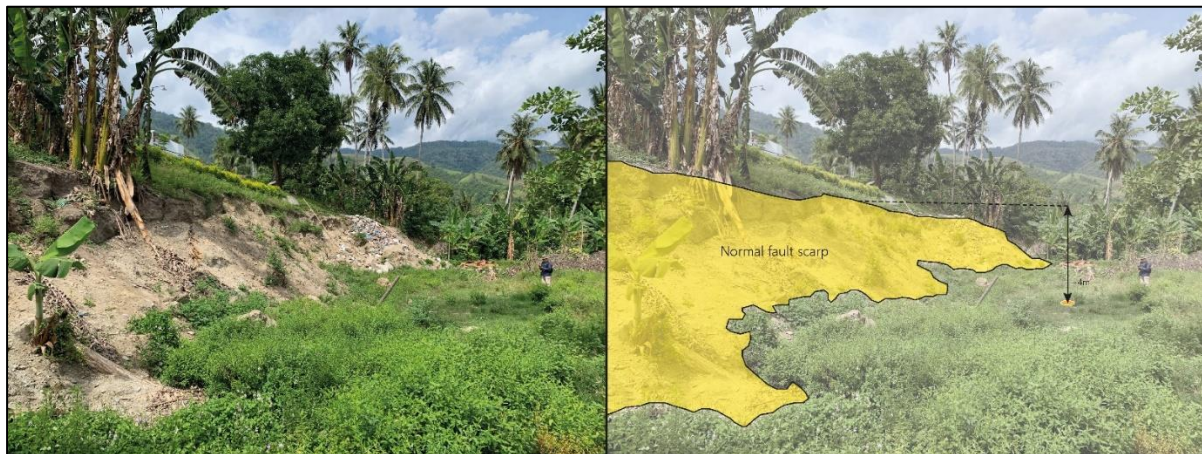


Figure 3.2 – Normal fault scarp displaying vertical displacement of approximately 4m in the south of Palu valley.

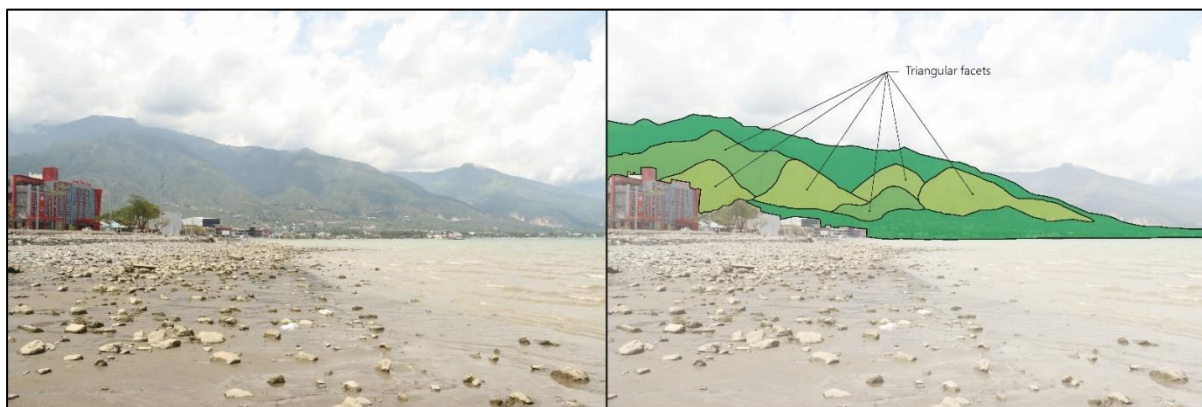


Figure 3.3 – Triangular facets on the western side of Palu valley.

Surface rupture of the fault was observed in the field with evidence of displacement identified at the Palu city bay-front area and at the far southern end of the Palu valley. Other instances of surface fault

rupture were identified on the western side of the Gulf of Palu at Tasiburi as well as on the eastern side of the bay near Dalaka. However, the interconnectivity of these ruptures with the surface rupture in the Palu valley area is inferred, particularly the undersea component.



Figure 3.4 – Offset road due to strike-slip fault displacement.

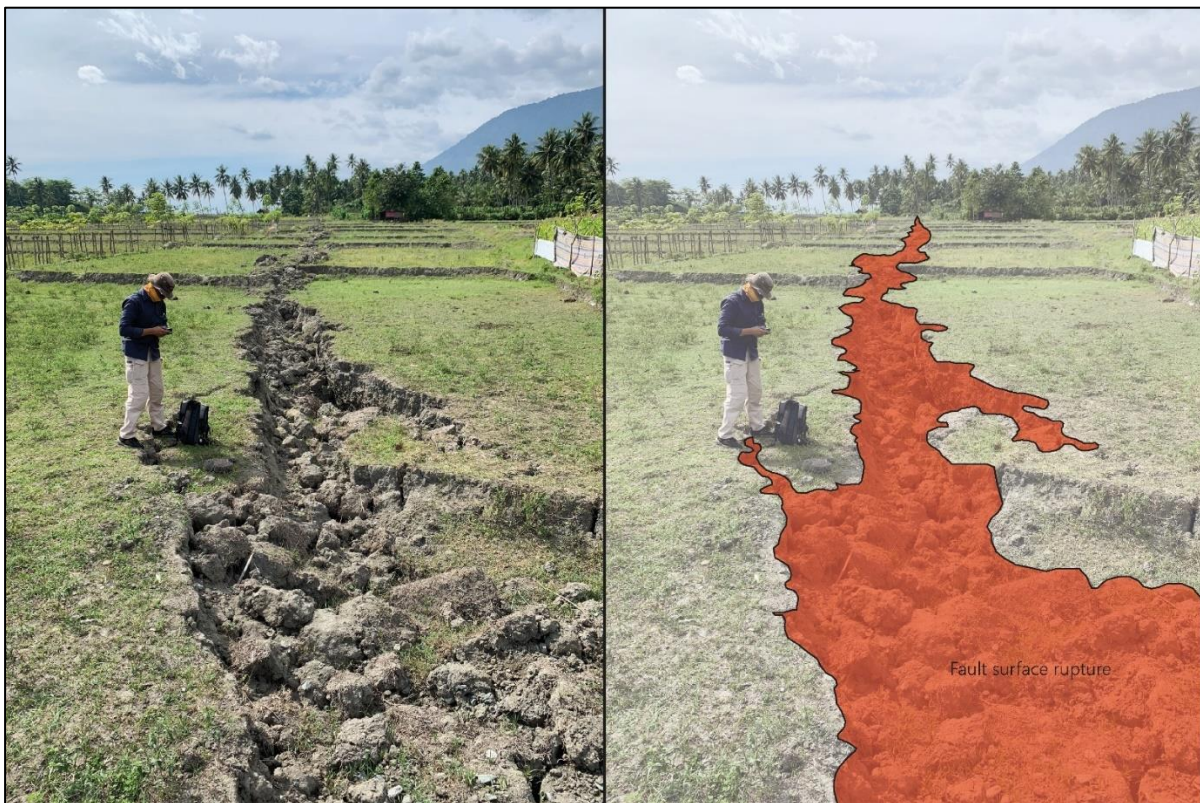


Figure 3.5 – Fault surface rupture through rice paddy field.



Figure 3.6 – Displacement of approximately 5m along fault surface rupture shown due to offset rice paddy terraces.

Numerous expressions of the fault surface rupture were identified throughout the area, typically by the offset of linear features such as roads (Figure 3.4), but also dramatic continuous surface ruptures through agricultural land (Figure 3.5). Left-lateral strike-slip displacement was measured by the Team to be a maximum of 5m at Pewunu (Figure 3.6), and typically between 3-4m. It is possible that, given the proximity of the Pewunu area to the valley sides and steep terrain, the soil is thinner and thus the greater displacements in the bedrock are more closely represented at the surface.



Figure 3.7 – Normal faulting observed North of Labua on the East side of Palu Bay. Photo taken facing North East



Figure 3.8 – Damage to water channel on North side of large rupture at Labua indicates observed total displacement may be only partly due to 28th September event

To the East of Palu Bay and north of the settlement of Labua, two surface expressions of predominantly normal displacement were observed in close proximity as shown in Figure 3.7. Vertical offsets of 0.5 m were measured for the smaller, more westerly point (nearer the camera in Figure 3.7) and 2 m for the larger rupture. Although surface debris indicated recent movement had occurred on these surfaces, it is unclear whether these measured offsets were entirely caused by the 28th September earthquake, as a water channel alongside the larger fault surface showed a breakage with an offset of 0.6 m vertically and 0.4 m to the right (Figure 3.8). This channel also showed evidence of prior patchwork repairs, suggesting that it is possible that previous events may have also contributed to the 2 m total that was measured. Figure 3.9 presents an overview of the mapped and inferred fault locations.

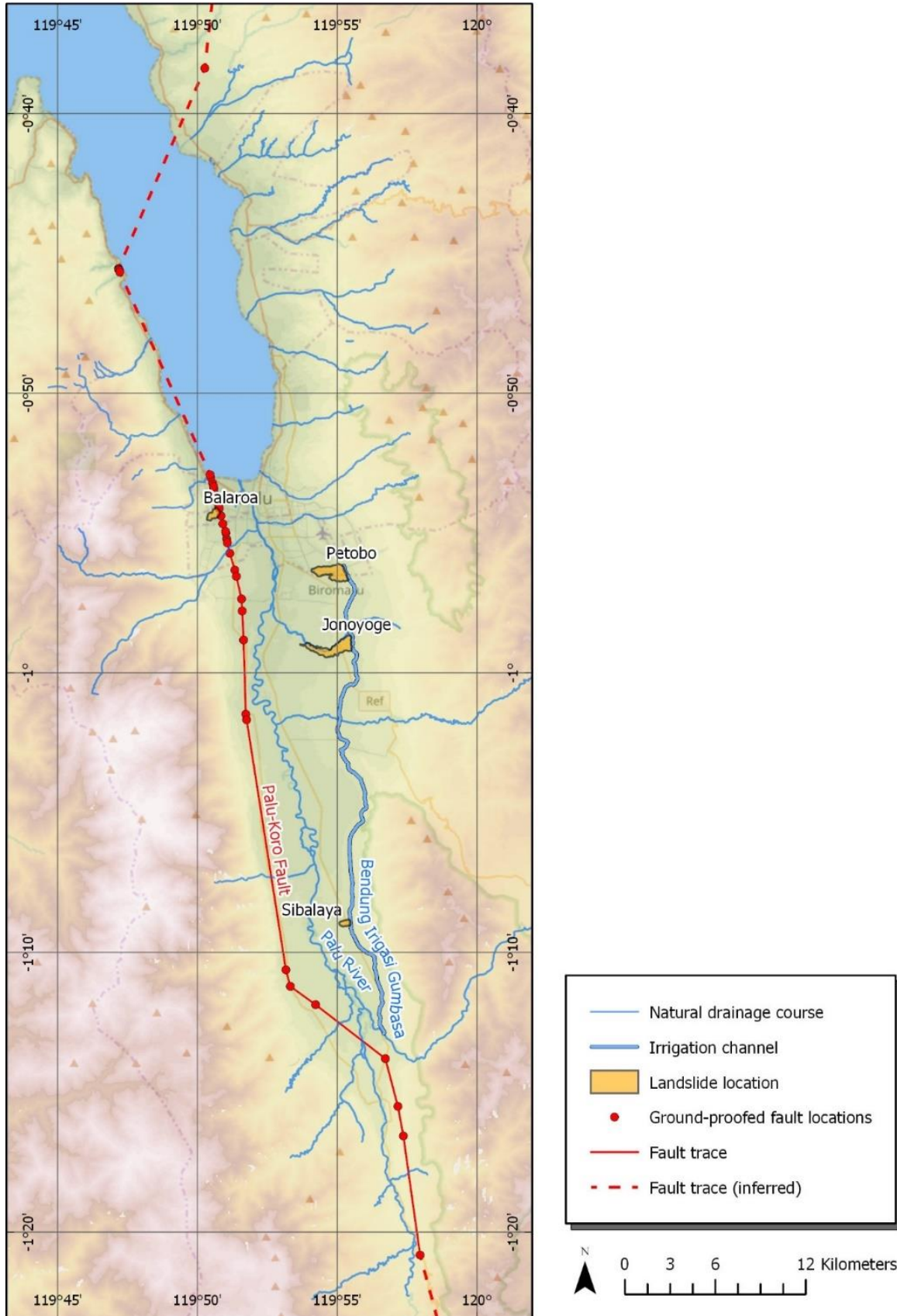


Figure 3.9 – Overview of Palu valley showing the Palu-Koro Fault, major landslides, Bendung Irigasi Gumbasa irrigation channel and the major natural drainage courses.

4.0 Landslide Investigation (Lagesse, R., Brennan, A.; Rusydy, I.)

As a result of the earthquake, several significant landslides occurred in the Palu area, in addition to many other smaller landslides observed in mountainous areas around the city and in road cuttings. During the field mission, most attention was paid to the three largest mass movement occurrences, namely: the Balaroa, Petobo, Jono Oge and Sibalaya landslides (Figure 3.7), named after the districts where they occurred. Although fatalities occurred due to tsunami and building collapse caused by severe ground shaking, the Balaroa and Petobo debris flows alone possibly account for more than half of the human losses for the wider disaster and thus warranted special attention.

The landslide that occurred in Jono Oge (in Sigi regency) was the largest in terms of runout (210 ha according to Indonesia's National Board for Disaster Management – BNPB) but led to reduced losses (although still significant building damage and some human losses resulted) due to its occurrence in a mostly rural area to the south of Palu city.

The main objectives of the field mission, in terms of the landslide investigation, was to establish the cause and the factors that could have led to the failures as well as establishing the failure mechanisms. It should be noted that the field mission took place approximately seven weeks after the events and significant clearing of debris had taken place, particularly in the more developed areas of Balaroa and Petobo. As such, it is likely that some evidence that could have contributed to the findings may have been removed.

The key field observations, supplemented by observations made using aerial photography and satellite imagery, for each landslide occurrence are described below.

4.1 Balaroa

The Balaroa Landslide occurred in the western district of Balaroa in Palu city with anecdotal evidence suggesting the landslide occurred within 1-2 minutes of the earthquake ground shaking commencing. The landslide has a head scarp approximately 0.5km wide and a runout approximately 1km long; the head scarp was measured to be approximately 8-9m at its highest. The overall slope angle from the top of the head scarp to the toe is approximately 3.5°. It has reasonably well-defined zones of depletion and accumulation with most debris being deposited 0.4km east of the head scarp (Figure 4.1). The surface rupture of the Palu-Koro Fault also runs along the toe of the landslide.

Before to the landslide, Balaroa was a densely populated residential area with historical aerial photos suggesting this was one of the oldest urbanised parts of Palu; as a result, damaged buildings and man-made debris was observed throughout the landslide area. Much of the debris in the lower depositional part of the landslide remained with most of the upper part having been cleared. Some buildings and vegetated areas remained intact but had been transported significant distances from their original location. This may suggest an underlying flow transport mechanism with shearing occurring deeper than many structure foundations and vegetation roots.

Subsurface materials were exposed at the head scarp (Figure 4.2) demonstrating the following succession:

- <1m granular engineering fill, predominantly sandy gravel and cobbles;
- 1-2m of fluvial deposits comprising sandy gravel, gravelly sand, silty sand, sandy silt; and
- Underlying granitoid subangular to sub-rounded cobbles and boulders in a gravelly medium to coarse sand matrix – suspected colluvium / previous landslide deposit, base not proven.

Many large boulders, similar to those observed in the colluvium, were also noticed scattered across the zone of depletion across the upper part of the landslide. Accounts from local geologists and engineers suggested colluvial material was widespread in the valley side areas.

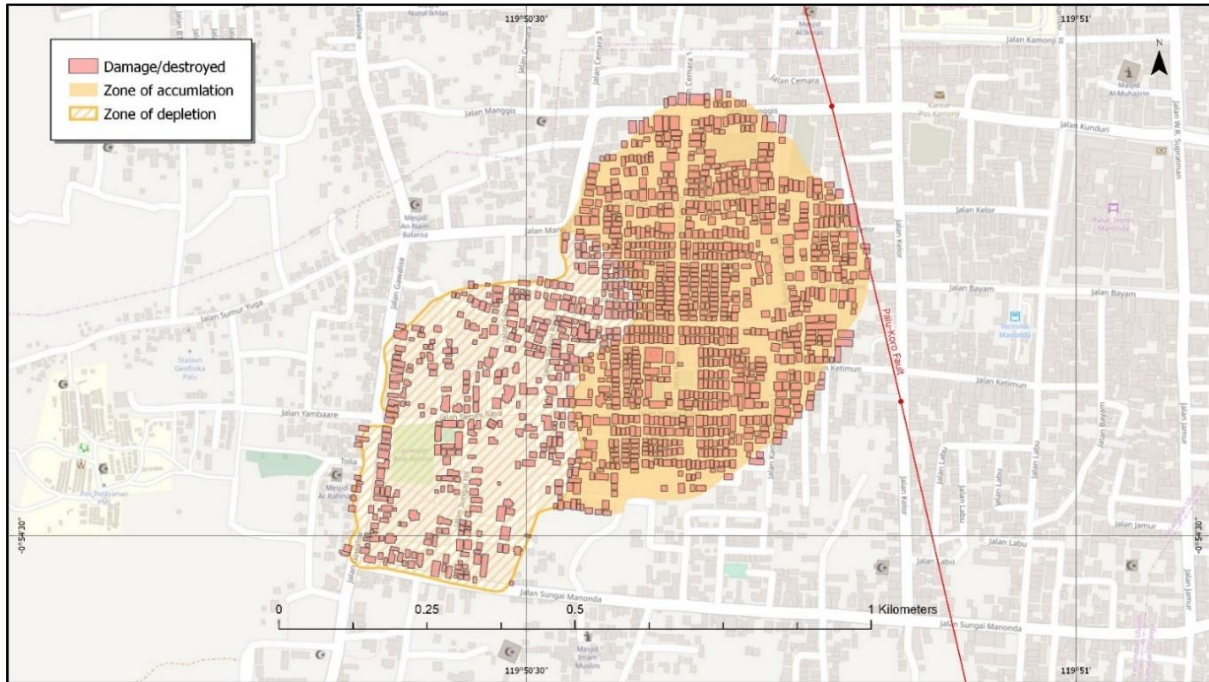


Figure 4.1 – Overview of the Petobo landslide area showing zones of depletion and accumulation as well as damaged buildings and the Palu-Koro Fault surface rupture.

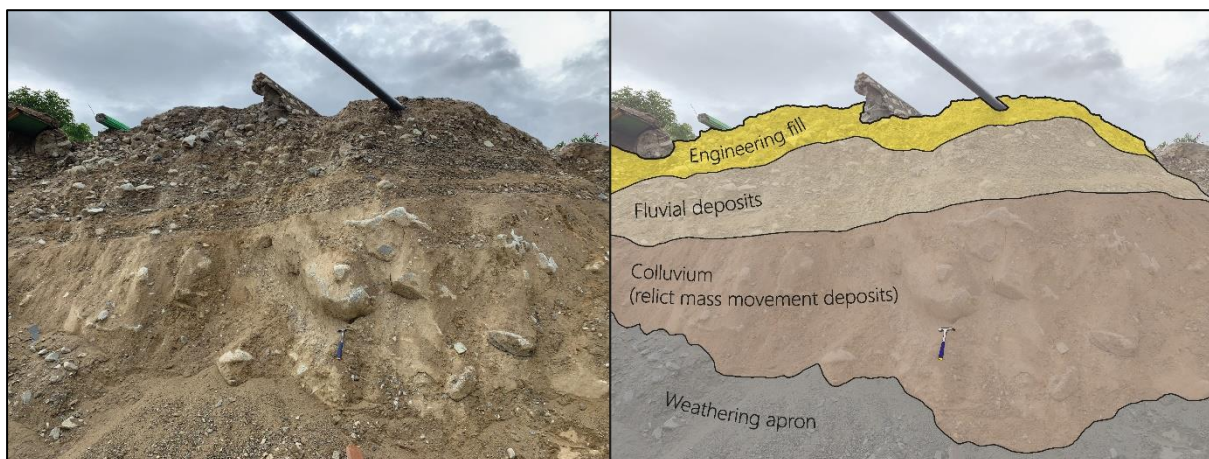


Figure 4.2 – Geological profile exposed in Balaroa Landslide head scarp.

Follow-up investigation in the immediate aftermath of the landslide by geotechnical representatives from Tadulako University identified evidence of liquefaction in the underlying soils. A 4m deep borehole hand-drilled one week after the event revealed localised sand material that has undergone liquefaction. Although based on only one borehole, it is possible that liquefiable material occurred in pockets rather than in mass. A 20m deep CPT located at the Anutapura Hospital, 200m from the toe of the landslide, revealed mostly silty clay and loose sand material with no refusal at 20m and a highest cone resistance (q_c) value of 8MPa.

Accounts from local residents, geologists and engineers suggest the groundwater levels on the western side of Palu Valley are relatively high with springs observed by locals in the slopes above Balaroa. A local resident and representative of the Meteorological, Climatological and Geophysical Agency (BKMKG) commented that prior to the earthquake groundwater levels were 4m below ground level at the location of his house at the toe of the landslide. He also noted that during the landslide his house

was raised by 3-4m and travelled 260m to the north from its original location. Significant ponding was observed during the walkover in the zone of accumulation and debris lobe.

A walkover of the area immediately above the landslide scarp revealed significant tension cracking but none were recorded further back than 30-40m from the scarp, with limited evidence of displacement or deformation beyond this distance. One account revealed that the area around the central portion of landside scarp was previously a football pitch where many local residents migrated to during the earthquake seeking open ground and safety from falling structures. Unfortunately, the ground underlying the pitch failed during the landslide and the group perished.

4.2 Petobo

The Petobo Landslide occurred in the south-eastern district of Petobo, Palu city with evidence suggesting the landslide occurred during the earthquake ground shaking. The landslide has a head scarp of approximately 1km wide with a runout approximately 2km long; the head scarp was measured to be approximately 8-9m at its highest. The overall slope angle from the top of the head scarp to the toe was approximately 3°. It has reasonably well-defined zones of depletion and accumulation with most debris being deposited 1km to the west of the head scarp (Figure 4.3) along the main runout. There is also partial back-sloping of the main debris lobe around the central area of the landslide.

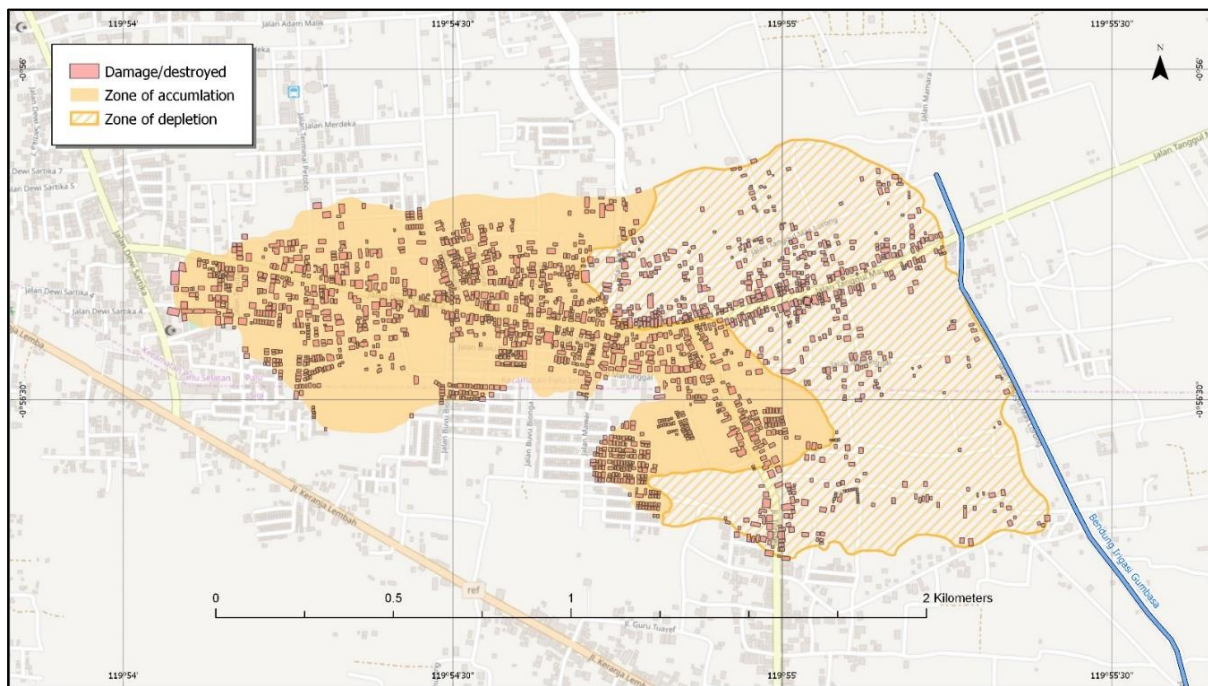


Figure 4.3 – Overview of the Petobo landslide area showing zones of depletion and accumulation as well as damaged buildings and the location of the Bendung Irigasi Gumbasa irrigation channel.

In the upper part of the landslide there is a finger of ground that has been partially inundated with debris but has largely stayed in situ and as a result this has led to a secondary runout, approximately 1km long, to the south of this finger. Much of the lower depositional part of the landslide had been cleared, however, a damaged house situated in a gully formed in the debris with the base at original ground level suggested the deposited debris thickness was approximately 4m (Figure 4.4). Elsewhere, debris has been used to form an embankment for an access road.

Prior to the landslide, Petobo was largely a residential area along a main road than ran down what is now the central axis of the main runout path. Along the flanks of what is now the landslide area, was predominantly open ground and some swamp areas (Figure 4.5). The upper part of the landslide was mostly agricultural land and rice paddies prior to the ground failure. A map published by Dutch settlers

in the early 20th Century (Kruyt, 1938) suggests that this area, as well as large parts of Palu, were also largely rice paddies during this time (Figure 4.6). Significant urbanisation occurred from 1952 onwards.



Figure 4.4 – Deposited debris thickness in the accumulation zone of the Petobo Landslide.



Figure 4.5 – Swampland adjacent to the toe of the Petobo Landslide.

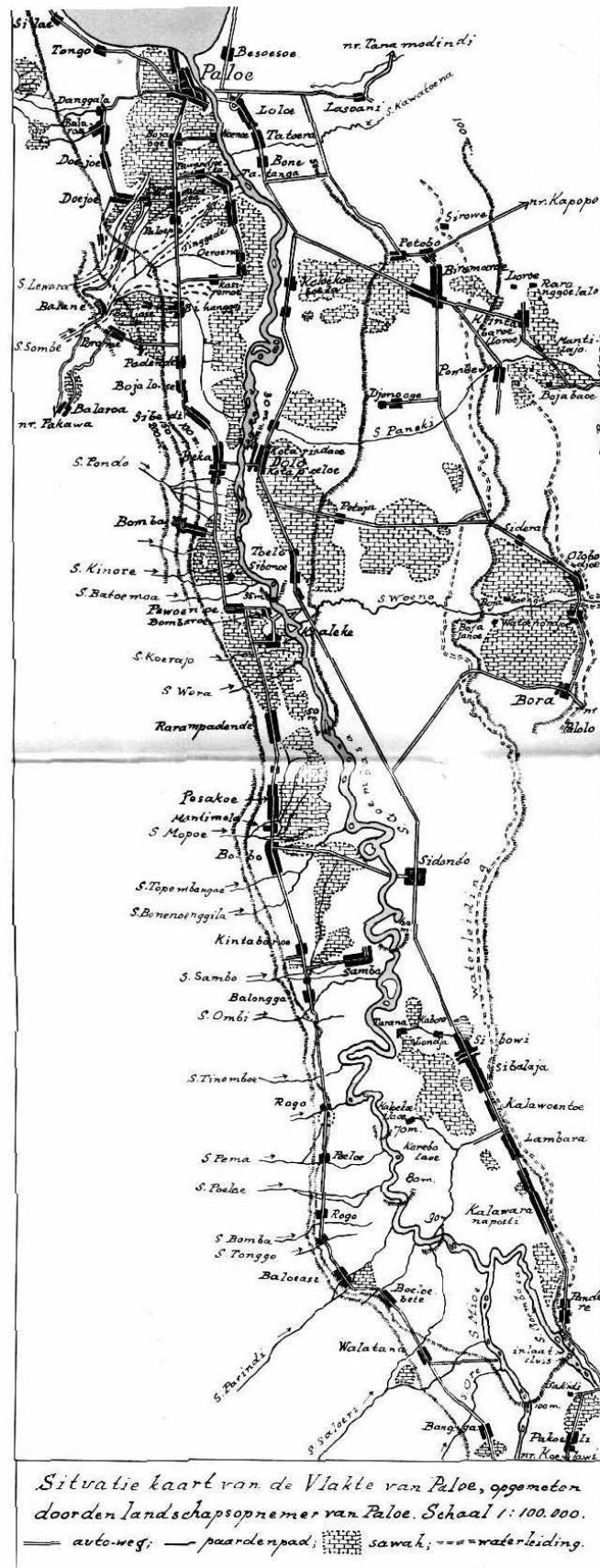


Figure 4.6 – Historical map of the Palu valley area in the 1930’s (Kruyt, 1938).

The Central Sulawesi, Indonesia Earthquake and Tsunami of 28th September 2018

Similarly to Balaroa, some buildings and vegetated areas remained intact but had been transported significant distances from their original location. This suggests an underlying flow transport mechanism with shearing occurring deeper than many structure foundations and vegetation roots.

Subsurface materials were exposed in the head scarp (Figure 4.7) demonstrating the following succession:

- <1m of agriculturally reworked topsoil; and
- Underlying fluvial/alluvial deposits comprising occasionally gravelly fine to medium sand with occasional layers of increased fines content – base not proven.

This succession was confirmed by a 3m deep borehole hand-drilled prior to the earthquake in the area that is now the upper part of the landslide. Bulk samples of material were collected by EEFIT-TDMRC team from the northern end of the head scarp at depths of 1.6m and 3.1m. These were tested for particle size distribution at University of Dundee as shown in Figure 4.8. The particle size distribution suggested a profile of silty fine sand. Darker patches of wet/damp material were observed in the exposed head scarp suggesting ongoing seepage of groundwater. At a location approximately 1km from the head scarp along the runout natural debris also comprised slightly gravelly silty fine to medium sand.

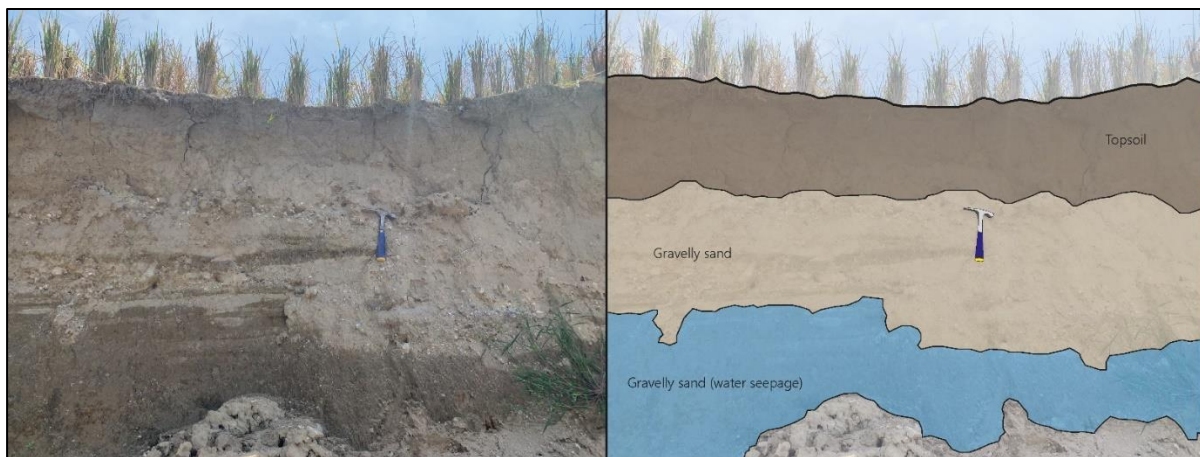


Figure 4.7 – Geological profile exposed in Petobo Landslide head scarp.

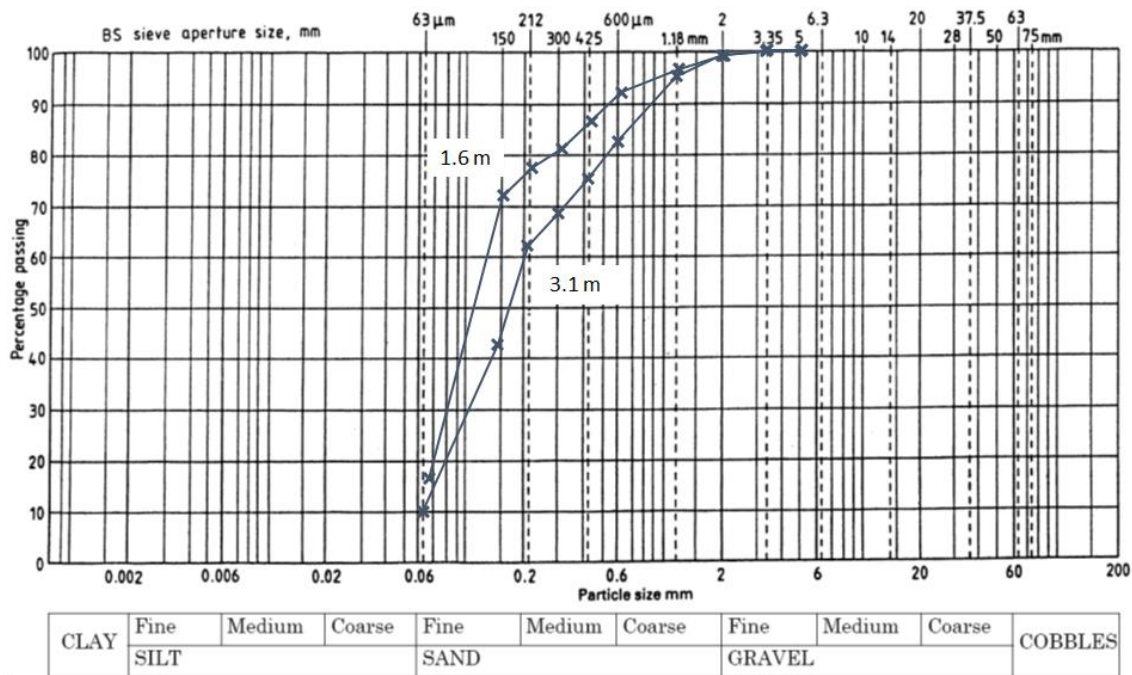


Figure 4.8 – Particle size distribution of samples taken from Petobo head scarp

Representatives of the provincial office of the Ministry of Public Works and Public Housing (MoPWPH), suggested in a conversation with the EEFIT-TDMRC Team that the agricultural land was quite permeable and farmers have trouble saturating the ground for agricultural purposes as the water flows away; this suggests permeable granular material underlying the area. However, following a meeting with a geologist and hydrogeologist from the local office of the Department for Energy and Minerals (DfEM), evidence suggests that there is indeed clay material interbedded with the sand deposits with the shallowest significant clay layer occurring at approximately 10m below ground level in the Petobo area. This interbedding is illustrated on cross-sections of the local geological map provided by the DfEM, which show the dip of interbedded layers run parallel to the ground profile. Further discussion with the DfEM revealed that their drilling showed the clay layer is confining an aquifer that was under artesian water pressures.

Conflicting accounts (by different locals and officials) of groundwater depths in the area suggest that the interbedding of clay layers may have resulted in multiple confined aquifers as well as the shallow unconfined groundwater. Accounts suggest that prior to the earthquake groundwater levels in the lower part of Petobo were between 8 and 12m below ground level, whereas after the earthquake and landslide they had risen to 2m below ground level. Significant water flow was observed coming from the toe of the landslide into local drainage networks. An area of swampland was observed to the north of the toe, likely reflecting the original conditions prior to urban development.

As mentioned, the upper part of Petobo area was predominantly rice paddies and other agricultural land prior to the landslide. Rice paddies require inundation of 20cm of water for a 15-day period during growing phases. This saturates the subsurface. The control of irrigation water is managed via a man-made network of channels and sluice gates which runs along the valley side, approximately at the location of the concave break of slope between steeper mountainous terrain and flatter valley sides. This system requires a large volume of water to always be present in the main irrigation channel such that farmers can syphon off the water via the sluice gate network as required. Over time, as the rice paddies have proliferated, the discharge of water into the ground, rather than local drainage networks, has increased as farmers have diverted more water onto their land. As a result of this dynamic use of irrigation water it is likely that groundwater conditions in the Petobo area are not hydrostatic and there is a flow component.

The main irrigation channel, called the *Bendung Irigasi Gumbasa*, is approximately 32km long and runs from south to north along the Palu Valley from its confluence with a major tributary of the Palu River in the south of the valley (Figure 4.3). The local office of the Ministry of Public Works and Public Housing (MoPWPH), are responsible for the operation and maintenance of the irrigation channel, which was constructed in 1973. However, on the historical map published by Kruyt (1938), (see Figure 4.6), the channel is delineated and labelled ‘*waterleiding*’ (*water pipe* in Dutch), which suggests that a man-made channel was also present at that time. The MoPWPH also stated that there is a network of underground water pipes supplying fresh water to residents in the area; and the EEFIT-TDMRC Team observed exposed subsurface pipes in areas of broken ground.

The main irrigation channel terminates in the Petobo area, with two much smaller channels located at the end, presumably to transport water into local man-made and natural drainage networks. However, the dimensions of the smaller channels (2m width, 1m depth) are significantly smaller than the main irrigation channel (14.5m width, 3.5m depth), and would not be sufficient to discharge significant amounts of water quickly. Instead, as the main channel is predominantly unlined, there is likely significant seepage of irrigation water into the ground in this area.

Anecdotal evidence suggests that ground water in the area above the irrigation channel, as terrain steepens, is much deeper between 15-30m below ground level. This is reflected in the aerial photography and satellite imagery of the area, with the land above the irrigation channel observed to be brown (no vegetation), whereas below the channel the ground is green in colour, indicating significant vegetation growth and agriculture (Figure 4.9). There is also limited urban development upslope of the channel as groundwater extraction is likely more challenging.

It is notable that both the Petobo and Jono Oge landslides, as well as a much smaller (but still significant) failure in the town of Sibalaya to the south, all initiated along the irrigation channel (Figure 4.3). Eyewitnesses remarked that prior to the earthquake the irrigation channel was full of water and rapidly emptied during the ground shaking (Figure 4.10). Local eyewitnesses at the confluence where the main channel flow control structures are situated reported that flow to the irrigation was stopped in the evening after the earthquake and, at the time of the mission, the entire channel was observed by the EEFIT-TDMRC to be dry except for some localised ponding.



Figure 4.9 – Difference in vegetation growth due to groundwater conditions on either side of the Bendung Irigasi Gumbasa in the Petobo area. Green vegetation growth (left) indicates wetter ground conditions as opposed to brown land with lack of vegetation growth (right) indicating mostly dry ground.



Figure 4.10 – Far northern end of the Bendung Irigasi Gumbasa irrigation channel above the head of the Petobo Landslide before (left) and after (right) the earthquake.

Given the subsurface materials (predominantly sand, overlying clay) and the hydrogeological conditions in the area, it is likely that flow liquefaction of the sand material occurred. This, coupled with shear stresses induced by the slope angle, (even if the latter is slight), led to a catastrophic failure of the slope, which in turn initiated a highly mobile translational debris flow.

Back-tilted blocks in close proximity to the head scarp suggest that the initial failure mechanism also had a rotational component. Given the height of the back scarp (8-9m) and the reported depth of the shallowest clay layer (10m) it is also possible that increased pore pressures at the boundary between the sand and clay led to a reduction in effective stress, and therefore that a shear surface developed along this horizon. It is further noted that, if the clay layer breached during the landslide this would introduce significant additional groundwater from the underlying confined aquifer, possibly with higher than normal pressures. Further, if the local water supply pipes ruptured this would, again, increase the water in the ground.

Representatives from the MoPWPH suggested that there were plans to restore the irrigation channel following the landslide, adding to it an impermeable geosynthetic clay liner (GCL) as well as upgrade the local drainage network. They also remarked that a new residential area was planned at the southern end of the airport, to the north of the Petobo Landslide. The airport was pre-existing to the development of the main irrigation channel and it is possible the continuation of the channel was restricted by planning restrictions related to the airport (see Figure 4.8).

4.3 Jono Oge

The Jono Oge Landslide occurred to the southeast of Palu city, in a more rural area. Evidence suggests the failure occurred during the earthquake ground shaking. The landslide has a head scarp of approximately 1km wide with a runout of the main debris lobe of 4.5km. However, at the toe of the landslide, debris became entrained in a natural drainage channel, and was transported as far as the Gulf of Palu via the main Palu River.

The exposed part of the head scarp was measured to be 3-4m at its highest, although measurement was partially obstructed back-tilted blocks. Significant minor scarps were observed due to abundant back-tilted blocks remaining intact (Figure 4.11). The overall slope angle from the top of the head scarp to the toe was less than 1° – the length of the runout and this low angle suggests the landslide was extremely fluid and thus mobile. The landslide is bounded to the north by a major drainage line – the same drainage line that it eventually becomes entrained in.

The evidence and characteristics of the landslide suggest the failure mechanism and causal factors were similar to the Petobo failure, however, with some notable differences. In contrast to Balaroa and Petobo, the Jono Oge area is much more rural, and the main area of damage was a 700m long section of the town (mainly comprising one row of houses). There were also some localised developed areas that were partially inundated with debris. However, similarly to in Balaroa and Petobo, some buildings and

vegetated areas remained intact but had been transported significant distances from their original location. This suggests an underlying flow transport mechanism with shearing occurring deeper than many structure foundations and vegetation roots. This is supported by video evidence which shows large areas of ground with buildings and vegetation moving as one block. Eyewitnesses also suggested that the landslide had a ‘swirling’ motion.



Figure 4.11 – Upper part of the Jono Oge Landslide with the main scarp and minor scarps indicated.

In the head scarp and minor scarps, a maximum of 2-3m of natural material was exposed demonstrating the following succession:

- <0.5m of agriculturally reworked topsoil;
- <0.5m of an organic rich relict topsoil layer; and
- Underlying fluvial/alluvial deposits comprising occasionally gravelly silty sand.

Geotechnical representatives from Tadulako University suggested that the Jono Oge area had more clay rich soils in comparison to Petobo and Balaroa, with a thick clay layer proved in a hand-drilled borehole. During the field walkover, a rotary core borehole drilling rig was observed at the head scarp area of the landslide. The operator suggested they were conducting a geotechnical investigation on behalf of the MoPWPH, with the borehole scheduled for termination at 30m below ground level.

The Jono Oge landslide also initiated at the Bendung Irigasi Gumbasa main irrigation channel, with the channel forming a large graben behind the main head scarp. The large blocks of intact material at the upper part of the landslide suggest that any liquefied layers were likely at depths below 3-4m. Lateral spreading liquefaction was observed in the main part of Jono Oge town to the north of the landslide. Significant differential settlement and tension cracking, along with evidence of sand boils, was observed.

4.4 Summary

The three main landslides that occurred following the earthquake are considered to be low-angle liquefaction-induced debris flows that were extremely mobile due to significant water content. The causal factors are largely thought to be related to the hydrogeological regimes’ interaction with the topography as well as possible anthropogenic factors. Most notably, a man-made irrigation channel running along the eastern side of the valley appears to be the initiation point of the two largest landslides within evidence suggesting the underlying hydrogeological regime is significantly affected by its’ presence. Whether or not the irrigation channel alone directly led to the failures is cause for discussion, but it is likely at the very least that it contributed to the long runouts due to the significant volume of additional water introduced into the ground.

EEFIT



Further investigation is needed to establish a clearer picture of the landslide causes and mechanisms, ideally with some detailed intrusive geotechnical investigation. At the very least the role of the anthropogenic influences on ground failure should be clarified where possible and potential mitigation options, such as drainage infrastructure and modifications to irrigation systems should be considered.

5.0 Liquefaction and Ground Subsidence Investigation (Brennan, A.; Lagesse, R.; Rusydy, I.)

In the aftermath of the 28th September 2018 Sulawesi earthquake, news media widely reported liquefaction as a significant cause of damage. However, the associated descriptions of the effects – complete burial of towns – was not consistent with conventional understanding of liquefaction damage. From the field reconnaissance, the EEFIT-TDMRC team identified three distinct manifestations of ground failure:-

1. “Conventional”, localised liquefaction-induced settlements and tilting of individual structures, with associated ejecta features. These seemed to affect a small number of isolated areas.
2. Liquefaction of seafront areas near estuary mouths, resulting in significant areas of land mass slumping into Palu Bay. The Team identified areas on both sides of Palu Bay affected by this. It is possible that some of the reported coastal inundations were caused by backwash over these slumps.
3. Landslides. Very large mass movements of soil that have buried settlements, as reported in Section 4.0.

The Team noted that public perception was that the term “liquefaction” related (incorrectly) to the landslides. As described in Section 4.0, liquefaction may have been a triggering factor in causing the landslides to occur, but the large-scale ground failures at Balaroa, Petobo and Jono Oge should be treated as landslide hazards. In the following Sections, observations made on the localised liquefaction and liquefaction of seafront areas are presented.

5.1 Local Liquefaction

Liquefaction as commonly observed elsewhere, with structural settlements, tilting and ejecta as key features, seemed to affect a small number of isolated areas, and the EEFIT-TDMRC Team identified three of these, shown in Figure 5.1, as being: (i) near the fault within Palu City, at Lasoso district, (ii) the town of Sigi in the Eastern suburbs, and (iii) The reclaimed land alongside Donggala Dolphin Park on the West shore of Palu Bay.

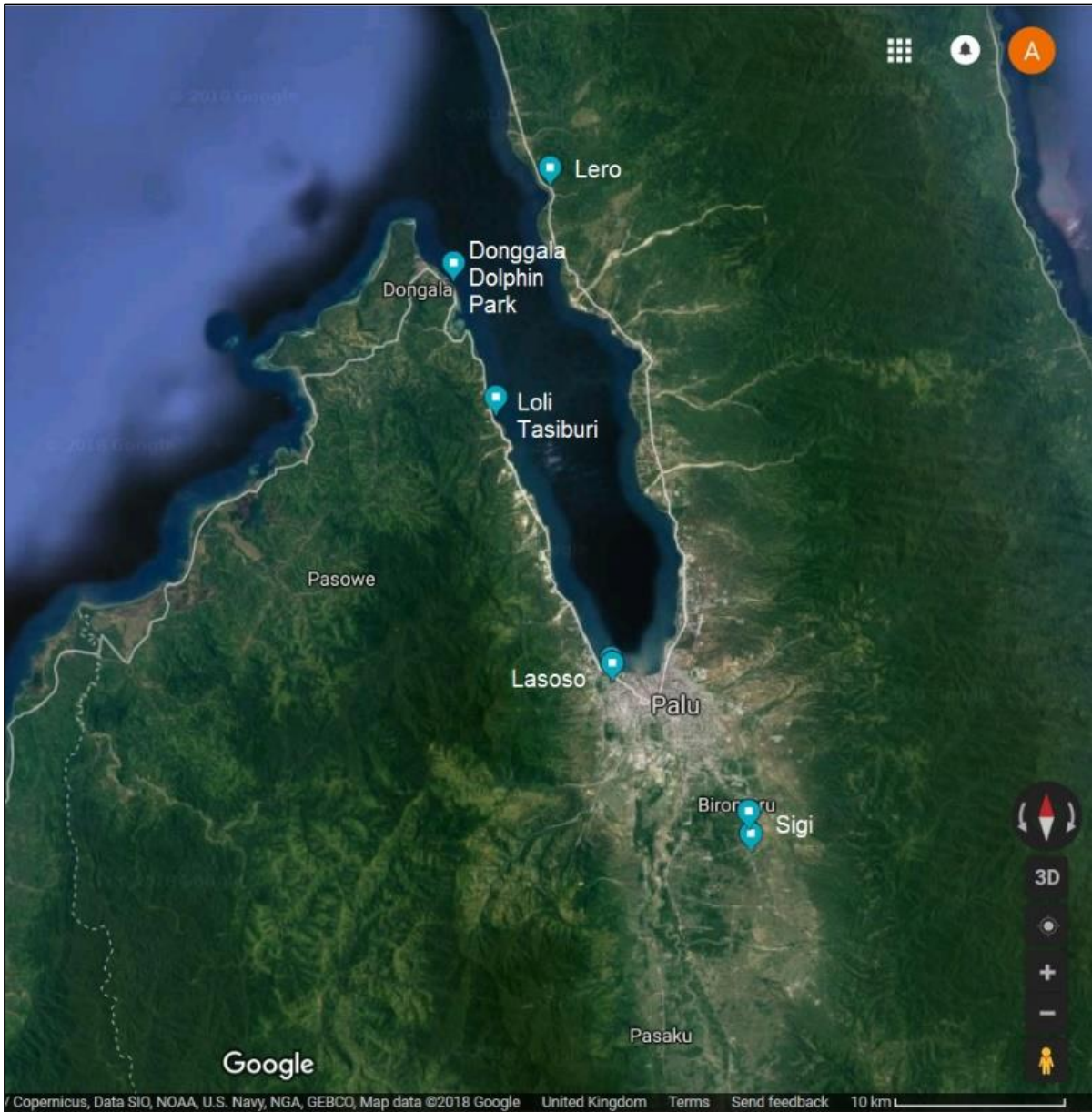


Figure 5.1 - Map of sites observed by the EEFIT-TDMRC Team to be affected by localised liquefaction (map: Google).

5.1.1 Palu City

Near the fault in Palu City, particularly in the Lasoso suburb, a small number of liquefaction-induced settlements of structures were observed (e.g. Figure 5.5 and 5.6). Furthermore, the Gelanggang Mahasiswa sports field in Kabonena was crossed by the fault and was observed to be covered in ejecta (Figure 5.2 and 5.3) classified as very gravelly sand (Figure 5.4). A vertical offset of 300 mm around the field suggested settlement of this amount, relative to nearby soils that showed no evidence of liquefaction.



Figure 5.2.- Liquefaction ejecta in a field at Gelanggang Mahasiswa, Kabonena. Observe the vertical offset in front of the pavilion where the field has settled relative to nearby intact ground.



Figure 5.3.- Liquefaction ejecta in a field at Gelanggang Mahasiswa, Kabonena. The ejecta, is seen to follow the path of the fault across the field, although the soil on both sides appears to have settled by a similar distance.

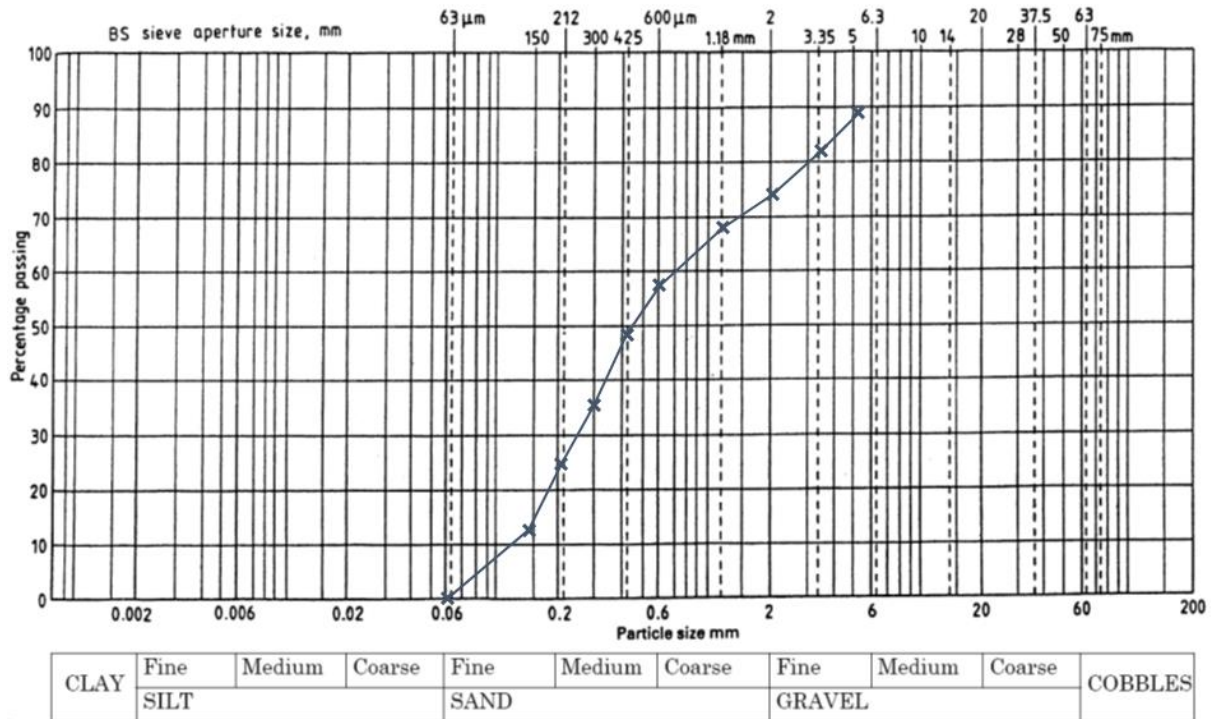


Figure 5.4 - Particle size distribution of ejecta collected at Kabonena

A single-storey house just South of the Kabonena field was noted to have undergone differential settlement and a lateral displacement of 2.6m, due to a combination of liquefaction and the permanent displacement of the fault. The owner reported having observed the ground “bubbling” and fountains of soil and water reaching about 1m above the ground. The owner reported a general settlement of ~30 cm in the area (although it was not clear how he had arrived at this value). House total settlement appeared minor relative to the soil, in line with expectations for a one-storey domestic structure, (Figure 5.5).



Figure 5.5. - Damage to a one-storey building in Lasoso due to differential settlement induced by liquefaction. Sandy ejecta in garden.

Opposite the dwelling in Lasoso was Masjid Iqra. This mosque had undergone severe liquefaction-induced damage, with ejecta clearly visible in the garden of the mosque. The mosque suffered large settlements (up to ~50 cm relative to surrounding land), and significant rotation of minarets (Figure 5.6).



Figure 5.6 – Left: Front of Masjid Iqra. Right: Masjid Iqra in Lasoso. Severe liquefaction-induced damage and tilting of minaret due to liquefaction beneath base.



Figure 5.7 -. Masjid Iqra. Failure of garden paving above sandy soil, and ejecta in background.

These examples were rather localised and many similar structures in the locality had not undergone such failures. It may be that strong shaking very close to the fault was notably stronger, such that only

soils above the fault experienced sufficiently strong shear stresses to liquefy. More likely is that the sandy soils across Palu are largely medium dense to dense – this information was noted by Dr Sukiman Nudin at Tadulako University - and as such far less likely to experience liquefaction. The suggestion is corroborated in part by data collected by Thein et al. (2014)- as part of their micro-tremor study of the city’s soils. Figure 5.8 shows their survey locations and corresponding shear wave velocity profiles along Line B through the city. This shows the profile at Lasoso (LSS, in orange) as having a shear wave velocity in the top 30 m $V_{s,30} \sim 180$ m/s. Sites further East appear to have greater values of shear wave velocity, with $V_{s,30}$ being 240 m/s – 300 m/s.

To give context to these values, Figure 5.9 from the study by Andrus and Stokoe (2000) shows the relationship between shear wave velocity (at the point where effective stress equals 100 kPa, typically approximately 5-10 m depth depending on water table) and the cyclic stress ratio, (which may be thought of loosely as earthquake “strength” and is closely related to peak acceleration). In this graph, it appears that soil at $V_s \sim 150$ m/s liquefies readily in modest earthquakes whereas soil at $V_s > 200$ m/s has very little history of liquefiability. Thus the majority of Palu’s soils are too stiff (and hence too densely packed) to liquefy. Only a few isolated places have soils with $V_s < 200$ m/s, which are able to liquefy.

The site of Great Mosque Darassalam (measurement MSQ, in red) was not visited by the team as there were no reports of damage, and the mosque appeared in good condition when viewed from surrounding areas. Therefore, despite the apparent lower $V_{s,30}$ shown in Figure 5.8b for site MSQ catastrophic failure of Great Mosque Darassalam was not seen, although closer inspection would have been instructive.

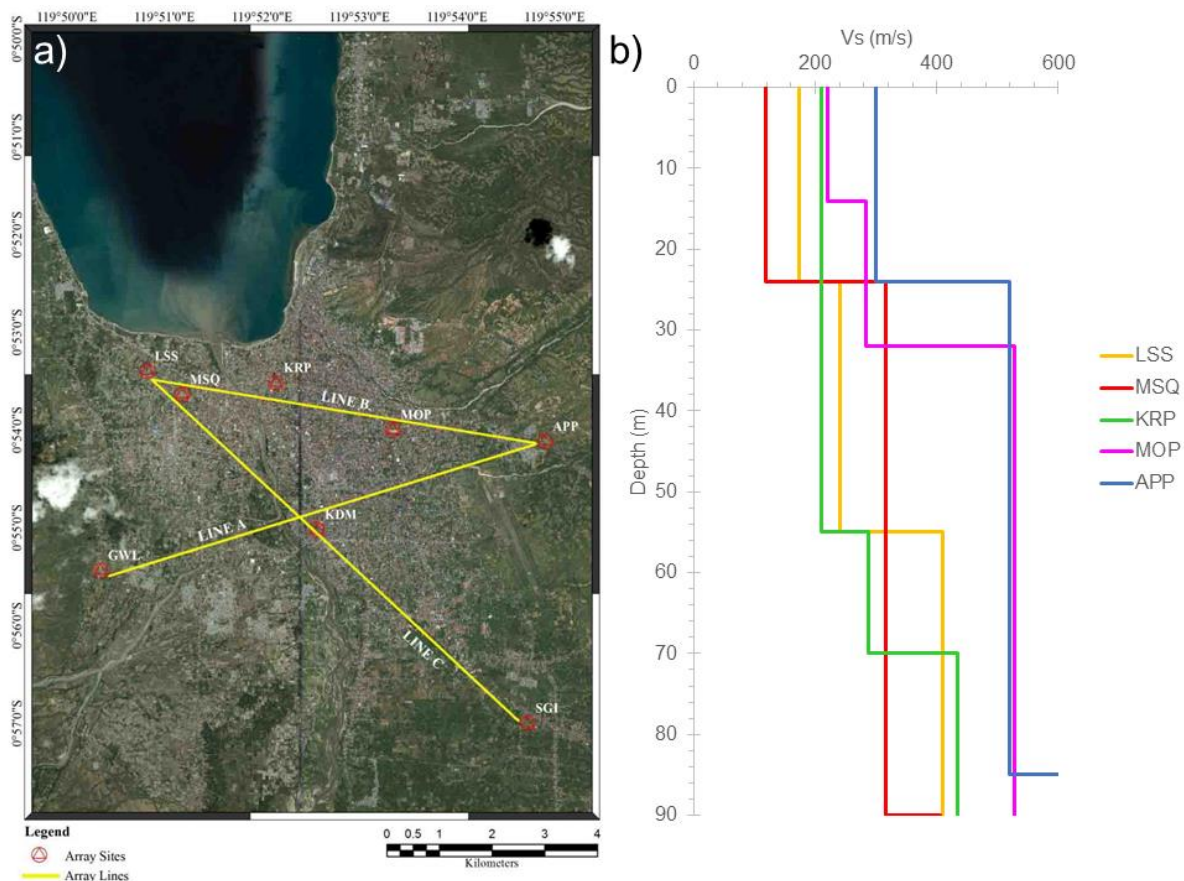


Figure 5.9 – Microtremor data for urban Palu reported by Thein et al. (2014) a) survey locations: LSS is Lasoso, MSQ is not the Masjid Iqra but rather the Great Mosque Darassalam Palu b) shear wave velocity measurements along Line B, redrawn for near surface soils following Thein et al. (2014)

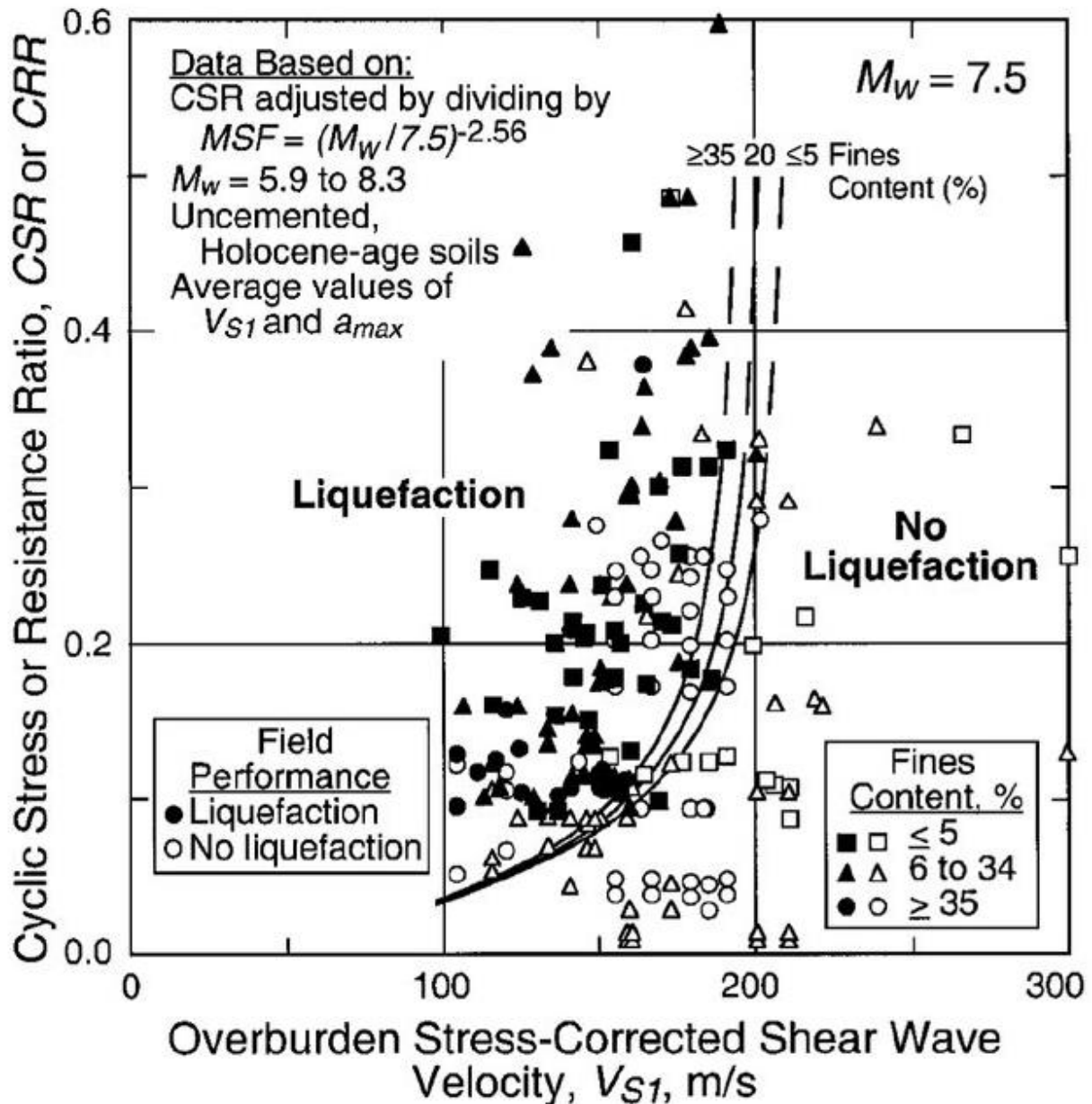


Figure 5.10 - Relationship between shear wave velocity and cyclic resistance ratio for sands, Andrus & Stokoe (2000)

5.1.2 Sigi

In Sigi, the liquefaction was rather more extensive, with differential settlements affecting many structures through the town, and sandy ejecta on the streets. Outside the town, the settlements had dropped the soil level to below the water table, and lateral spreading had opened large cracks in the ground, now filled with water (Figure 5.11). In the town, differential settlement beneath structures had resulted in structural failure. Evidence of lateral spreading – cracks perpendicular to slope contours – was observed (Figure 5.12), and the pattern of offsets being formed reappeared (Figure 5.13), similar to the seafront spreads at Lero, (see below).



Figure 5.11 - Settlement and spreading cracks outside the town of Sigi



Figure 5.12 - Differential settlement and ground disturbance in Sigi. Pipework in foreground appears to be new rather than uplifted.



Figure 5.13 - Large settlements with sandy ejecta adjacent to relatively unaffected soil in Sigi.

Ejecta was identified on the site and provisionally classified as a uniform sand (Figure 5.14), as has commonly been noted at historic liquefaction sites in other locations worldwide. The micro-tremor survey of Thein et al. (2014) included a site at Sigi in which (Figure 5.15) a clear low V_s (~140 m/s) surface layer of approximately 8 m thickness overlies more competent material nearer $V_s \sim 300$ m/s. Cross referencing again with the chart of Andrus and Stokoe (2000) (Figure 5.10) puts this near surface soil firmly in the “liquefiable” regime for all but the smallest earthquakes, in line with the observations.



Figure 5.14 - Ejecta at Sigi. Uniform sand, in damp condition.

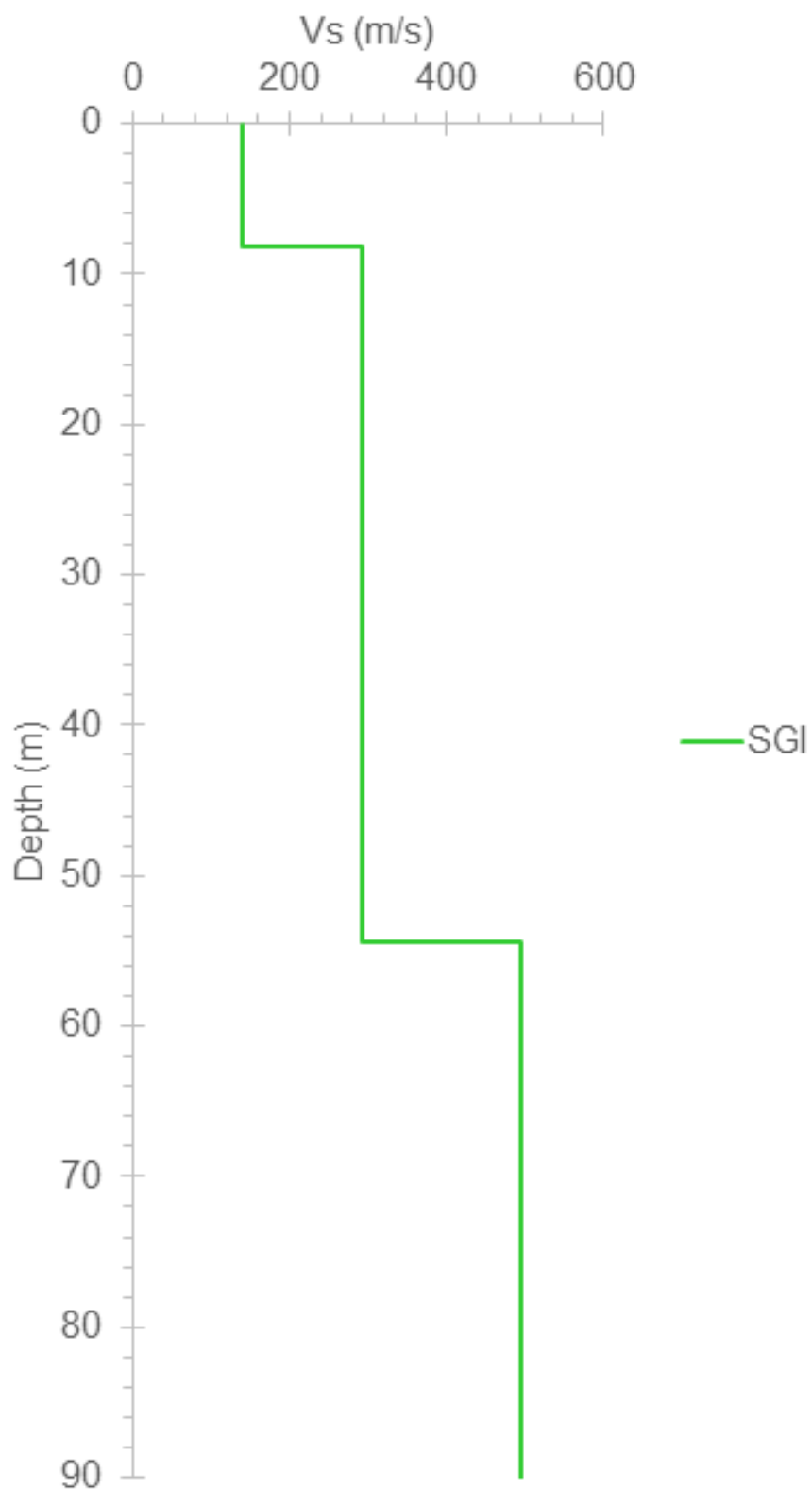


Figure 5.15 -. Data for Line C (see Figure 5.9a) for point SGI in Sigi. redrawn after Thein et al. (2014)

5.1.3 Donggala Dolphin Park

A final notable liquefaction site visited by the EEFIT-TDMRC Team was the Donggala Kota Wisata (Dolphin Park). Here, an area of land had been reclaimed in order to enclose an expanse of water for housing dolphins, (which were not, nor have ever been, present). Looking across the enclosure from the main road showed that the bridge on the far (seaward) side of the dolphin tank had been damaged, consistent with soil displacements and possibly liquefaction (Figure 5.16). Near the bridge, large cracks were found parallel to the coast consistent with lateral spreading in the land forming the seaward side of the tank (Figure 5.17), and large areas of the seaward side had collapsed into the sea. In parts, a piled wall had supported the land and acted as a seawall. This had now been displaced seawards and in places overturned (Figure 5.17 and 5.18). Exposures on the sea side (Figure 5.19) revealed that the relatively competent upper layers overlaid sandy material that may have been susceptible to liquefaction.



Figure 5.16 - View across dolphin enclosure to sea road. Slight damage to bridge abutments consistent with soil displacements, though bridge remains operational.



Figure 5.17 - Cracks parallel to coastline, consistent with lateral spreading of the ground.



Figure 5.18 - Failure of piled sea wall at Donggala Koto Wisata



Figure 5.19.- Soil layers exposed by lateral spreading at Donggala Koto Wisata.

5.2 Seafront Loss Due to Liquefaction

The team identified areas on both sides of Palu Bay affected by seafront loss due to liquefaction. The EEFIT-TDMRC observed this at Loli Tasiburi on the Western shore and at Lero on the Eastern coast. Anecdotal and map evidence suggested the problem occurred at a number of other locations particularly North of Lero, but this was not verified with ground inspection.

5.2.1 Loli Tasiburi

The road at Loli Tasiburi ran near the coast, through tsunami damaged/destroyed dwellings. Locals reported that large areas of coastline had broken off and fallen into the sea, with one indicating Palu, visible in the distance around a headland, which he reported had previously been obscured by the land (Figure 5.20). An eyewitness described the soil “bubbling”, and two large upwards spurts of water on the beach (at this point he ran for cover up the hill). The soil at the site was very gravelly sand (Figure 5.21), and black in colour. It was reported that “Tasiburi” means “black sand” in the local Kaili dialect.

The soil type and inevitable high groundwater level suggest liquefaction was a clear possibility, and the eyewitness reports are consistent with soil liquefying. The team concluded that liquefaction had therefore occurred in the coastal soil, and either the resultant large settlements were sufficient to submerge the coastal land or (more likely) lateral spreading has taken the shoreline into the Bay.



Figure 5.20 - Waterfront at Loli Tasiburi. Note the headland in the background which locals had indicated is now far shorter than before.

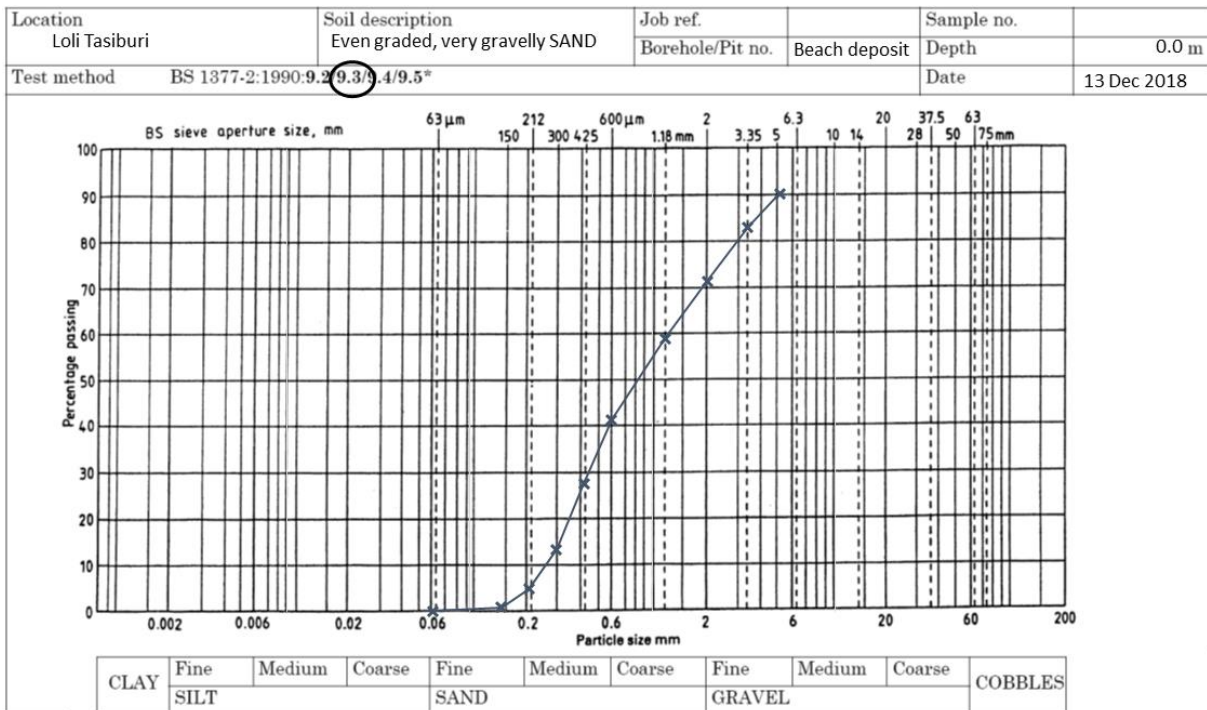


Figure 5.21 - Particle size distribution for surface soils at Loli Tasiburi

5.2.2 Donggala Town

North of Loli Tasiburi was the town of Donggala, with a small port. Further shoreline-reducing liquefaction was seen here, as indicated by the “bite” into the current land shape compared to the overlay of roads shown in Figure 5.22, which is taken from Google Maps. Figure 5.23 shows a photograph of the bay post-earthquake, first across the “bite” (Fig 5.23a) and secondly showing evidence of soil having displaced from beneath a heavy concrete structure (Fig 5.23b). This soil displacement may have occurred through liquefaction induced spreading, as seen in other places, although scour may also have played a part, especially if the soil generated excess pore pressures and was in a softened state at the moment of tsunami wave inundation.



Figure 5.22 - Aerial photograph of post-earthquake Donggala port, overlain by prior road map showing missing land around the estuary mouth.



Figure 5.23.- Photographs of Donggala Port, looking a) South East across the estuary towards the partially collapsed metal rooved storage houses b) detail beneath the concrete structure seen tilted on the South edge of the bay, showing evidence of soil having been displaced from beneath the structure.

5.2.3 Lero

At Lero, an estuary at the East side of Palu Bay, the team first identified liquefaction beneath a local school beside the main road (Figure 5.24). Here, ejecta remained and differential settlements had occurred under the school buildings (Figure 5.25). This showed that liquefaction had occurred in the town.



Figure 5.24 – Settlement in the road with sandy soil ejected through cracks.



Figure 5.25 – Differential settlement of School in Lero, with liquefaction ejecta in the yard

The land sloped down towards the beach (Figure 5.26), and large cracks parallel to the shore were observed South of the estuary (Figure 5.27 and 5.28), with some ejecta of a uniformly graded fine silica sand. According to local reports, the seafront road and seven dwellings had moved into the sea (Figure 5.29), experiencing both large settlement and lateral displacement consistent with liquefaction and lateral spreading.

Since the first draft of this report, subsequent publications have been produced by other teams. Amongst these, Widiyanto et al. (2019) have also identified the coastal loss at both Lero and in Donggala port identified in this report. These authors describe reported sudden drops in the surface level consistent with a soil instability. Sassa and Takagawa (2019) speculate that lateral movement of these break-offs may be a driving force for the main tsunami. From evidence examined by the EEFIT-TDMRC team, it would be hard to say what offshore movement might have been present without bathymetric data and an indication of slope into the bay. However, we would corroborate that these areas experienced significant downwards and outwards movements, and that based on observed evidence (ejecta, lateral spread cracks, presence of saturated sandy soils) and anecdotal evidence (observed high pressure fountains of water and soil) the driving force for this would almost certainly be liquefaction of the soil.



Figure 5.26 – Lero: View down towards the sea. The seafront had previously been the site of seven homes and a road.



Figure 5.27 – Lero: Cracks observed parallel to shoreline consistent with lateral spreading.



Figure 5.28 – Further cracks, and submerged land and palm trees, in Lero.



Figure 5.29 – More ground cracks at Lero, and view across the estuary towards a now submerged restaurant.

5.3 Summary

Liquefaction proved the principal geotechnical hazard, manifesting most notably as a factor in the mass movements described in Chapter 4. Only limited incidences of liquefaction – manifested as structure settlement and ejecta features - were observed in Palu city itself. It was noted that whilst saturated sandy soils made up much of the ground on which the city of Palu was built, these were in a medium dense to dense condition as evidenced by the shear wave velocity profiles obtained. This provides some evidence that V_s -CRR charts originating with Andrus and Stokoe (2000) that appear to show liquefaction to be near-impossible above $V_s \sim 200$ m/s provided a reasonable match to observed behaviour, as the sites of observed liquefaction correlated with the only soils identified to have a V_s lower than 200 m/s.

Outwith the landslides and the city, liquefaction was observed frequently around the coastline of Palu Bay in the form of spreading and subsidence of material into the Bay. This was observed in both natural coastal soils and made ground such as that found at the Dolphin Park. The village in Sigi Regency near the Jono Oge landslide was the main inshore site of “conventional” liquefaction damage, with widespread differential settlement and ejecta being observed.

6.0 Tsunami Investigation (Raby, A.; Robinson, D.; Rossetto, T.)

6.1 Tsunami terminology

When discussing tsunami and their inundation onshore, this report will use an adapted version of the terminology defined within Fraser et al (2013), shown in Figures 6.1 and 6.2.

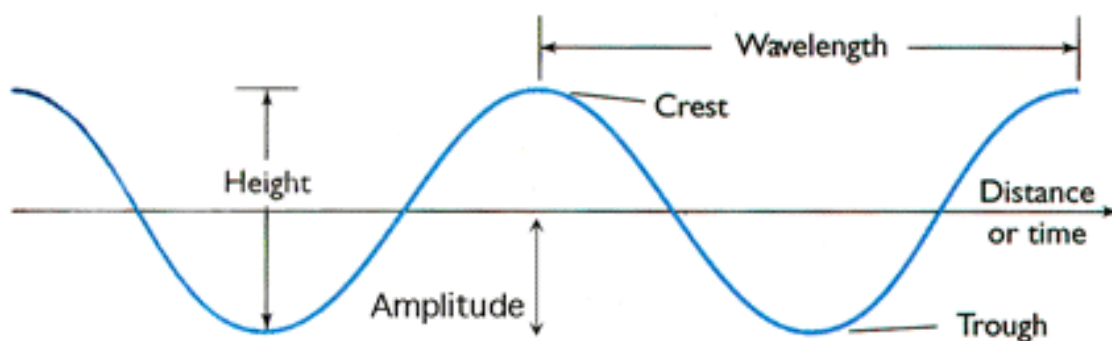


Figure 6.1 - Definition of offshore tsunami wave trace terminology

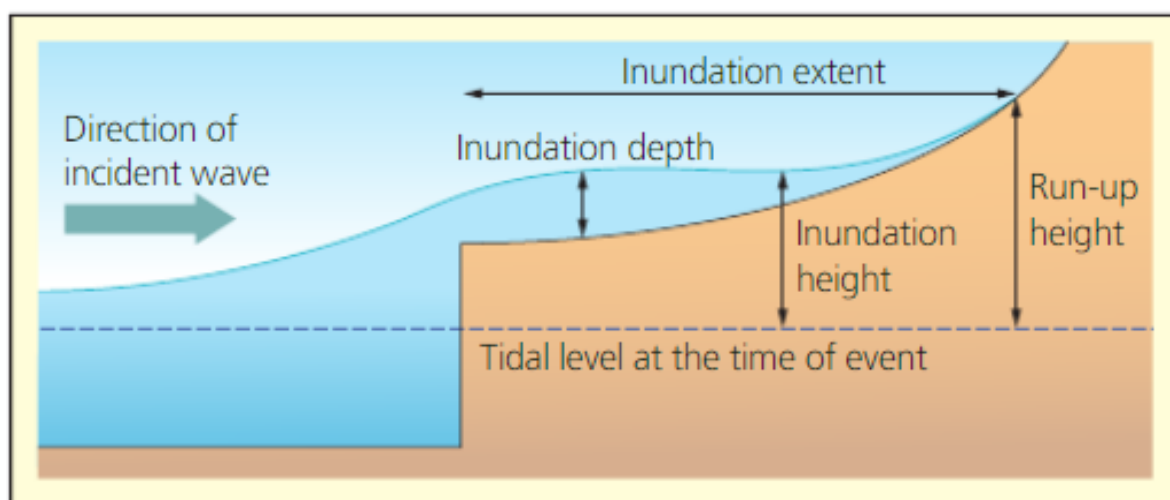


Figure 6.2 - Definition of tsunami inundation terminology (adapted from Fraser et al., 2013)

6.2 Past tsunami in the Palu Bay area

The central part of Sulawesi, where Palu Bay is situated, has experienced a number of significant tsunami during the twentieth century. Figure 6.3 and Table 6.1 present information gathered by Pelinovsky et al. (1997). These indicate a periodicity of the order of a few tens of years, with earthquake sources that are relatively local.

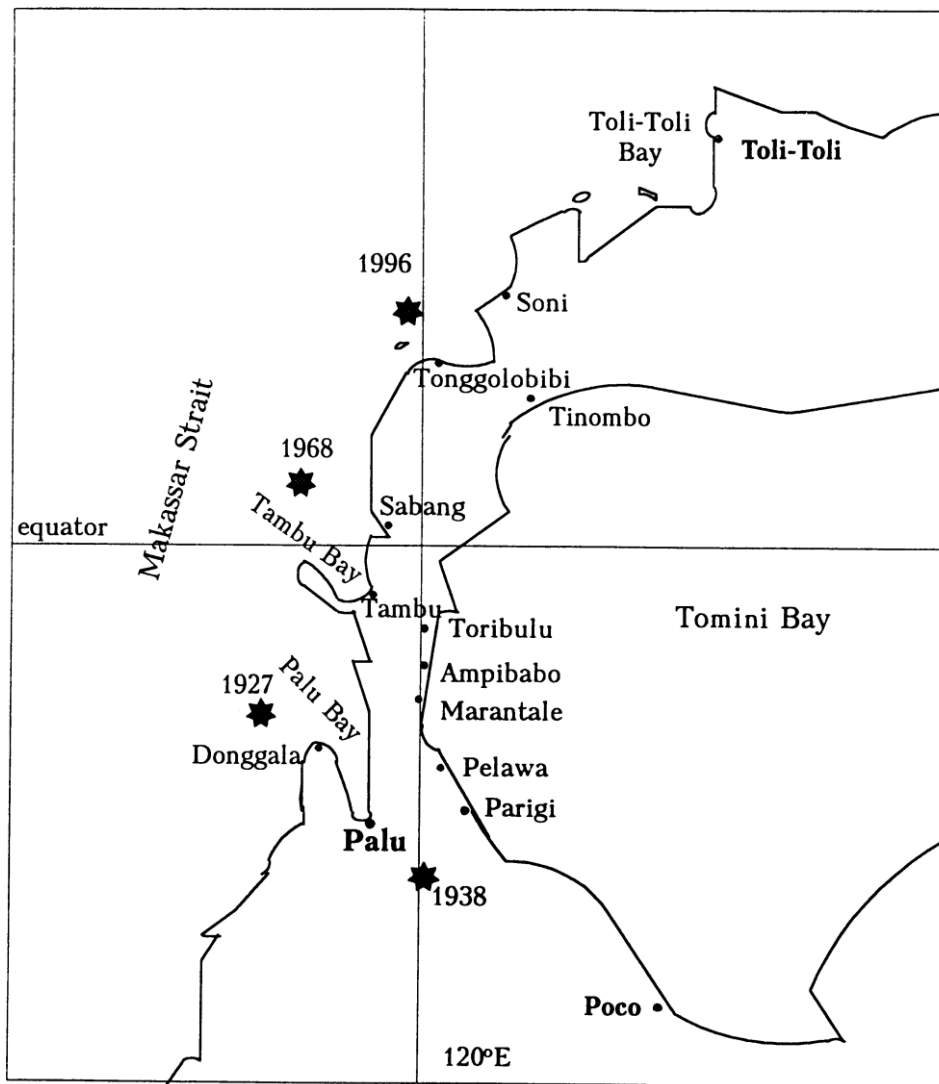


Figure 6.3 - Epicentres of the tsunamigenic earthquakes of 20th century in the region around Palu Bay (Pelinovsky et al., 1997).

Table 6.1 - Details of earthquakes and subsequent tsunamis in central Sulawesi (Pelinovsky et al., 1997)

Year	Date	Latitude	Longitude E	Magnitude M	Wave height (m)
1927	01.12	0.7° S	119.7°	6.3	15
1938	19.05	1° S	120°	7.6	3
1968	14.08	0.2° N	119.8°	7.4	10
1996	01.01	0.83° N	120.01°	7.7	3.4

6.2 The 28th September 2018 Tsunami and its characteristics

6.2.1 Cause of tsunami in Palu Bay

As described in Section 3.0, the 28 September 2018 event was a predominantly strike-slip earthquake. The relative movements of the plates in this type of earthquake are largely horizontal, and hence would not typically cause a tsunami, though due to the steep bathymetry of the bay (see Figure 6.4) it is not inconceivable that horizontal movement could displace water (STEER, 2019). Measurements from outside of the bay suggest that a tsunami originating from a location close to the epicentre would not have had time to reach the bay before the first waves were observed (Muhari *et al.*, 2018). There are a variety of causal mechanisms now suggested, amongst which are landslides triggered by the earthquake. This seems plausible given the number of observed sub-aerial landslides that occurred and some slides on the west of the bay that were seen to cause tsunamis (STEER, 2019). However, to date the location of a single submarine landslide of the size required to cause a tsunami of the size recorded has not been identified.

From observations made during the mission by the TDMRC-EEFIT Team, a further possibility is a combination of vertical fault movement under Palu Bay, combined with triggered submarine landslides. As mentioned in Section 3.0, it is possible that a step-over fault underlying the bay formed a contractional bend and resultant thrust faulting has led to vertical displacement of the sea bed. This was not proven by any of the bathymetric survey data available to the EEFIT-TDMRC Team at the time of the mission. However, a secondary tsunami source within Palu Bay might explain the short arrival time of waves seen in video recordings made from the Grand Mall in Palu City (Figure 6.8) and Wani (Figure 6.11).

An analysis of arrival times sourced from several video recordings at the Grand Mall was published by Takagi *et al.*, (2019). This analysis suggests a source approximately 5 km from the Grand Mall. Heidarzadeh *et al.*, (2019), performed spectral analysis of the Pantaloan tide gauge reading and found two dominant sources: one large 3.6-4.4 minute period wave, sourced 3.4-4.1 km from Pantaloan; and one smaller 10 minute period wave, sourced from 32.5 km from Pantaloan. A source approximately 3-4 km south of Pantaloan would also be approximately 5 km north of the Grand Mall.

Although Takagi *et al.*, (2019), assumed a landslide source, results from a coupled physics-based earthquake displacement model published by Ulrich *et al.*, (2019) instead conclude that the primary tsunami source may have been co-seismically generated vertical displacement occurring in approximately the same region. Jamelot *et al.*, (2019), conclude from the results of two heterogeneous earthquake models that the earthquake would have been able to trigger devastating water waves compatible with field survey reports at Pantaloan and at the southern tip of Palu bay. However, the authors do not exclude that coastal collapses contributed to the generation of destructive breaking waves very locally.

6.2.2 International tsunami surveys

In the few weeks preceding the EEFIT survey, a number of international teams visited Palu Bay, undertaking runup and inundation measurements. Figure 6.2 is an excerpt from the 16th November DG ECHO Daily Map from the Research Centre for Water Resources, using data prepared by Dr Leo Sembiring, of the Indonesia Ministry of Public Works (ERCC, 2018). It consolidates the measurements that had been made prior to the 16th November 2018 by teams from Indonesia, Japan, Turkey, Russia, Portugal, Italy and Austria. The first Japanese team arrived at the location very soon after the event (4th October 2018) and had to sleep outdoors due to the lack of available facilities (Muhari *et al.* 2018).

Evident from Figure 6.4 is that, in general, the inundation heights increase towards the head of the bay, with 7m inundation height consistently measured. Figure 6.5 provides an indication of what an inundation height of 7 – 8 m looks like. The left-hand image is a photograph of a team member standing against an advertising board at the southern tip of the bay, (Jalan Taman Ria, Balaroa, 0 53' 1.6" S 119 50' 53.4" E), alongside 3 frames taken of the same sign (rear side) during the tsunami. Obviously, some of the wave is highly aerated so it does not have the same force as green water loading.

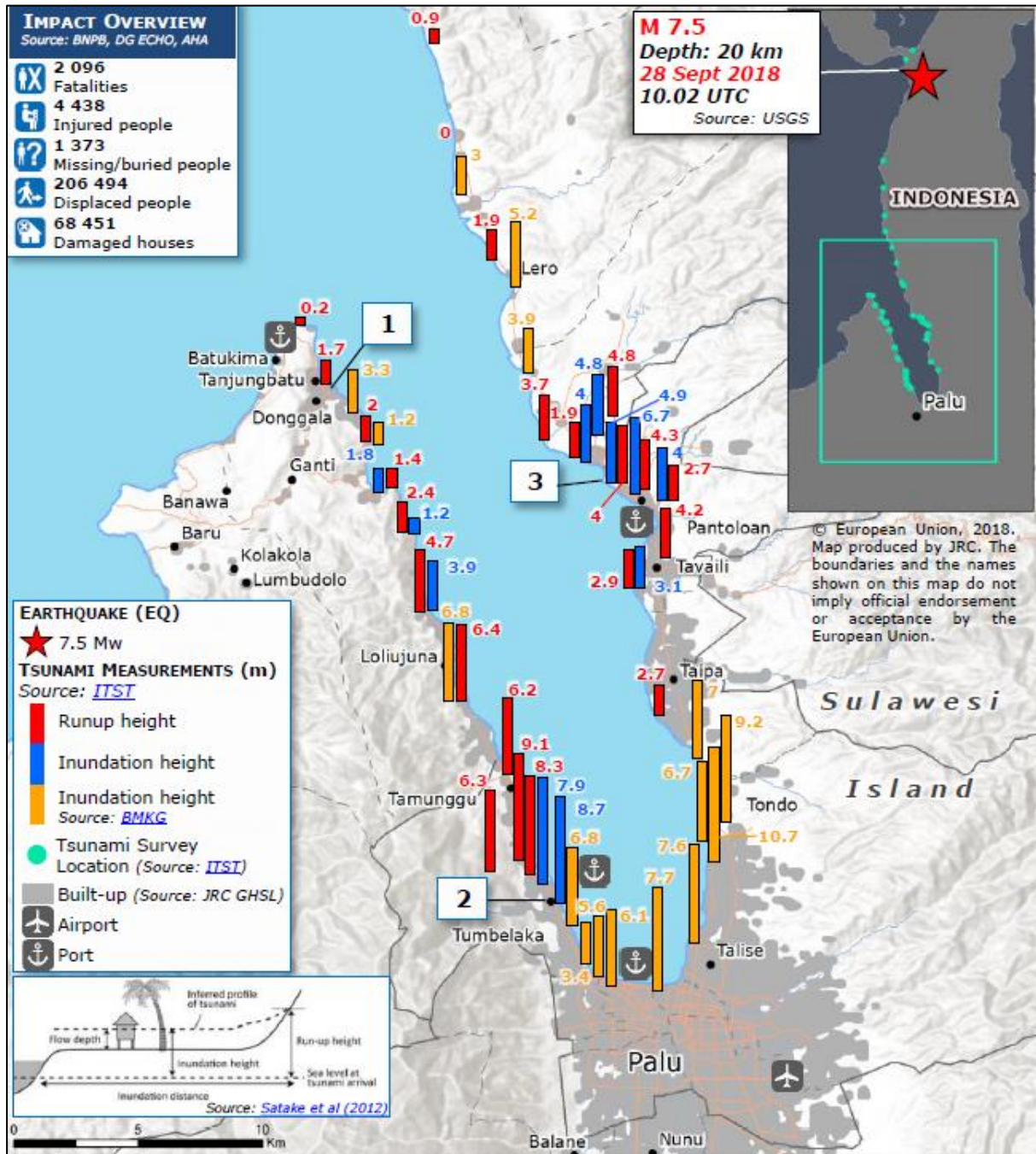


Figure 6.4 - Measurements of tsunami inundation heights and runup (see definition in Figure 6.2) measured by International survey teams as of 16 November 2018 (ERCC, 2018).

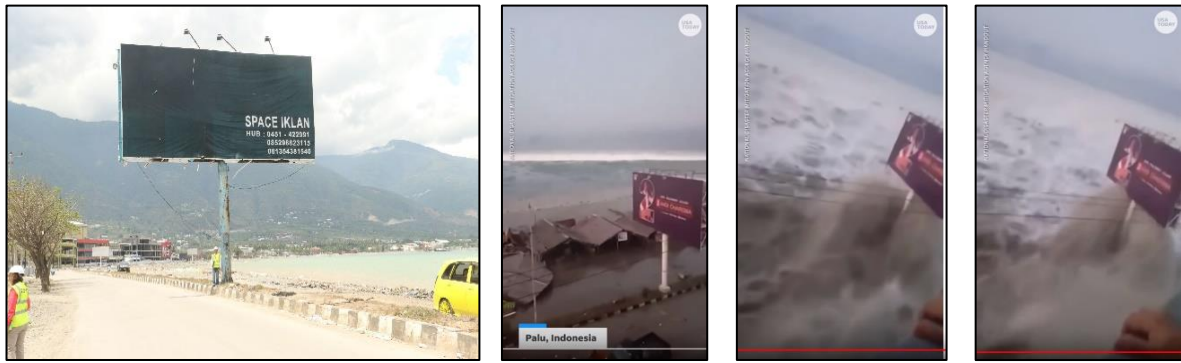


Figure 6.5 - Tsunami inundation at Jalan Taman Ria, Balaroa ($0^{\circ} 53' 1.58'' S$ $119^{\circ} 50' 53.42'' E$).

6.2.3 Tsunami characteristics

The shape of the bay clearly influences the tsunami inundation height and runup, so it is instructive to consider the Palu Bay bathymetry. Figure 6.6 is a fairly low-resolution contour map of Palu Bay's bathymetry, as known before the 28th September 2018 event. Notable is that the sides of the bay are extremely steep. There are maximum depth contours of 700 m only 4 km from the shoreline in places. The depth and steepness of the bathymetry are related to the occurrence and type of wave breaking, respectively. The type of wave breaking can be predicted for periodic waves propagating on a plane beach using the Iribarren number, which relates the beach steepness to the offshore wave steepness (Battjes, 1974). When beach slopes are gentle, waves are more likely to form spilling breakers. For steeper beaches, there will be an increase in the occurrence of plunging breakers. For the steepest beaches, some waves will form collapsing or surging breakers. In many interviews around the coastline, people reported that the main tsunami was a plunging wave. Tsunami often arrive with broken fronts, or as bores, but they rarely steepen sufficiently to form plunging breakers at the shoreline. Another notable observation was that a number of waves were reported (in some locations up to five). These reports consistently describe the second or third waves as being the largest.

Whether the tsunami was crest or trough-led seemed variable, at least if survivor observations are assumed to be accurate. For example, at Wani, on the east coast of the bay, a man had been standing in the water along the shoreline, up to his knees. After the earthquake stopped he reports that the water depth increased to waist depth, suggesting it was crest-led. However, at Loli Tasiburi Banawa on the west coast of the bay, the tsunami was described by eye-witnesses as trough-led. The only measurement of the tsunami was made by a tide gauge at Pantaloan Port (on the east coast), see Figure 6.7. This tide gauge reading suggests a very small crest followed by a much larger trough (measuring ~ 6.74 m at 18:08), followed by a crest (measuring ~ 10.55 m at 18:08) (Valkaniotis et al., 2018).

It needs to be borne in mind that some of the tsunami waves, as described by eye-witnesses, may have been generated very locally, immediately following liquefaction and subsidence of the shoreline (with this phenomenon being fairly extensive along the Palu Bay coast, as mentioned in Section 5.0). In the latter cases, to some extent the tsunami at that locations would have been a 'backwash', (i.e. water travelling seawards from the land), a characteristic not reported previously.

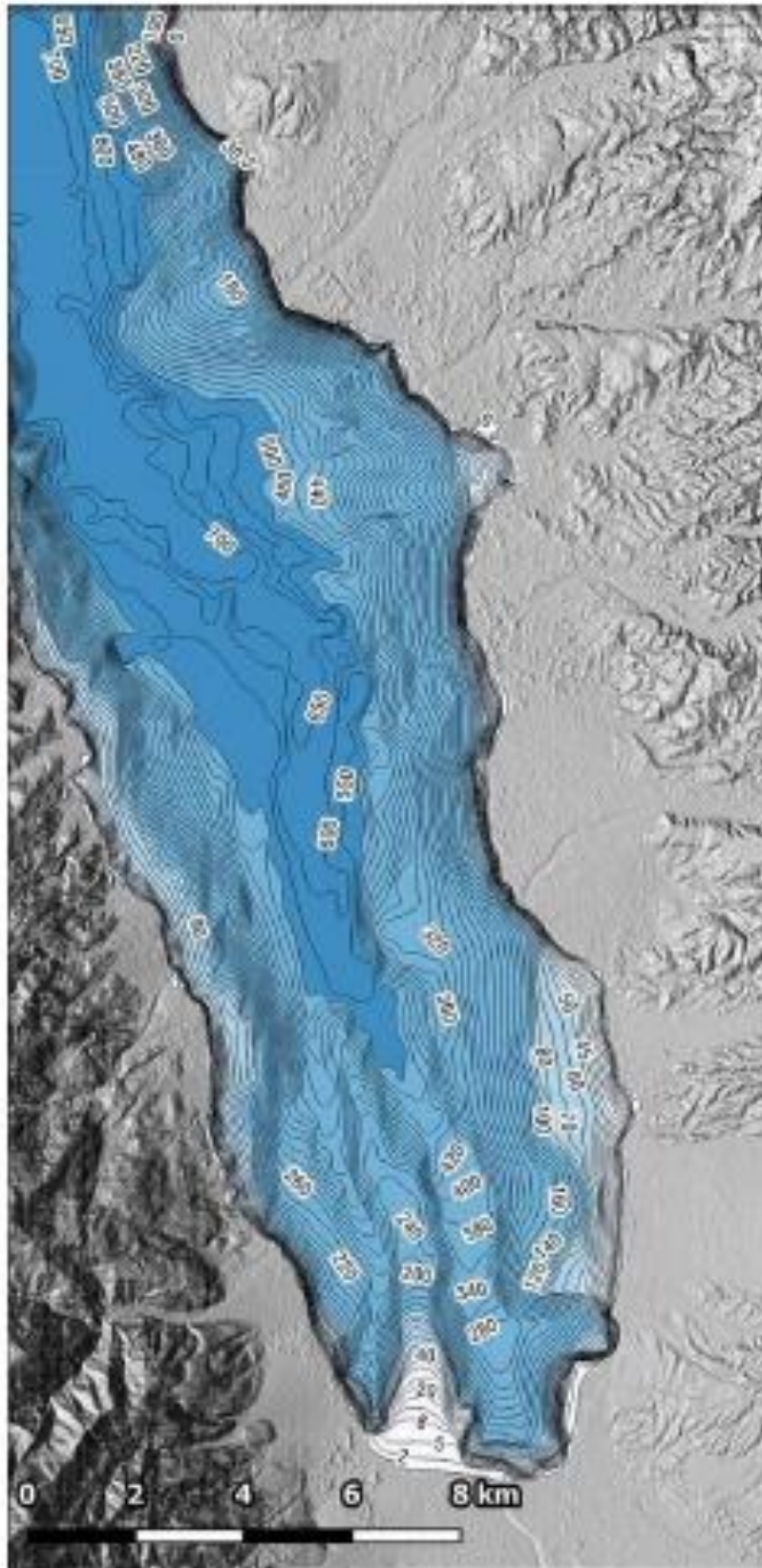


Figure 6.6 - Badan Informasi Geospasial Contour map of Palu Bay before the earthquake, Retrieved from <https://cloud.big.go.id>. Accessed 30 Oct 2018.

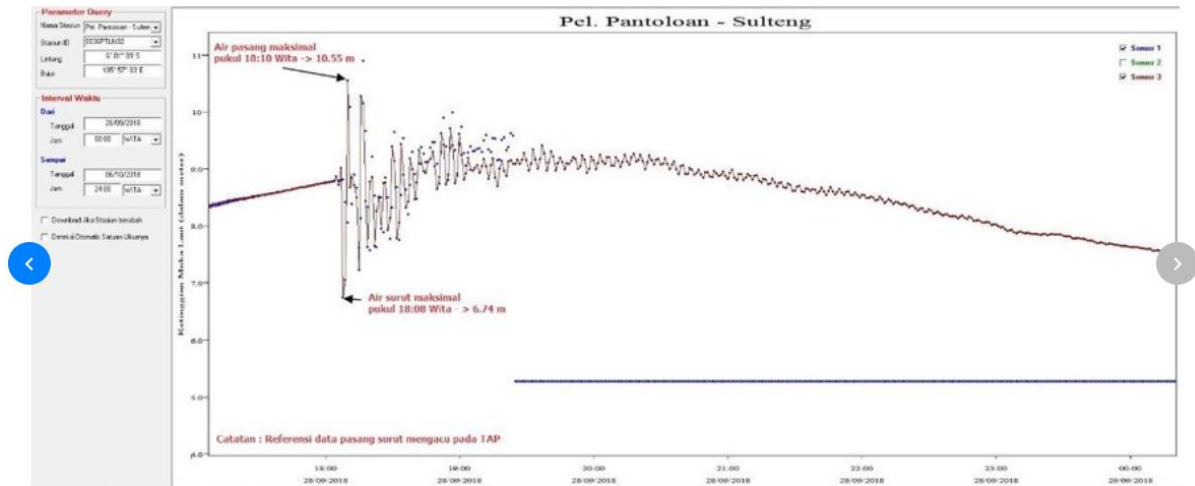


Figure 6.7 - Tide gauge data from Pantoloan Port (Valkaniotis et al., 2018)

Those people unfortunate enough to have been caught up in the wave described it as being ‘black’ and ‘itchy’. Black waves with white crests were also reported by some. This blackness could indicate suspended sediment or debris. Other observers just south of Mambo, describe seeing waves coming from different directions and interfering with each other. Figure 6.8 shows a sequence of frames from a YouTube video that shows what was seen of the waves from the Palu Grand Mall. In the top left frame, the first breaking tsunami wave is seen along the shoreline.

At this time traffic is still driving along the coast road, and pedestrians are apparently unaware. In the next frame shown, the camera operator points out much larger breaking (plunging) waves coming; the top right frame shows 5 individual waves travelling towards the coast. The effects of the waves that have inundated the shoreline are seen in the bottom three frames: shoreline buildings have been lifted off their foundations and vehicles have been caught up in the flow.

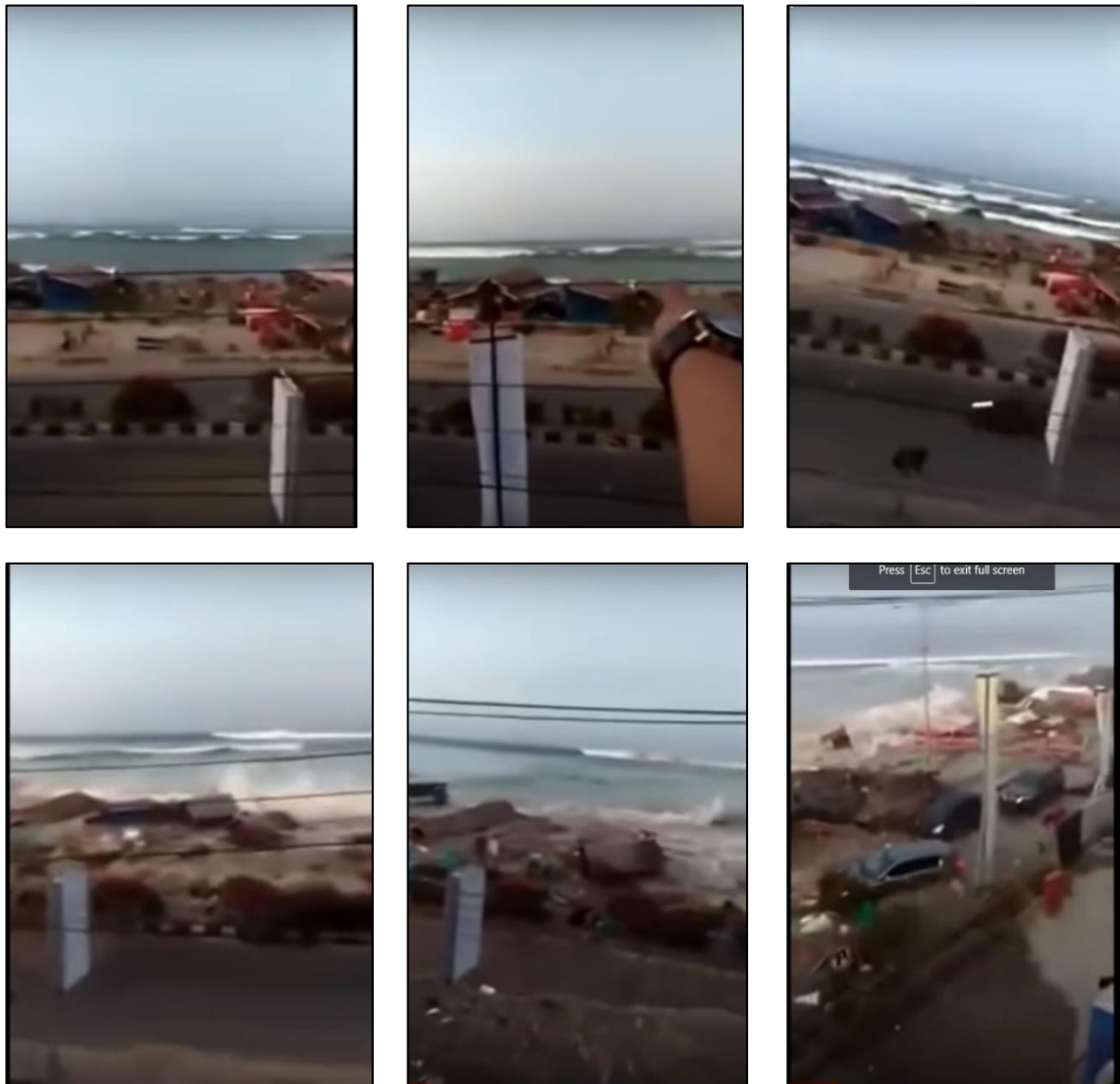


Figure 6.8 - Frames of YouTube video recorded from the Palu Grand Mall car park (https://www.youtube.com/watch?v=rCQ_hPZF1bM). The earthquake occurred at 18:02:45 (UTC+8) and several waves were seen to arrive from multiple directions between 18:08:15 and 18:10:49, Takagi et al (2019).

6.3 General tsunami observations obtained through interviews and video footage by TDMRC-EEFIT Team

The TDMRC-EEFIT Team visited several locations along the Palu Bay coastline, conducting tsunami damage surveys and interviewing local people. General observations of the tsunami made at three locations along Palu bay, as shown in Figure 6.9, are presented here.

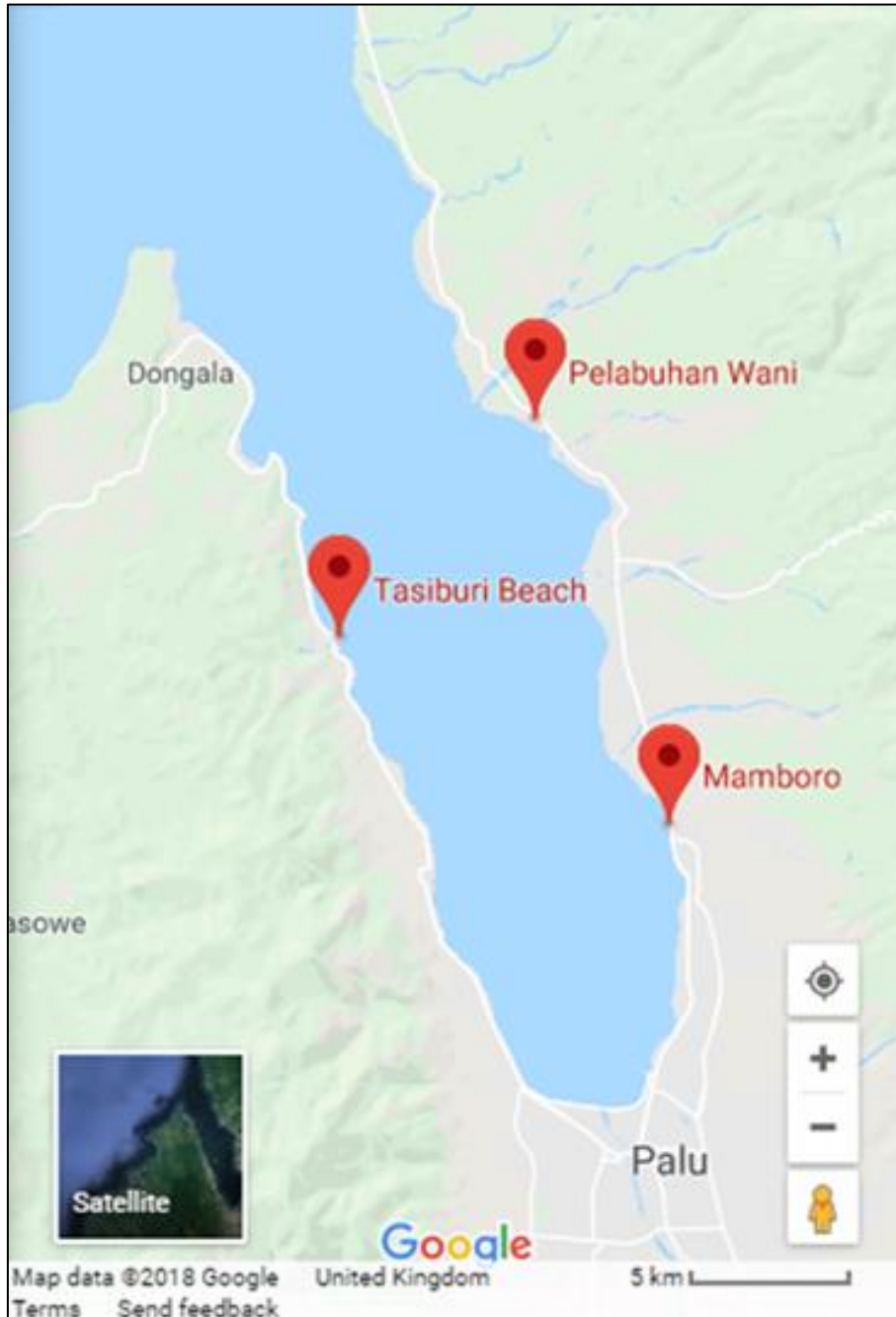


Figure 6.9 - Location of the observations presented

6.3.1 General tsunami observations from Wani

Wani is a town on the east coast of Palu Bay that suffered considerable damage due to the tsunami, (see Figure 6.10), and was made famous as the location of a household CCTV footage that showed the effect of the earthquake followed three and a half minutes later by the tsunami (Figure 6.11). The Team identified the house at which the CCTV was recorded (coordinates: 0 41'38.532" latitude; 119 50'31.422" longitude), and from comparison of measurable features of the house that were visible in the video, estimate the maximum inundation depth (above grade) at the site of the house to have been around 1.2m.



Figure 6.10 - Wani village on the east coast of Palu bay which experienced considerable damage



Figure 6.11 - Video frames at 18:03:01, 18:06:29, 18:06:30, 18:06:36 and during the EEFIT mission. Notice the mopeds have fallen over, following by the bore-like tsunami about 3 minutes later. This short arrival time supports the argument, discussed in Section 6.2.1, for a secondary tsunami source within Palu Bay.

Whilst in Wani, at the location shown in Figure 6.12 (left), the Team heard the dramatic account of a man who saw the water coming out of the ground during the earthquake so got into his car to pick up his wife and mother. Having got into his car, the man only had time close the window, before he felt water rise up to his knees. It then went dark due to the wave, then light again. The car stopped and he broke the window to climb to the balcony of the house shown in Figure 6.12 (right). Whilst he was at top of the rear stairs he heard the next wave and the sound of debris. He then saw a fast-flowing stream of water and people screaming for help. After the water receded he was reunited with his wife and mother.



Figure 6.12 - Location (left) and photograph (right) of the house where the man in the car ended up at around 50 m inland from the sea

6.3.2 General tsunami observations from Kampung Muara near Tasiburi

According to eye witnesses several earthquakes occurred that day, but the community only evacuated for the last one as the water looked strange; “it was ‘boiling’”. The earthquake had a duration of about 30 s. Then 25 s to 30 s later the first of the three waves, followed 20 s later by the second and third waves (separated from each other by about 1 minute).

A coastal landslide occurred shortly after the earthquake, creating local tsunami at the river mouth and with subsequent land subsidence causing a number of houses to collapse into the sea. The cross-shore profile of shallow water bathymetry reveals the depth, suggesting the size of the landslide. Figure 6.14 is an annotated YouTube video frame showing the wave rundown which reveals the cliff-like structure on the seabed, presumably following a submarine landslide.

Observations and interviews provide an unclear picture of what exactly happened in this area. The “boiling water” could be consistent with liquefaction of submarine soils in shallow water depths, that might then have produced a landslide. More plausible is that a wave could have been triggered by the land masses shifting into the sea.

Figure 6.15 shows a hand-written list of casualties in Kampung Muara, stating that 22 adults and 19 children died in the area, with 6 adults and 6 children still missing at the time of the mission.



Figure 6.13 - Photos of TDMRC-EEFIT Team interviewing locals and recording a piece for the mission video blog.



Figure 6.14 - Youtube video frame indicating wave rundown and the sharp change in bathymetry following a submarine landslide.

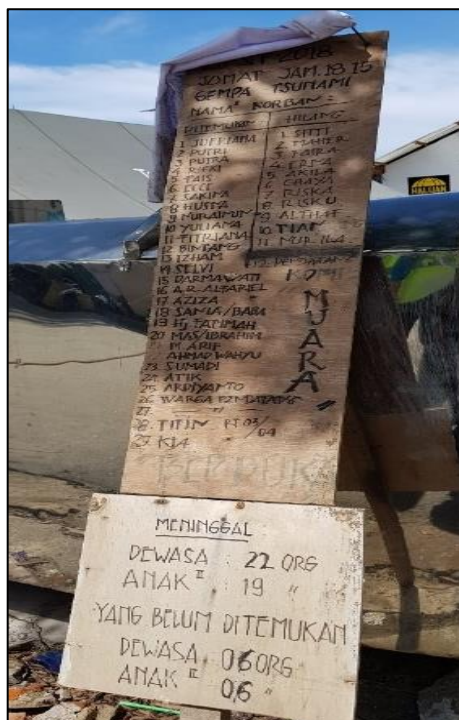


Figure 6.15 - List of dead and missing at Kampung Muara

Close by, in Labuhan Bajo (Figure 6.16), according to the eye-witnesses the first wave was clear foam, only ankle depth and the second and third came up to midriff. The first wave had a period of just seconds, and the second and third wave occurred in rapid succession, about 10 minutes after the first wave. This separation in time between the first wave and the following two, together with their different appearance, is possible supporting evidence for their being two separate tsunami sources, as discussed in Section 6.2.1.



Figure 6.16 - Damage in Labuhan Bajo.

6.3.3 General tsunami observations from Mamboro

In Mamboro a tropical fish fisherman was very keen to be interviewed by the TDMRC-EEFIT Team (Figure 6.17). He reported that he was swimming about 400 m along the shore to the north, in a water depth of about 3 – 4 m. During the earthquake he sensed a current which made it difficult to swim, so got out of the water. When he looked across the bay he saw the white water of a breaking wave. On the nearshore side the water receded by about 30 m, then the 1st wave came in. It was only gentle but came into the house.

He could then see a 2nd wave coming so told his family to evacuate. He wanted to stay to watch the wave but then decided to go inland. However, he spotted an 11 year old boy by himself and so ran back towards the sea to rescue him. He reached the boy but they were both knocked onto their backs by the wave. The 3rd wave was not quite as strong as the 2nd, and the 4th and 5th waves were smaller still. There was only about a minute between waves. The boy could not walk for 14 days afterwards because of blisters/puncture wounds.



Figure 6.17 - Interview being conduct with the tropical fisherman who was swimming in the sea when the earthquake occurred

6.4 Tsunami Inundation Observations

6.4.1 Tsunami inundation inland

The horizontal extent of the tsunami is regarded to be modest, which is indicative of a landslide generated tsunami i.e. one with relatively short wavelength (Buldakov, 2013). The team investigated inundations along a transect along a southerly direction i.e. from north to south. Three locations are indicated in Figure 6.18, then described in Figure 6.19.

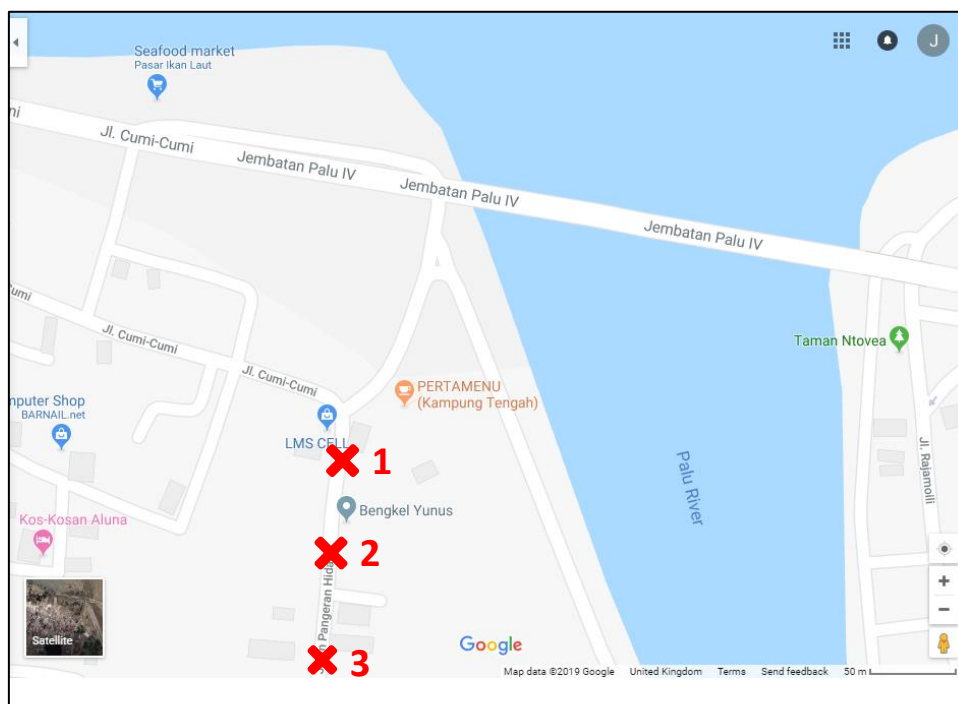


Figure 6.18 - Locations 1, 2 and 3 where inundation was observed and described below

The left-hand column of Figure 6.19 shows Google Streetview scenes from before the earthquake/tsunami and the right hand column show the same locations captured during the TDMRC-EEFIT mission. North of Location 1 (Figure 6.18), there was severe devastation and damaged structures had already been cleared. The first row of Figure 6.19 corresponds to Location 1 looking westwards, surrounded by ornamental walls and a gate. There was simply no sign of the house when we visited. Also, at Location 1 but looking eastwards, the timber structure with rusty steel roof evident from Google Street-view had also disappeared, but the neighbouring house seemed largely unaffected. The photographs at Location 2 which are shown in the third row of Figure 6.19, about 50 m further south, illustrate the care with which vertical inundation needed to be established, as the pre-tsunami photograph shows a significant discolouration line which is due to rising damp, common in that area.

Only by obtaining additional clues *e.g.* from a faint black line on the white timber door can an accurate level be ascertained. The fourth row of Figure 6.19, corresponds to Location 3 facing westward, a further 50 m or further south, which revealed a watermark on a set of metal gates, protecting a house which seemed unaffected. Finally, the bottom row, also at Location 3 but looking eastwards, shows remediation work that has been undertaken. Here, a wide, sloping kerb had been constructed right up to the timber doors. Enquiries at that location solicited the fact that due to local coastal subsidence the high tides were reaching the same extent as the horizontal inundation of the tsunami, so this protective kerb had been erected to address on-going flooding issues. This new flooding hazard was apparently also bringing crocodiles into Palu.

Location 1, looking westward



Location 1, looking eastward



Location 2, looking eastward



Location 3, looking westward



Location 3, looking eastward



Figure 6.19 - Evidence of inundation and the respective effects: (Left column) Pre-earthquake/tsunami images from Google Streetview (Right column) EEFIT observations at same locations Descriptions of each location are provided in the paragraph above.

6.4.2. Tsunami inundation along Palu river

In contrast to another EEFIT mission to Japan in 2011, the tsunami did not evidently travel up the Palu river, despite its considerable height at the southern end of the bay. Considering the substantial building damage seen at the shoreline near the mouth of the river, one would expect to see building damage continued some way upstream along the river, on the riverbanks. It was verified by visiting the neighbourhood on the west side of Palu river, just inland from the coast, that there was no damage. Eyewitnesses also said they just saw boats bobbing up and down but no significant overtopping of the river wall (Figure 6.20) close to their house. It is probable that there was a mitigating effect on the tsunami from the collapsed Palu Bridge IV (Figure 6.21). The bridge collapsed during the ground shaking, and fallen bridge deck is likely to have acted as a barrier to the tsunami, mitigating its effects on the river.

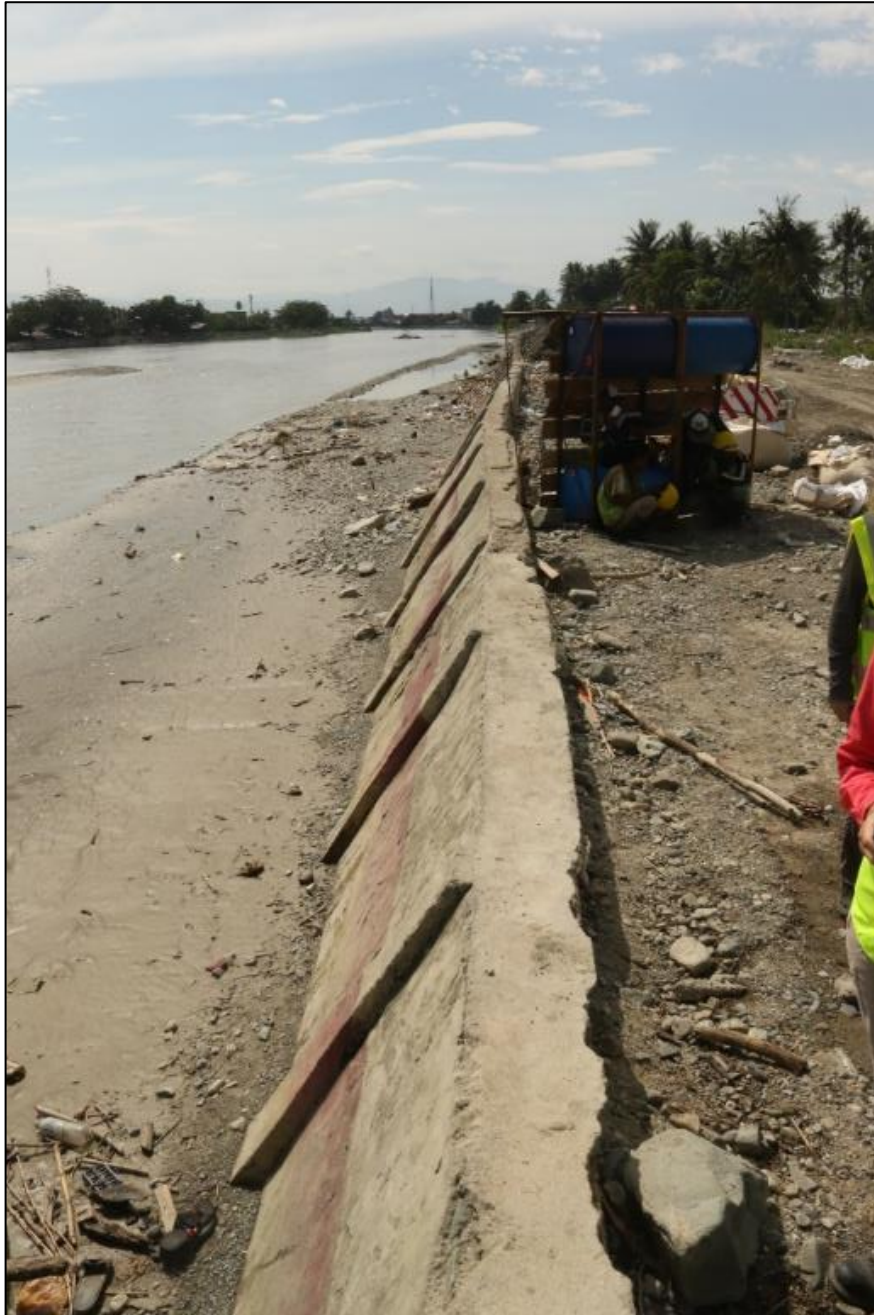


Figure 6.20 - Concrete river wall near entrance to the Palu river



Figure 6.21 - Submerged bridge deck of the Palu Bridge IV which may have acted as a submerged breakwater to the tsunami waves, preventing them travelling up the river

6.4.3 Sheltering effects

Evidence of assets and vegetation sheltering housing from the tsunami inundation were evident in a few of the locations surveyed.

To the south of Mambo, on the east side of Palu bay, inundation depths of around 1m were visible, which is much lower than elsewhere. Damage due to the tsunami was highly variable along a transect from the shoreline, travelling inland, due to sheltering effects and construction types. A man interviewed at this location talked about an upturned boat, a container and truck providing some level of protection to the houses behind, limiting inundation. The building closest to the shore that had survived, was a large masonry structure that appeared largely undamaged, possibly due to this protective effect. However, immediately inland of this house, there had apparently been a wooden house which had been destroyed, even with this limited inundation depth. It should be noted that wooden structures are known to be more vulnerable than masonry structures in tsunami flow and that the wooden house would be expected to experience greater damage than the masonry one, even for the same flow conditions.

Mangroves are native to Indonesia, and in some locations were seen to provide some limited protection from the tsunami inundation. Mangroves in Labuan Bajo were said to have provided some protection to some poor quality 1960s housing (Figure 6.22), locally resulting in no damage.

According to our Indonesian team members there is some desire to convert areas of mangroves to palm oil production, and mangroves are being also cut down for use as temporary props and scaffolding in construction projects. However, evidence on the ground was more positive, with new mangrove plantations and a mangrove park for tourists observed (Figure 6.23).



Figure 6.22 - (top) Poor quality 1960s housing in Labuan Bajo that has been sheltered by a large area of mangroves at the shoreline. (below) A map showing the position of the building within the port, behind the large green area of mangroves



Figure 6.23 - Mangrove plantations to the west of Palu bay: (Top row) Newly established mangrove plantation (Bottom row) Tourist park dedicated to mangroves.

6.5 Tsunami warning and evacuation

The Indonesian tsunami early warning system was designed as a partnership between Indonesia and Germany, in response to the 2004 Boxing Day tsunami. The partnership created a large database of numerical modelling results of possible tsunami inundation scenarios, assuming a range of earthquake epicentre locations and magnitudes. The system uses the database of pre-calculated tsunami scenarios, together with live tide gauge data, (see Figure 6.24), to give real-time inshore inundation estimates.

A tsunami warning was issued at 17:07, but because of the recorded 0.06 m tsunami at 17:27 at the Mamuju tidal gauge, which is located approximately 180 km from the epicenter, the tsunami warning was cancelled at 17:36 (European Commission, 2018). The Pantoloan tide gauge inside Palu Bay recorded a wave height of 3.81 m, but this information could not be sent to headquarters because of a power cut (UNDRR and UNESCO-IOC, 2019).

Eye witnesses that the Team interviewed were aware of tsunami hazards and seemed to rely upon self-evacuation. On 28 September there had been a number of earthquakes but the one that occurred at 17:02 was by far the largest. At Loli Tasiburi Banawa the eye-witness reported that he had only evacuated following the large earthquake event and when they saw ‘boiling water’ (liquefaction). In Figure 6.25 a TDMRC-EEFIT Team member is indicating a typical evacuation route close to where we conducted the interview. There is a small pedestrian thoroughfare with vegetated higher ground just beyond. Most of local villagers at Kampung Muara and Labuhan Bajo immediately ran uphill across the coastal road following the earthquake.

In Mamboro there was some appreciation of past tsunamis *e.g.* 1938, which informed their instinct to evacuate. This appreciation of the older events mostly came from the younger generation in the family

group that we interviewed. In Wani instead, evacuation was triggered by the shouts of an elder of the village who had been standing in the sea near the shore at the time of the earthquake ground shaking, felt a strong current in the water, and raised the alarm.

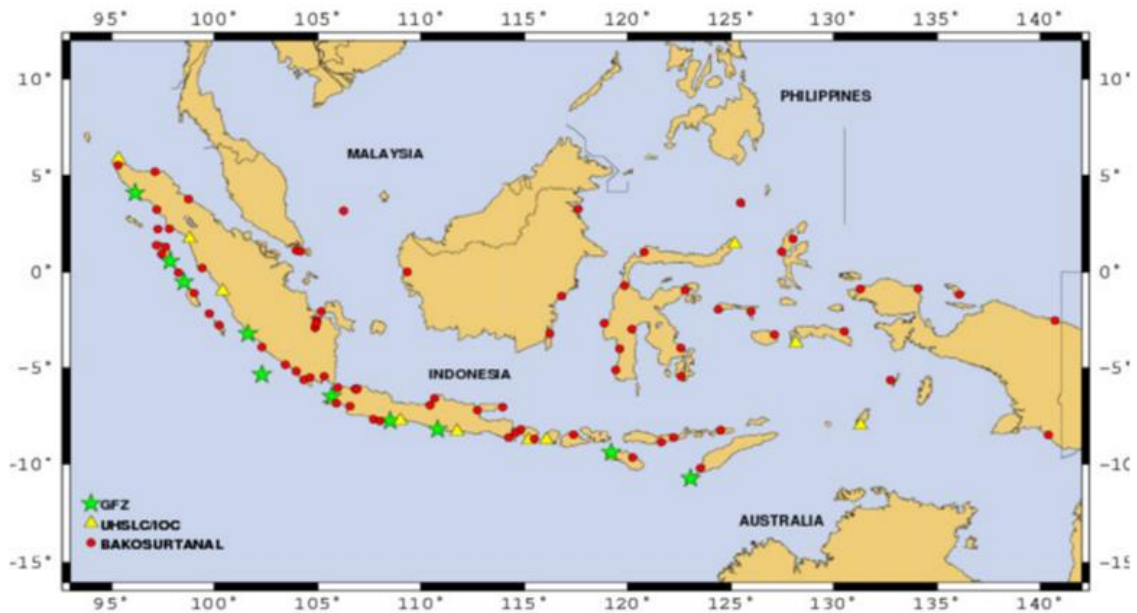


Figure 6.24 - Tide gauges installed in Indonesia by German, US and Indonesian organisations (Lauterjung and Letz, 2017)



Figure 6.25 - EEFIT member indicating a typical evacuation route inland from the main road through Loli Tasiburi Banawa.

6.6 Summary

The tsunami generation mechanism was not established at the time of the EEFIT survey, with many theories circulating and surveys being conducted. During our visit, extensive bathymetric surveys were taking place but not able to scan the seabed to full depth, given very steep bathymetry down to 700 m depth in the bay. At the time of writing the report, there are still multiple tsunami generation theories comprising combinations of seismic and landslide sources.

We noted that survey teams were regulated by the Indonesian authorities to an extent not witnessed before, perhaps not surprising given the large number of international teams.

Inundation heights of ~ 7m were evident at the head of Palu Bay and unusual reports of plunging type wave suggesting landslide generation. Tsunami inundation was observed to be affected by distance from shoreline, building type and sheltering effect of neighbouring buildings.

Eye-witnesses described seeing both crest and trough-led waves. They also described the effects of the earthquake, the subsequent tsunami and had even been caught up in the tsunami. They provided helpful observations that substantiated liquefaction theories.

Finally, no formal tsunami warnings were provided, but lives were saved due to self-evacuation: people had gained knowledge from previous events, where ground-shaking was associated with tsunamis.

7.0 Observation of Impact on Buildings and Infrastructure (Rossetto, T.; Adhikari, R.; Idriss, Y.; Raby, A)

7.1 Damage Scale and Survey Sheet

As a result of the Central Sulawesi earthquake and ensuing tsunami, many buildings within the tsunami inundation zones were also damaged both by the earthquake ground shaking. The assessment of these buildings by EEFIT-TDMRC therefore required the development of a new damage scale and survey form, which could be used to capture both the damage mechanisms typical of ground shaking and those of tsunami. Such an approach provides a consistent evaluation of the damage for both hazards. An alternative approach would have been to adopt separate and different damage scales, chosen from the literature, for the evaluation of damage to buildings affected predominantly by one or other of the hazards. This approach was not followed as the Team wanted to be able to compare damage from the two hazards, and be able to capture damage in buildings affected by both hazards.

The developed damage scale is presented in Table 7.1 and is based on the European Macroseismic Scale 1998 - EMS 98 (Grünthal 1998), the Japan Cabinet Office (2013) damage scale used for evaluating tsunami damage after the 2011 Tohoku tsunami, and the damage scale developed by EEFIT for the 2004 Indian Ocean Tsunami reconnaissance (Rossetto et al. 2007). The damage scale has 5 damage states, referred to as DET0 to DET4, which range from no damage to collapse, and which are described for 4 different structural types. The damage state equivalence with EMS 98 is also shown in Table 7.1.

A damage survey form should be designed to aid the surveyor capture all the essential information on the structure being assessed, i.e. location, building characteristics that affect structural vulnerability to a hazard, and damage state. However, the form needs to be short enough to be completed in a few minutes, in order to allow for the survey of many buildings. For the Central Sulawesi earthquake and tsunami reconnaissance, the survey form shown in Figures 7.1 and 7.2 was designed and used. This survey form was developed from those designed by UCL for the World Bank Global Program for Safer Schools project (World Bank, 2019) and for the assessment of buildings damaged in the 2016 Italian earthquakes by EEFIT (Stone et al. 2018).

Building and environmental characteristics known to affect a building's vulnerability to tsunami are also incorporated into the survey from consideration of past tsunami reconnaissance findings and vulnerability studies (Rossetto et al. 2007; Dall'Osso et al. 2009; Suppasri et al. 2013). The survey takes between 5-15 minutes to complete (depending on the level of detail entered) and captures confidence levels in the damage assessments made. For more rapid visual assessments, only critical information categories need be filled in. These are denoted with an asterisk.

All survey forms were collected, scanned and stored at the end of each day in the field.

Table 7.1 - The adopted new Earthquake and Tsunami damage scale

Damage State Name	Damage state description			Usability
	Unreinforced Masonry (URM) and Confined Masonry (CM)	Reinforced Concrete	Timber Frame	
No Damage (DET0): <i>equivalent to EMS-98 DG0</i>	No visible structural or non-structural damage observed during the survey. Inundation with contents damage is possible.			Immediately occupiable
Slight Damage (DET1): <i>equivalent to EMS-98 DG1</i>	<p>No structural damage.</p> <p>Damage to non-structural elements only e.g.</p> <ul style="list-style-type: none"> • loss of plaster on walls, • damage to cladding, windows, doors and fixtures • URM & CM: hairline cracking (<1mm) visible in masonry walls • CM - hairline cracking (<1mm) visible or in tie-beam/column joints. 	<p>No structural damage.</p> <p>Damage to non-structural elements only, e.g.:</p> <ul style="list-style-type: none"> • Minor damage to infill walls and partitions. • Damage to cladding, windows, doors and fixtures. 	<p>No frame damage.</p> <p>Light damage in wall panels (full or perforated).</p> <p>Damage in non-structural elements like windows, doors and roof cover.</p>	Immediately occupiable. Minor repair needed.
Moderate damage (DET2): <i>equivalent to EMS-98 DG2&3</i>	<p>No structural component fails.</p> <p>URM: Cracks up to 3mm in masonry walls (or in most of the tie beam/column joints and/or at the base of the columns) without compromising structural integrity. Masonry wall can be repaired or rebuilt to restore integrity.</p> <p>CM: Cracks up to 3mm in masonry walls or in most of the tie beam/column joints and/or at the base of the columns, without compromising structural integrity.</p> <p>Repairable damage from tsunami debris impact to individual or few structural members, without compromising structural stability.</p> <p>Tsunami scouring at corners of the structures leaving foundations partly exposed but repairable</p>	<p>No structural member failure.</p> <p>Fine cracking to spalling of concrete in structural elements.</p> <p>Repairable damage from tsunami debris impact to individual or few structural members, without compromising structural stability.</p> <p>Tsunami scouring at corners of the structures leaving foundations partly exposed but repairable by backfilling.</p> <p>Out-of-plane failure or collapse of parts of or whole sections of infill walls without compromising structural stability.</p>	<p>No frame component fails.</p> <p>Some frame connections damaged (e.g. pull-out of some nails or fixings) but structural stability maintained.</p> <p>Failure of some wall panels.</p> <p>Repairable damage from tsunami debris impact to individual or few structural members, without compromising structural stability.</p> <p>Tsunami scouring at corners of the structures leaving foundations partly exposed but repairable by backfilling.</p>	Suitable for occupancy after repair

	<p>by backfilling. Cracks caused by undermined foundations are visible on walls but not critical.</p> <p>Heavy damage to collapse of non-structural components (e.g. roof cover, gables or parapets)</p>		<p>Heavy damage to collapse of non-structural components (e.g. roof cover, gables or parapets, windows or doors)</p>	
<p>Very Heavy Damage (DET3): <i>equivalent to EMS-98 DG4</i></p>	<p>The structure is standing but is very heavily damaged. Structural integrity compromised and determines entry into this damage state.</p> <p>URM: Out-of-plane failure or collapse of masonry wall panels beyond repair.</p> <p>CM: Major cracks, >5mm, and/or rebar yielding in concrete elements and joints. Out-of-plane failure or collapse of wall panels beyond repair.</p> <p>Roof structure damaged.</p> <p>Excessive foundation settlement and tilting beyond repair.</p> <p>Partial collapse or corner failure of walls due to scouring.</p> <p>Collapse of most (>70%) non-structural components (e.g. roof cover, gables or parapets), but structural element damage dominates damage state definition.</p>	<p>The structure is standing but is very heavily damaged.</p> <p>Collapse of a few columns or of a single upper floor possible.</p> <p>Structural elements damaged or failed (e.g. large cracks in structural elements, compression failure of concrete, buckling/fracture of rebar).</p> <p>Excessive foundation settlement and tilting beyond repair.</p> <p>Roofs are damaged and have to be totally replaced or repaired.</p> <p>Collapse of most (>70%) non-structural components (e.g. roof cover, gables or parapets), but structural element damage dominates damage state definition.</p>	<p>The frame is standing but is very heavily damaged. Structural integrity compromised.</p> <p>Roof structure damaged.</p> <p>Excessive foundation settlement or frame tilting beyond repair.</p> <p>Collapse of most (>70%) non-structural components (e.g. roof cover, gables or parapets), but structural element damage dominates damage state definition</p>	<p>Structure is unsafe and requires demolition.</p>
<p>Collapse/Washed Away (DET4): <i>equivalent to EMS-98 DG5</i></p>	<p>Complete structural damage or collapse. Structure might have been washed away, or structure highly unstable due to excessive foundation settlement and tilting.</p>			<p>Requires demolition.</p>

ASSESSMENT IDENTIFICATION*	
Inspection date (DD/MM/YYYY): _____ / _____ / _____ Hour: _____ : _____ <input type="checkbox"/> a.m. <input type="checkbox"/> p.m. Inspector's name: _____ Group ID: _____ Affiliation: _____ Signature: _____ <input type="checkbox"/> Earthquake <input type="checkbox"/> Tsunami <input type="checkbox"/> Liquefaction <input type="checkbox"/> Other	
BUILDING IDENTIFICATION	
General Data	Location*
Building ID: _____ City: _____ Neighborhood: _____ Address: _____ Type of ownership: <input type="checkbox"/> Public <input type="checkbox"/> Private	Geographical coordinates - GPS (In degrees with 3 decimals) Lat: + [] [] [] . [] [] [] Long: - [] [] [] . [] [] [] <hr/> Casualties Dead or injured: <input type="checkbox"/> Yes <input type="checkbox"/> No <input type="checkbox"/> Unknown Deaths _____ Injuries _____
BUILDING DESCRIPTION	
General Characteristics*	Primary Occupancy*
Orientation to coast line <input type="checkbox"/> Facing <input type="checkbox"/> At an angle Perimeter wall <input type="checkbox"/> High(>1.8m) <input type="checkbox"/> Low <input type="checkbox"/> None Sheltered <input type="checkbox"/> Yes <input type="checkbox"/> No Number of stories above ground: _____ Below ground: _____ Approx. Plan area (m2) _____ Construction year _____ Open ground story <input type="checkbox"/> Yes <input type="checkbox"/> No % Wall openings (max.) _____	<input type="checkbox"/> Residential <input type="checkbox"/> Office <input type="checkbox"/> Commercial <input type="checkbox"/> School <input type="checkbox"/> Hospital <input type="checkbox"/> Light industry <input type="checkbox"/> Governmental <input type="checkbox"/> Mixed use <input type="checkbox"/> Other: _____ Number of occupants: _____
Structural System*	
Reinforced Concrete (RC) <input type="checkbox"/> Frames <input type="checkbox"/> Shear walls <input type="checkbox"/> Combined <input type="checkbox"/> Slab - Column Load Bearing Masonry (LBM) <input type="checkbox"/> Unreinforced <input type="checkbox"/> Confined <input type="checkbox"/> Reinforced <input type="checkbox"/> Light Steel Framed Masonry Steel (SF) <input type="checkbox"/> Unbraced frame <input type="checkbox"/> Braced frame <input type="checkbox"/> Truss Earthen (E) <input type="checkbox"/> Adobe Walls <input type="checkbox"/> Rammed Earth Walls <input type="checkbox"/> Bahareque Walls <input type="checkbox"/> Timber (T) <input type="checkbox"/> Bamboo (B) <input type="checkbox"/> Frames <input type="checkbox"/> Walls <input type="checkbox"/> Combined <input type="checkbox"/> Truss <input type="checkbox"/> Other: _____	
Roofing System*	Non-structural Elements*
<input type="checkbox"/> Light steel structure <input type="checkbox"/> Light wooden structure <input type="checkbox"/> RC slab <input type="checkbox"/> Non engineered truss with precarious coverings (plastic, straw) <input type="checkbox"/> Dome, vault, or arch in masonry, earthen, or wood <input type="checkbox"/> Other: _____	Infill walls <input type="checkbox"/> Concrete block <input type="checkbox"/> Brick masonry <input type="checkbox"/> Wood panels <input type="checkbox"/> Other: _____ Internal Partition walls <input type="checkbox"/> Concrete block <input type="checkbox"/> Brick masonry <input type="checkbox"/> Wood panels <input type="checkbox"/> Other: _____
DAMAGE EVALUATION*	
Scope of the Evaluation*	Evaluation of Damage State*
Exterior <input type="checkbox"/> Partial <input type="checkbox"/> Complete <hr/> Interior <input type="checkbox"/> Not accessed <input type="checkbox"/> Partial <input type="checkbox"/> Complete	<input type="checkbox"/> DET0 <input type="checkbox"/> DET1 <input type="checkbox"/> DET2 <input type="checkbox"/> DET3 <input type="checkbox"/> DET4 Confidence Level H M L

Figure 7.1 - The earthquake and tsunami building rapid visual assessment survey forms-Page 1

DETAILED EVALUATION OF DAMAGES IN THE BUILDING														
Analyze the building and choose the corresponding column for each question (take at least one picture for each one):														
Structure stability:			Yes	No	Not Sure	Geotechnical problems:			Yes	No	Not Sure			
Total or partial collapse of the building:			<input type="checkbox"/>	<input type="checkbox"/>		Mass movements:			<input type="checkbox"/>	<input type="checkbox"/>	<input type="checkbox"/>			
Leaning of the building or a story:			<input type="checkbox"/>	<input type="checkbox"/>	<input type="checkbox"/>	Land cracking:			<input type="checkbox"/>	<input type="checkbox"/>	<input type="checkbox"/>			
Severe settlements, foundation damage:			<input type="checkbox"/>	<input type="checkbox"/>	<input type="checkbox"/>	Liquefaction:			<input type="checkbox"/>	<input type="checkbox"/>	<input type="checkbox"/>			
Others: _____			<input type="checkbox"/>	<input type="checkbox"/>	<input type="checkbox"/>	Others: _____			<input type="checkbox"/>	<input type="checkbox"/>	<input type="checkbox"/>			
Structural elements damage:					Debris and scour induced damage					Yes	No	Not sure		
Write the % of vertical structural elements with particular damage grade.														
Storey	G	1	2	3	4	5	6	7	Debris impact (vehicle, boat, container etc.)			<input type="checkbox"/>	<input type="checkbox"/>	<input type="checkbox"/>
Slight (S)	<input type="checkbox"/>	<input type="checkbox"/>	<input type="checkbox"/>	<input type="checkbox"/>	Scour damage (foundation exposed etc.)			<input type="checkbox"/>	<input type="checkbox"/>	<input type="checkbox"/>				
Moderate (M)	<input type="checkbox"/>	<input type="checkbox"/>	<input type="checkbox"/>	<input type="checkbox"/>	Describe: _____			<input type="checkbox"/>	<input type="checkbox"/>	<input type="checkbox"/>				
Very Heavy (VH)	<input type="checkbox"/>	<input type="checkbox"/>	<input type="checkbox"/>	<input type="checkbox"/>	_____			<input type="checkbox"/>	<input type="checkbox"/>	<input type="checkbox"/>				
S = hairline cracking (<1mm) in masonry walls or in tie-beam/column joints for C.M. Fine cracking to spalling of RC														
M = cracks up to 3mm in masonry walls or in tie beam/column joints or in tie-columns for C.M. Cracking and re-bar yield in RC. Connection damage in Timber														
VH = out-of-plane failure, shear failure or collapse of masonry walls, RC and Timber. Cracks >5mm, and/or rebar yielding in concrete elements and joints of C.M.														
Sketches and notes (please include information on construction materials, member dimensions, reinforcement detailing (size and numbers), wall thickness, external risks etc.):														

Figure 7.2 - The earthquake and tsunami building rapid visual assessment survey forms-Page 2

7.2 Observations on the characteristics and performance of typical low-rise houses

Typical low rise construction of Palu and Donggala is here divided into three different categories: timber “stilt” houses, timber framed houses with infills and confined masonry (clay brick and concrete block) houses. These three categories of buildings represent different eras of non-engineered building practice in the region.

7.2.1 Timber “stilt” houses

Traditional timber housing in Palu is two-storeys in height, where the main living quarters are on the 1st floor and the ground storey has no cladding i.e. the house is effectively on stilts (see Figure 7.3 left). These stilt houses could be found along Palu bay, though are not as common as the other two types of low-rise housing. Many such houses were founded on dry land but in the fisherman villages along Palu bay they were also seen built on the water. The ground floor of the frame is commonly seen to include some diagonal struts to improve stability under lateral loads. The roof consists of a wooden truss with light weight steel or corrugated iron covering. The timber struts forming the ground storey were seen to sit on individual concrete footings, which are called Umpak in Indonesia (e.g. Figure 7.5). This type of concrete footing usually has the form of a flat top prism, where the bottom of the footing sits at least 30cm underground. The maximum space between two footings is 1.5 m. The timber frame typically has nailed connections, but in a few cases mortise and tenon joints were seen. These houses were traditionally built of ebony (e.g. Figure 7.4-left), but are now made of coconut wood, as this is less expensive. The Sulawesi coconut lumber is a high quality hardwood, as seen in Figure 7.3.



Figure 7.3 –Picture of coconut lumber.

The stilt houses showed varied performance under the earthquake and tsunami. At the shore-front these structures performed badly due to ground subsidence and the tsunami inundation reaching the first floor. For example, Figure 7.4-right shows the remains of the stilt houses foundations of the fisherman village in Labuan Bajo Donggala. However, in other areas, where the tsunami inundation did not exceed the ground floor, this type of housing was seen to perform well due to their open ground floor offering little resistance to the flow. Only two examples of stilt houses were surveyed by the Team in an area of Palu that had not been inundated by the tsunami. These were both at the Heritage site of the palace of the Princes of Palu, with the first (Figure 7.4-left, the palace) being undamaged by the earthquake ground shaking, whilst the neighbouring very small structure exhibited severe tilting.



Figure 7.4 - Performance of timber stilt houses in Palu and Donggala, Central Sulawesi: Left – The palace of the Princes of Palu. This structure was affected by ground shaking but not tsunami inundation and was undamaged. Right - The remaining concrete foundations of the timber stilt houses in the Labuan Bajo Fisherman Village, shown in red circle. Collapsed stilt houses can be seen in the background.

Typical Column and Foundation of Stilt Houses

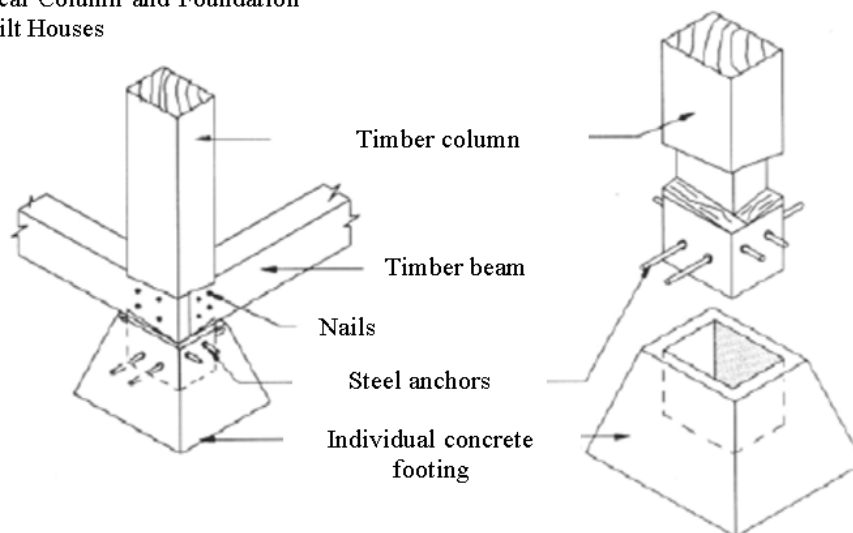


Figure 7.5 - Detail of individual concrete foundation for stilt house (Umpak). (Base image source: Pedoman Teknis Rumah dan Bangunan Gedung Tahan Gempa, Kementerian Pekerjaan Umum dan Perumahan Rakyat, Indonesia, 2006).

7.2.2 Timber frame houses with infills

A second category of low rise construction in Donggala and Palu comprises timber frames with either wire mortar or masonry infill. These construction types were observed in Donggala city and form the heritage of this old port city. According to locals, and confirmed by Mansur (2006) these buildings were built during the colonial time (i.e. during the Dutch period c1824 – 1942). The timber frame is made from hard timber called “Ulin”, which is similar to ebony and had been brought from Kalimantan. The infill walls are either made from mortar reinforced with barbed wire or wire mesh, or are masonry (red clay brick or concrete block), see Figures 7.6 and 7.7.

The typical earthquake induced damage observed in these buildings was out-of-plane failure of the infill walls or separation between the infill and frame due to differential settlement (see Figure 7.8).



Figure 7.6 - Examples of infilled timber frame construction in Labuan Bajo. Left - Timber framed house with wire-reinforced mortar. Right - Two storey timber framed house with mortar infill.



Figure 7.7 - Examples of infilled timber frame construction. Left - Timber framed warehouse with masonry infill in Labuan Bajo (left). Right - Elementary school at Wani, timber frame construction with mortar infill.



Figure 7.8 - Typical earthquake damage observed in infilled timber frame construction. Left - Out-of-plane failure of infill panels. Right - Separation of infill from frame due to differential settlement of foundations.

7.2.3 Confined masonry housing

The most common non-engineered construction observed in Palu is confined masonry (CM). CM construction is a load bearing type of construction in which the brick masonry walls are confined with reinforced concrete elements, called tie-elements. The vertical and horizontal tie-elements are called tie-columns and tie-beams, respectively. The tie-elements are of small cross-section, (usually the same as the wall thickness), and have poorly reinforced/detailed joints. Hence, the tie-elements cannot provide a moment-resisting frame action in the structure. Instead, these elements act as the confining elements to stiffen the masonry wall panels and thus increase the strength and stiffness of the masonry walls, where both the wall and tie-elements act together. This differentiates the behaviour of confined masonry buildings from that of a RC framed construction (e.g. see Figure 7.9).

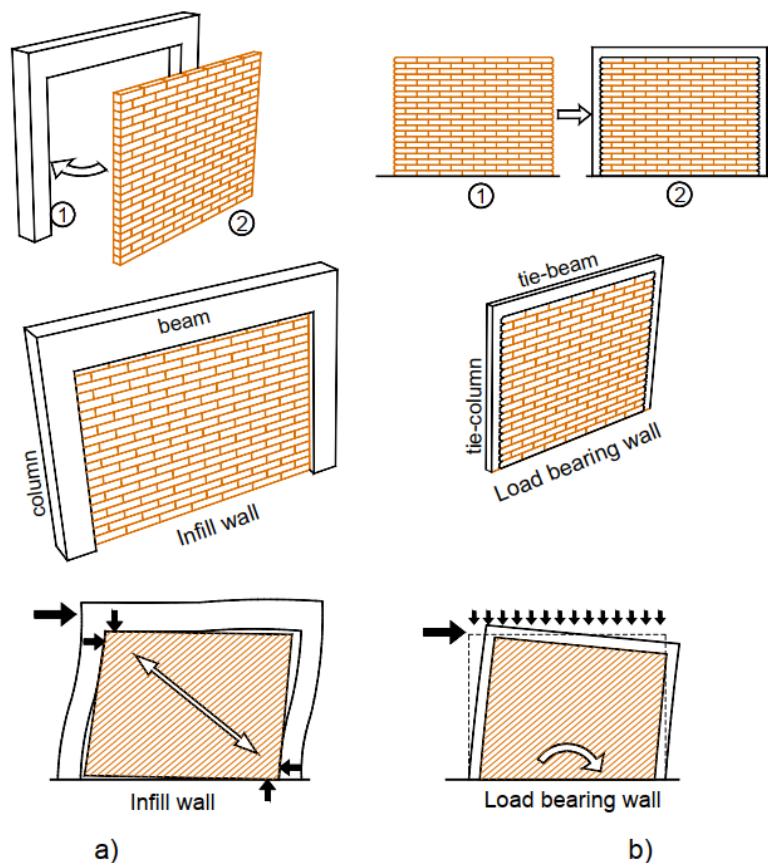


Figure 7.9 - Comparison of construction characteristics and seismic behaviour of a) RC frames with masonry infills and b) confined masonry construction: construction sequence (top); relative size of confining elements (middle), and the seismic response (bottom) (Source: EERI, 2011).

CM became the predominant type of construction for residential buildings in Indonesia after 1970. The growing adoption of this type of construction was however not accompanied by appropriate checks on material or construction quality. In these buildings, the walls are thin at about 100 – 150 mm and are lightly confined with weak RC tie-beams and tie-columns of similar sized cross-section. The roof structures are usually double pitched light timber framed structures. The foundations are usually strip type laid in stone masonry underneath the loadbearing walls.



Figure 7.10 – Heavily damaged CM houses in Palu bay area along the Jl. Rajamoili road, about 100m from coastline. The walls of this house were directly hit by the tsunami inundation.



Figure 7.11 – Undamaged CM houses in Palu bay area along the Jl. Rajamoili road. These houses were sheltered from the tsunami inundation by other houses-buildings.

Typical damage sustained by CM houses along the coast line in Palu bay area is shown in Figure 7.10. The main damage pattern is the out of plane failure of walls directly hit by the tsunami waves. The tie-columns, being small in size and having poor reinforcement detailing, also suffered shear damage. However, as shown in Figure 7.11, sheltered houses near the coastline were unaffected, indicating that the effect of ground shaking was modest in this area.

CM is also the predominant form of construction for school buildings built during the 1980s as a result of a presidential decree. These schools are named “*Inpres Schools*”. The performance of confined masonry low rise buildings is therefore discussed in Section 7.3.2 on schools.

7.2.4 Guidance for low-rise housing construction in seismic areas in Indonesia

In 2006 the Indonesian Ministry of Civil Works and Residential Houses published a technical guidance document for the construction of earthquake resistant houses and buildings in Indonesia, which is aimed at builders and contractors (Pedoman Teknis Rumah dan Bangunan Gedung Tahan Gempa, Kementerian Pekerjaan Umum dan Perumahan Rakyat, Indonesia, 2006). This guidance is based on the following reference documents (Cipta Karya 2006):

- UUBG No.28/2002 tentang Bangunan Gedung; The Indonesian Law of Building Construction
This law regulates the process of building construction, including siting, structure types and the architecture of building components.

- PPBG No. 36/2005 tentang Peraturan Pelaksanaan UUBG; The Government Law for implementation of the Indonesian Law No.28/2002 (The Indonesian Law of Building Construction). This law is aimed to ensure the effectiveness of the implementation of the building construction regulation (UUBG No.28/2002). The law includes articles to further explain about the evaluation approach and technical assessment of building construction.
- *Kepmen Kimpraswil No.403/KPTS/M/2002* regards the construction of simple houses (Ordinary, masonry houses, half masonry houses, stilt timber houses, and timber houses),
- Lampiran Surat Keputusan Direktur Jenderal Cipta Karya No. 111/KPTS/CK/1993 i.e. the guidelines for the earthquake design of buildings
- Guidelines for Earthquake Resistant Non-Engineered Construction, IAEE 1986;
- The Manual for simple buildings retrofitting damaged by earthquake by *Boen, Teddy, 1992*.
- SNI no 03-1726 – 2002 which was renewed in 2012 (Seismic Standard for the Construction of Engineered Buildings and Non-engineered Buildings).

Images from the *Pedoman Teknis Rumah dan Bangunan Gedung Tahan Gempa, Kementerian Pekerjaan Umum dan Perumahan Rakyat, Indonesia, (2006)* are shown in Figures 7.5, and 7.12 to 7.17.

For “stilt” timber framed housing (Figures 7.5, 7.12 and 7.13) it is interesting to note that the guidelines recommend the ground-floor columns be anchored inside the concrete footing, and that horizontal ties rather than diagonal braces are recommended for strengthening the lateral resistance of the ground floor. It is also recommended that the beams are connected to the columns using mortis and tenon joints, which were not commonly seen in Palu.

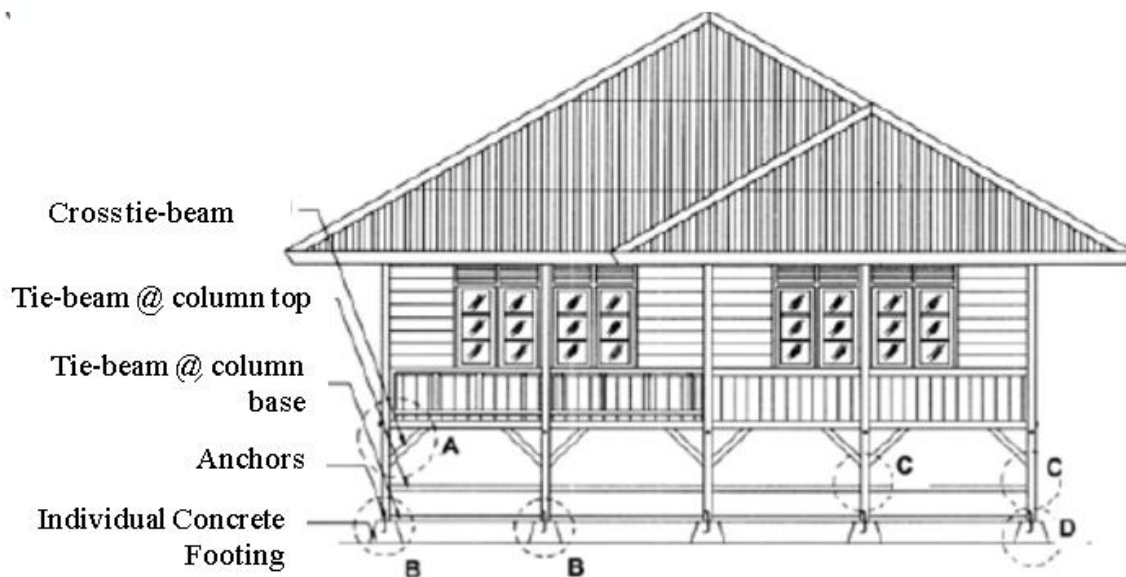


Figure 7.12 - Recommended detailing for “stilt” type timber frame construction from Technical guidelines of earthquake resistant houses and buildings construction published by the Indonesian Ministry of Public Works and Houses (Pedoman Teknis Rumah dan Bangunan Gedung Tahan Gempa, Kementerian Pekerjaan Umum dan Perumahan Rakyat, Indonesia).

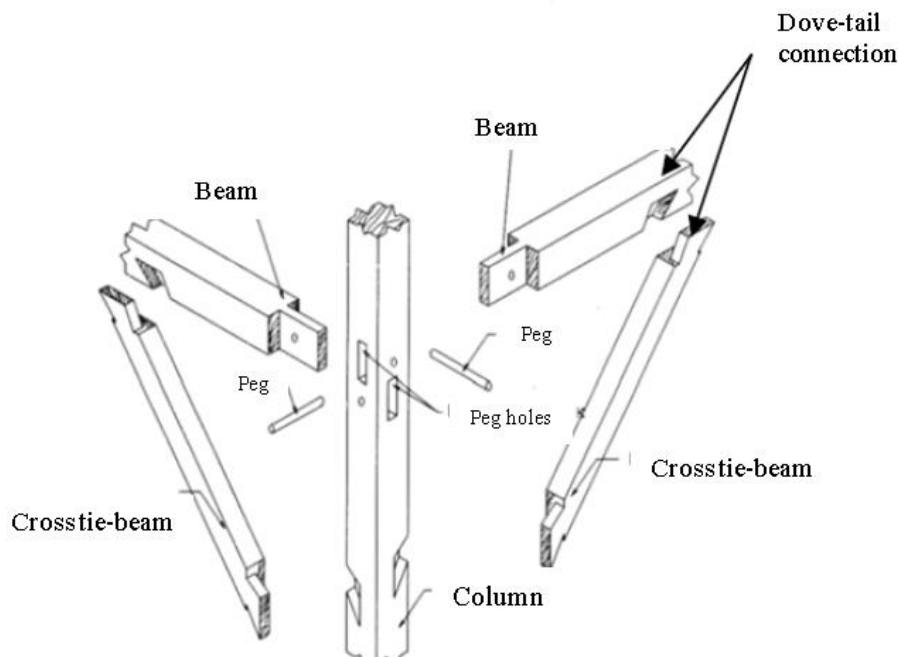


Figure 7.13 - Detailing for beam – to – column connections recommended in “stilt” type timber frames, from the Technical guidelines of earthquake resistant houses and buildings construction published by the Indonesian Ministry of Public Works and Houses (Pedoman Teknis Rumah dan Bangunan Gedung Tahan Gempa, Kementerian Pekerjaan Umum dan Perumahan Rakyat, Indonesia, 2006).

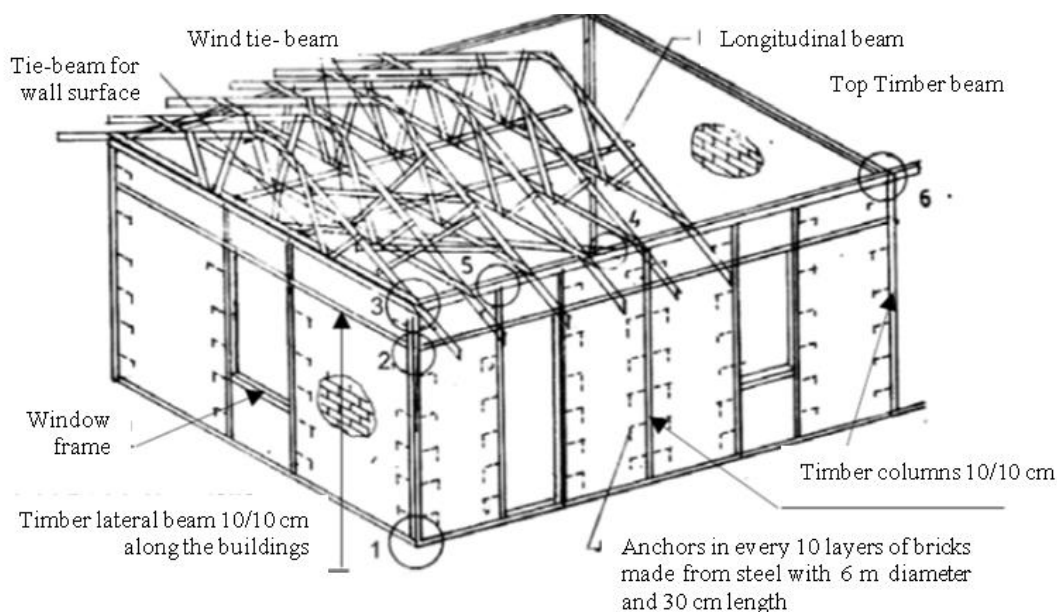


Figure 7.14 - Design of masonry infilled timber framed buildings, as recommended in Technical guidelines of earthquake resistant houses and buildings construction that published by the Indonesian ministry of public works and houses (Pedoman Teknis Rumah dan Bangunan Gedung Tahan Gempa, Kementerian Pekerjaan Umum dan Perumahan Rakyat, Indonesia, 2006).

In the case of masonry infilled timber framed buildings, Figure 7.14 shows that the guidelines recommend cross sections of 100x100mm² for both columns and beams. Details of recommended foundation design and of infill wall-to-frame connection are shown in Figure 7.15.

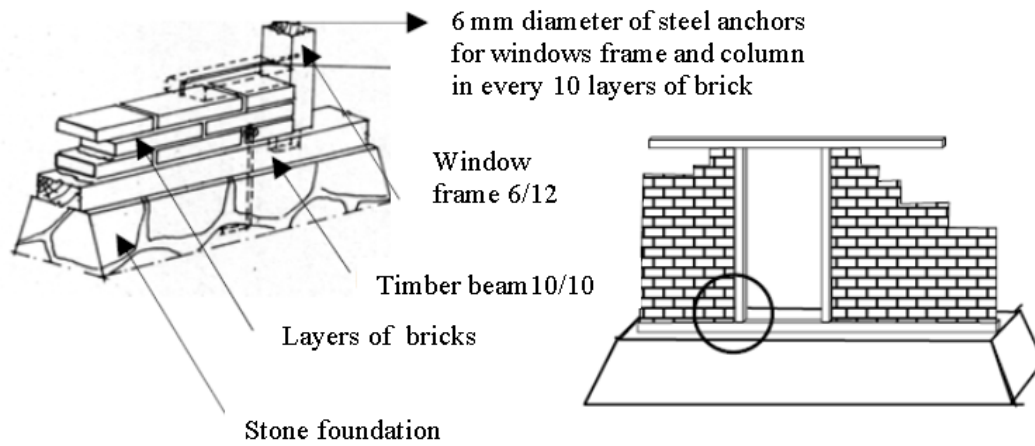


Figure 7.15 - Design of foundations and of the connection between the infill and timber frame in masonry infilled timber framed housing, recommended by the Technical guidelines of earthquake resistant houses and buildings construction published by the Indonesian Ministry of Public Works and Houses (*Pedoman Teknis Rumah dan Bangunan Gedung Tahan Gempa, Kementerian Pekerjaan Umum dan Perumahan Rakyat, Indonesia*).

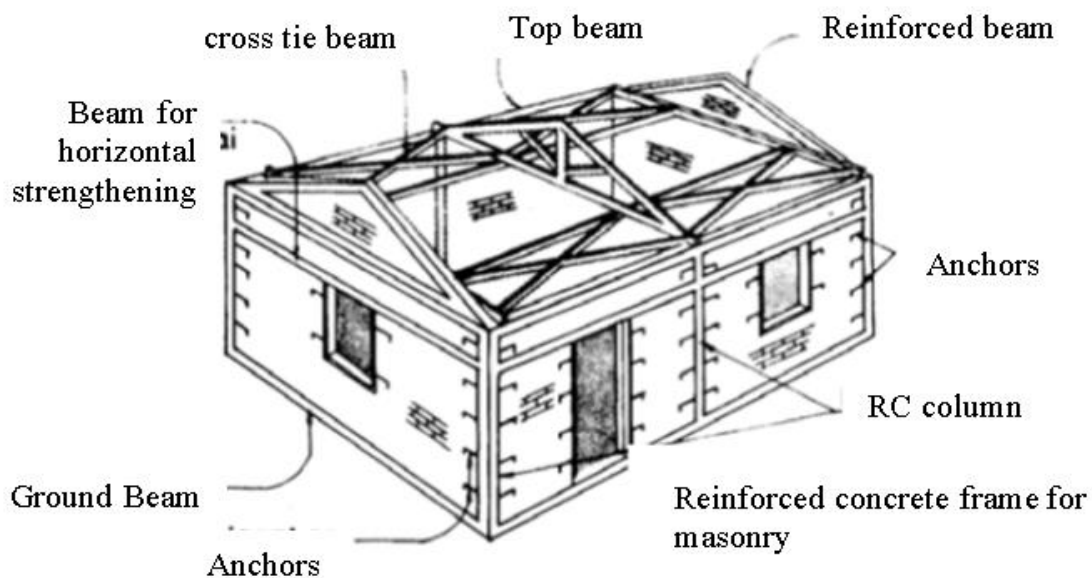


Figure 7.16 - Design of confined masonry buildings, as recommended in the Technical guidelines of earthquake resistant houses and buildings construction that published by the Indonesian ministry of public works and houses (*Pedoman Teknis Rumah dan Bangunan Gedung Tahan Gempa, Kementerian Pekerjaan Umum dan Perumahan Rakyat, Indonesia*).

In the case of confined masonry buildings, Figure 7.16 shows that the masonry walls should be anchored to the confining columns, and that the wall area confined should not be greater than 12m². Details of recommended stone and mortar foundation design and of the reinforced concrete confining elements are shown in Figure 7.17.

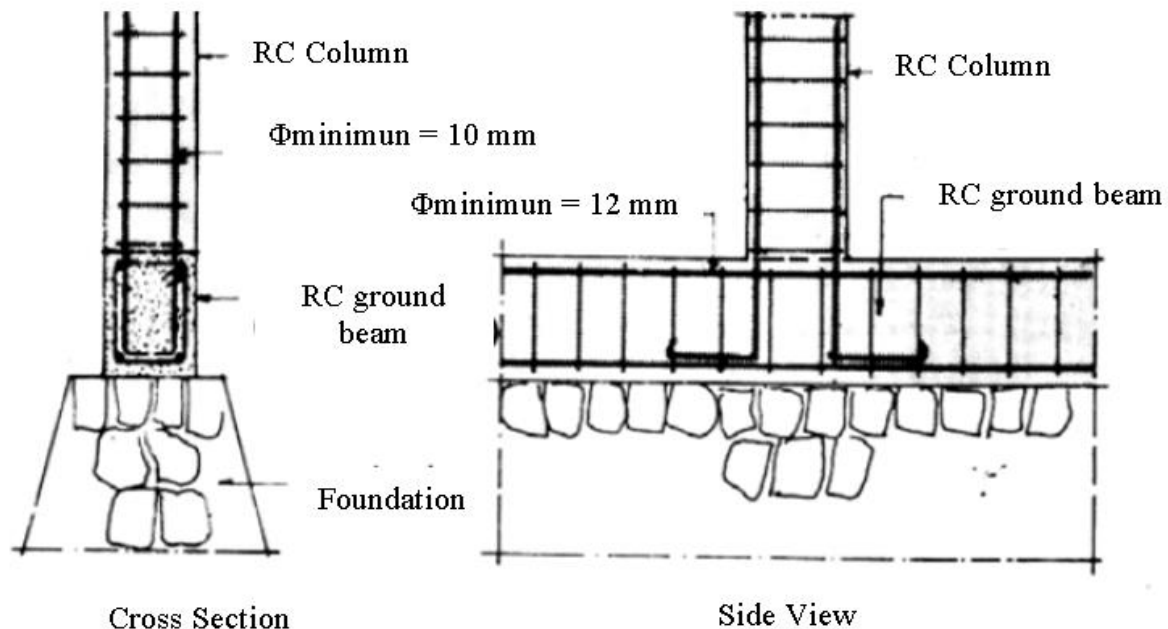


Figure 7.17 - Design of foundations, and confining reinforced concrete elements in confined masonry buildings, as recommended by the Technical guidelines of earthquake resistant houses and buildings construction that published by the Indonesian ministry of public works and houses (Pedoman Teknis Rumah dan Bangunan Gedung Tahan Gempa, Kementerian Pekerjaan Umum dan Perumahan Rakyat, Indonesia, 2006).

7.3 Observations on the performance of educational facilities

7.3.1 Tadulako University Campus

Tadulako University campus is located on a hill top North East of Palu city on the eastern side of Palu Bay and about 1.5 km from the shore. It is composed of masonry infilled reinforced concrete low- to mid-rise buildings, hosting 11 (eleven) faculties and 40,000 students. Buildings on this site were only affected by earthquake ground shaking. Most of the university buildings sustained no to slight damage (DET0-1). The EEFIT-TDMRC team observed that at least 3 buildings had sustained moderate damage (DET2), 1 sustained heavy damage (DET3) and 1 had collapsed (DET4).

The buildings inspected by EEFIT-TDMRC are identified in Figure 7.18. The moderately damaged buildings include the two buildings of the university hospital (discussed in Section 7.4.1) and the Rector's office building. Pictures of the latter are presented in Figure 7.19.

The Rector's office building is of 3 stories, has piled foundations and large open spaces at the ground storey. It is observed that the main damage is due to the in-plane shear cracking of brick partitions, the falling of suspended ceiling and breaking of windows. No damage to structural elements was observed and no casualties were sustained in this building. Some movement was apparent in a vertical construction joint at the south end of the structure, indicating a 2-5cm settlement of the north side relative to the south. This was evidenced also by displacement of paving outside the building. Also, relative movement of the structure and ground was seen to cause a reduction in the width of drains to

the north of the building. The structure was not being used at the time of the mission, but was to be re-occupied shortly, notwithstanding lack of repair.

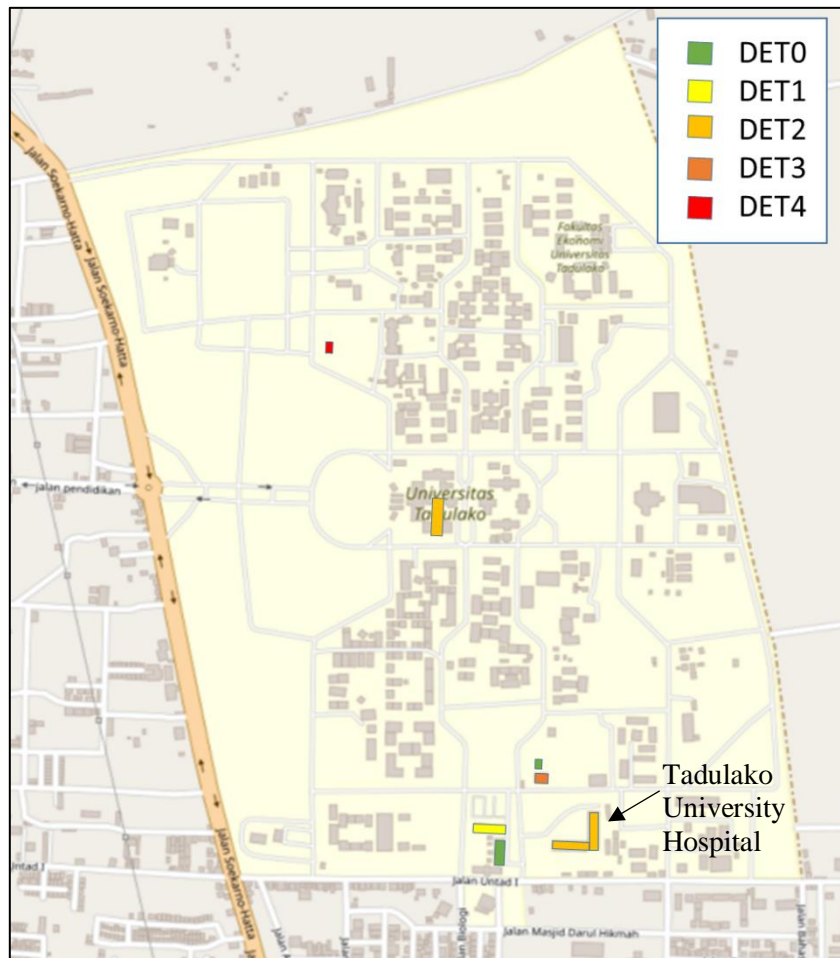


Figure 7.18 - Map of the Tadulako University Campus showing the damage states and location of the buildings surveyed by the EEFIT-TDMRC Team.



Figure 7.19 - Tadulako University Rektorat (DET2): exterior view (left); damage to internal infill panels (right)

Figure 7.20 shows the collapse of a 3-storey reinforced concrete frame building, part of the Faculty of Social and Political Sciences, at the university campus. This building had been built in 2016, and failure occurred through the activation of a soft-storey type mechanism, due to plastic hinge formation in the beam-column joints. The building has a plan approximately 20m x 12m. The primary beams are large (500mm deep by 300mm wide), span up to 6m in the shorter dimension of the building and have secondary beams of large size (250mm deep by 250mm wide) framing into them at 3m intervals. No columns support the primary beams at mid span, where there is the primary to secondary beam connection. The columns are larger than the beams (500mm x 500mm in plan) and are reinforced with 10 x 25mm ribbed diameter longitudinal reinforcing bars.

Shear reinforcement in the columns consists of smooth 10mm diameter hoops with 90degree hooks, at 140mm spacing. The roof is pitched and consists of a lightweight steel cover (CGI) on steel beams that terminate on the top beam of the frame. The floors consist of shaped sections of steel plate supporting concrete screed. The latter provides little/no contribution to the moment capacity or restraint of the beams. This, combined with the similar size of beams and columns, the soft-storey mechanism at ground level and lack of any shear reinforcement in the joints, has led to beam-column connection failure and building collapse. Concrete spalling of an exterior beam-column joint can be seen in Figure 7.21 – left and a failed exterior joint can be seen in Figure 7.21 - right).



Figure 7.20 - Tadulako Univerity collapsed 3-storey building of the Faculty of Social and Political Sciences. Left – front view. Right – back view.

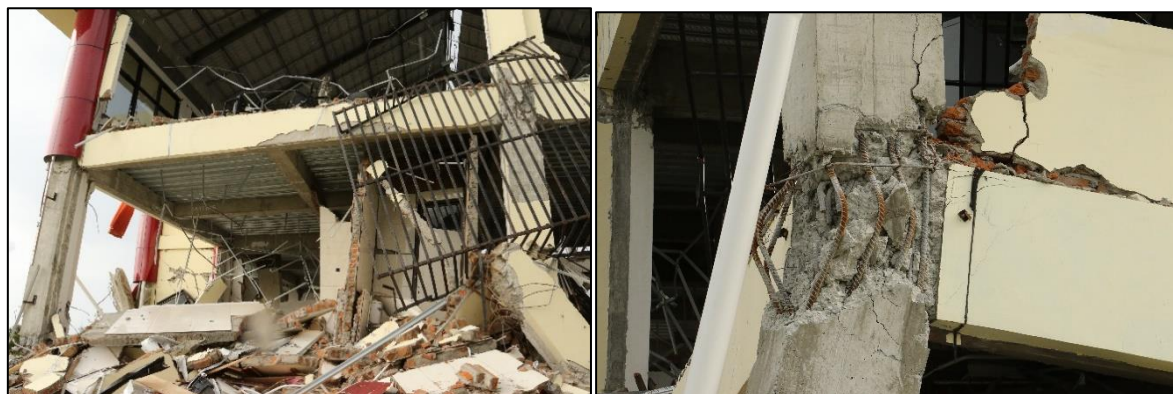


Figure 7.21 - Tadulako Univerity collapsed 3-storey building of the Faculty of Social and Political Sciences. Left – Side view of the building. Right – Failed external joint.

7.3.2 Schools

During the mission, the EEFIT-TDMRC Team surveyed and conducted damage assessments of a number of school buildings in several school compounds located in the Palu, Donggala and Sigi area as shown in Figure 7.22.



Figure 7.22 - Locations of schools visited in Palu, Sigi and Donggala Regency during the EEFIT-TDMRC mission.

The school buildings surveyed were mainly of two typologies: one-storey confined masonry (CM) buildings or two- to three- storey reinforced concrete (RC) buildings. The characteristics of these are described in more detail next, before describing the damage mechanisms observed.

7.3.2.1 Confined Masonry School Buildings

The majority of the school buildings in the school compounds visited during the mission were of CM construction type. The plan, number of classrooms, storey height, gable confinement details etc. of CM buildings were seen to vary within and across different school compounds. However, Figure 7.23 provides a representative layout and typical detailing for observed CM school buildings in Palu.

Most of the CM buildings observed in the visited school compounds suffered very heavy damage (DET3), and a few buildings were seen to have collapsed (DET4). Figure 7.24 show the damage states associated with buildings in three school complexes.

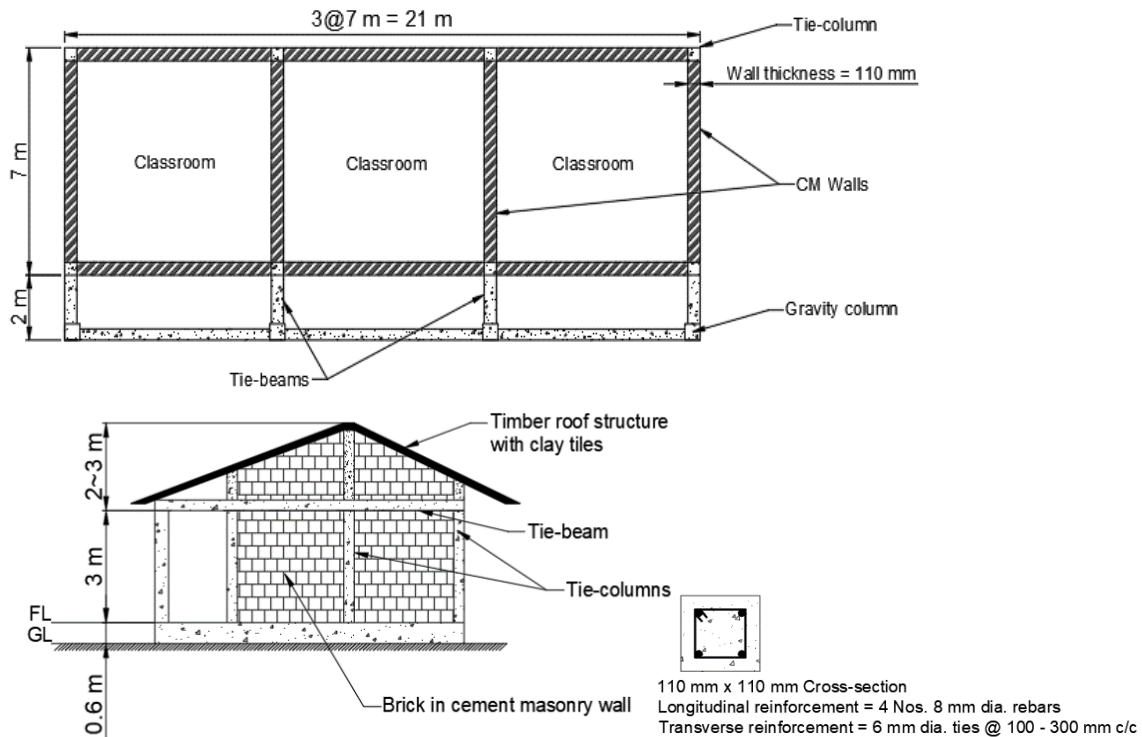


Figure 7.23 - Typical layout and construction details of a representative CM school building in Palu.

In many cases failure included damage to poorly confined heavy gables and the out-of-plane damage/collapse of long and poorly confined CM walls. The poor performance of these buildings in the earthquake was observed to be due to a number of construction defects and poor construction practices:

- Poor material quality of brick units, mortar and concrete. The latter often observed to be deteriorated and have corroded reinforcement (especially near the coast).
- Poor reinforcement detailing in tie-elements. Small rebar cross sections, very low longitudinal reinforcement ratio and large spacing of transverse ties.
- Large and poorly confined spans, which make walls vulnerable to out-of-plane failure.
- Low confinement level of thin walls (e.g. 110 mm) in both horizontal and vertical directions.
- Large and poorly confined/unconfined gables: Tie-columns in many cases not seen to extend to the full gable height, and gables are unconfined along their slopes (i.e. tie beams are absent).



(a)



(b)



(c)

Figure 7.24 – Damage observed in buildings at three school complexes.

(a) SMP Negeri 1 Biromaru School in Sigi. Building A is a 2 storey RC infilled frame structure, whilst all other buildings are one-storey CM construction). Building B was reduced to rubble, whilst most of the other CM buildings suffered range of damage states – from slight (DET2), very heavy (DET3) to partial collapse of their shorter walls (DET4).

(b) SD Inpres 1 Talise School in North Palu. Affected only by shaking (not ground failure) from the earthquake. All three buildings are single-storey CM buildings. All suffered unrepairable damage (DET3). Main damage mechanisms are separation of walls and gable failure, due to poor quality materials and ineffective confinement.

(c) SD Negeri Pengawu School in Palu. Two small-plan single-storey CM buildings (B and C) suffered minor, repairable damage. The large plan CM single-storey building D suffered heavy damage to collapse of some walls (DET4) due to differential ground movement. Building E is CM but was under construction at time of earthquake. Building A is a 2-storey RC infilled frame structure.

Figure 7.25 shows a collapsed CM school building, which suffered out-of-plane failure of the short cross wall, followed by roof collapse due to insufficient load carrying capacity of the load bearing elements.



Figure 7.25 - Collapse of a CM school building in SMP Negeri 1 Biromaru School, Sigi.

Figure 7.26a shows the complete collapse of the shorter wall of a CM school building in Sigi area. All the cross walls of this building suffered either collapse or detachment due to extensive damage in the out-of-plane direction. However, the in-plane damage was limited (Figure 7.26b). The heavy damage suffered by this building is attributed to the long, thin and poorly confined cross walls, poorly reinforced tie-elements and deteriorated material quality.



(a)



(b)

(c)

Figure 7.26 - Heavy damage sustained by CM school buildings at SMP Negeri 1 Biromaru School. (a) Out-of-plane collapse of the shorter wall in Building C (see Fig. 7.24). All the other cross walls either collapsed or are on the verge of collapse. (b) In-plane flexural and shear cracks through the spandrels. (c) In-plane flexural and shear cracks through the tie-columns.

Figure 7.27 shows another typical example of the type of damage observed in CM buildings. The heavy, tall and poorly confined gables suffered partial out-of-plane collapse. The (short) cross walls suffered damage where they separated from the confining columns, and out-of-plane deformation of the walls has commenced. Interestingly, cracks were observed to pass through both the bricks and mortar indicating the poor material quality of bricks.

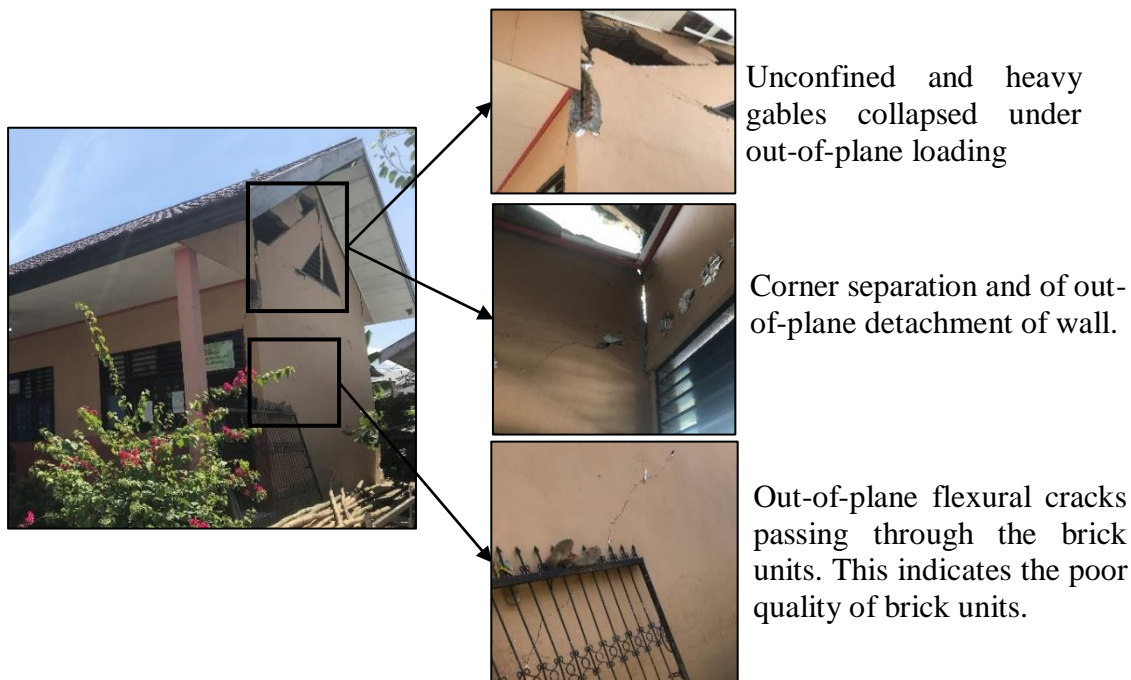


Figure 7.27 - Typical failure mechanisms observed in CM school buildings. Picture shows damage in building A at SD Inpres 1 Talise school.

The EEFIT-TDMRC visited one school that was still under construction at the time of the earthquake. This CM school building, shown in Figure 7.28, did not suffer any apparent damage. The level of confinement of the masonry panels and gables was seen to be good, but a construction defect was observed, in that the middle tie-column is not continuous up to the full gable height.

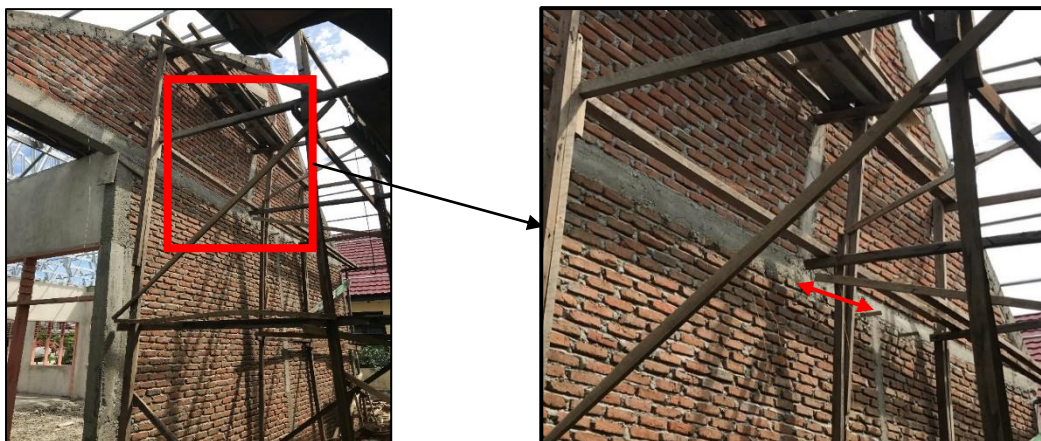


Figure 7.28 - Confined masonry school building (E in Fig. 7.24) in SD Negeri Pengawu school in Palu that was under construction at the time of the earthquake. Note the offset of the middle tie-column at the tie-beam level.

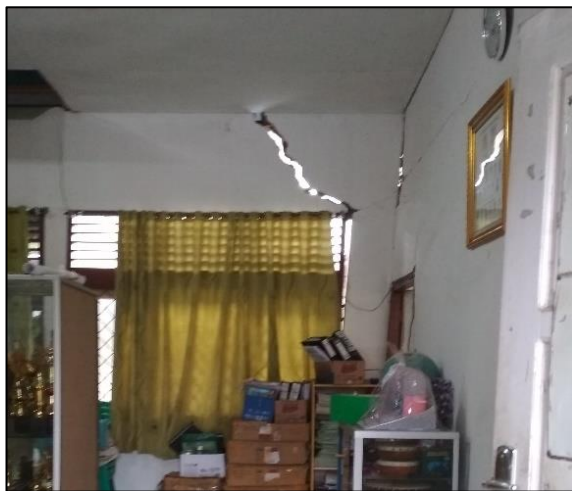
In many of the observed schools, ground failure precipitated damage. Differential settlement of buildings was common in the Sigi area and areas either side of Palu bay. Figure 7.29 shows some examples of the amplified damage due to the combined effect of the ground shaking and differential settlement.



(a)



(b)



(c)



(d)

Figure 1.29 - Extensive damaged in CM building (building D in Fig. 7.24c) in SD Negeri Pengawu school due to differential settlement. (a) differential movement of ground across a ground crack passing under the building caused failure of the floor. (b), (c) and (d) show crack opening induced by differential ground movement.

CM buildings with small plans and limited openings performed well, as expected, and only suffered no/slight damage (DET0/1) due to their box-like behaviour e.g. see Figure 7.30.



Figure 7.30 - A small plan box-type CM school building that suffered no damage (building B in Fig. 7.24c) in SD Negeri Pengawu school.

The following recommendations are suggested for improving the quality of CM school building construction in the reconstruction process.

- Good quality construction materials (concrete, steel, bricks etc.) should be used in the future school construction.
- Enough confinement (both horizontal as well as vertical) to all the wall panels should be ensured. An example of a high design CM school construction (which has similar architectural features as that of the existing CM schools in Palu area) is shown in Figure 7.31.
- Gables should either be confined properly both vertically and along the slopes (if masonry gables) or light material such as CGI (Corrugated Galvanized Iron) sheets should be used.

Although the cost will increase when improving the construction practice, this is justified by the fact that schools are important infrastructure in a community.

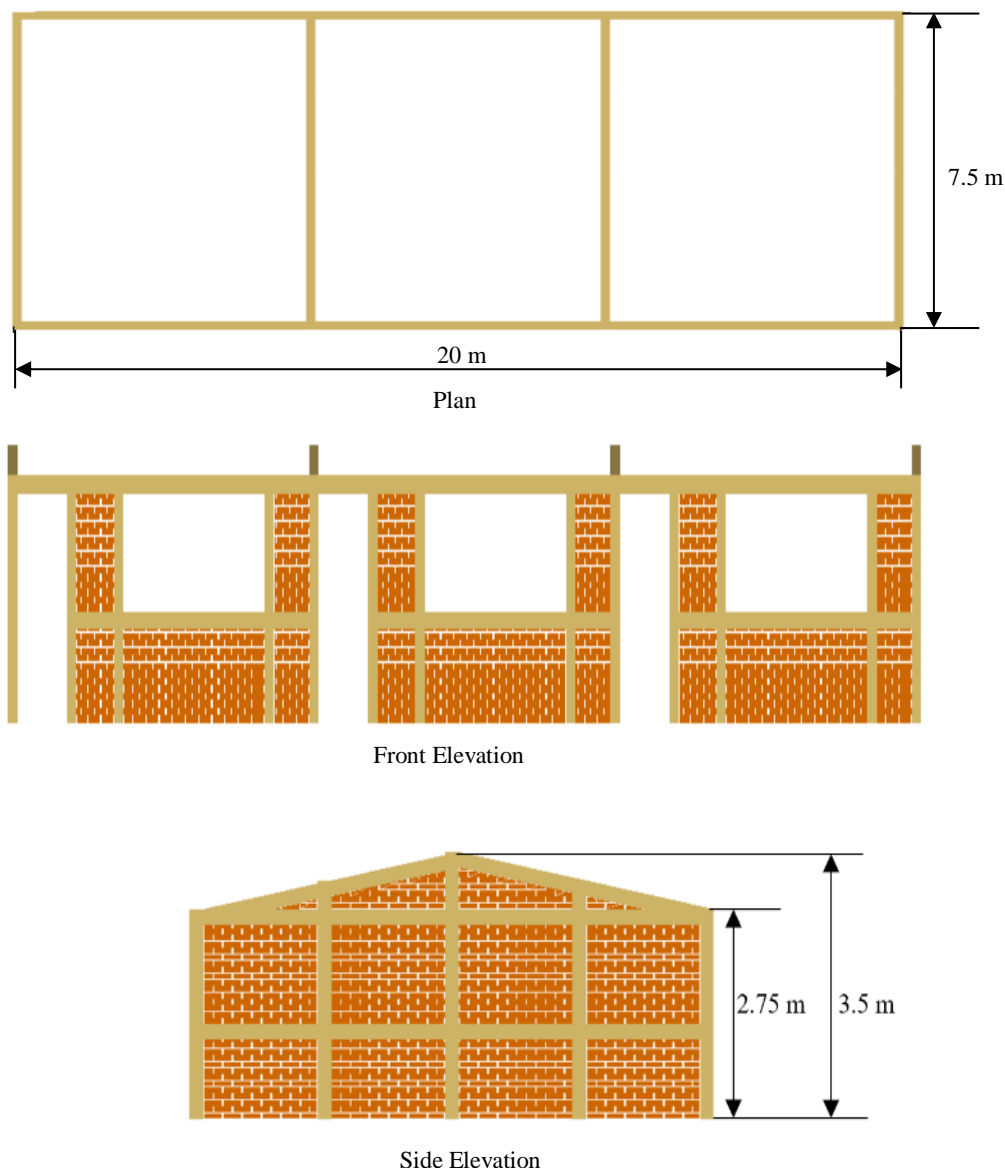


Figure 7.31 - Construction details of a well-designed CM school building from El Salvador (Credit: Rohit Kumar Adhikari, World Bank, 2019).

7.3.2.2 Reinforced Concrete School Buildings

Reinforced Concrete (RC) school buildings were observed to be 2 to 4 storeys high, RC frames with brick masonry infill, had some level of seismic design and good material quality. The RC frame school buildings observed were commonly 1 bay wide (bay-width typically 6.5-7m) and 8 bays long in plan (bay width 3-3.5m). They contained large columns (600mm x 300mm) and beams (600mm x 400mm), with storey heights of 3.4-3.5m. Roofs were commonly seen to be double-pitched timber frame roofs with light-weight steel or corrugated iron covering.

Generally, reinforced concrete school buildings performed well during the earthquake ground shaking. For example, MTS Alkhairaat Pusa Palu School contained 9 two-storey RC school buildings, all of which suffered no damage. Only one 3-storey RC building at this school complex had suffered light damage to its infill walls (Figure 7.32). In fact, damage to masonry infill walls was the predominant

damage observed in RC frame school buildings that were subjected to earthquake ground shaking only, and another example is shown in Figure 7.33.



Figure 7.32 - MTS Alkhairaat Pusa Palu School. Left – 3-storey RC frame building that sustained minor damage to infill panels. Right – Typical sizes of beams and columns in RC frame schools.



Figure 7.33 - SD Negeri Pengawu School in Palu (Building A in Fig. 7.24c). Left – 2-storey RC school building that sustained moderate damage to infill panels. Right – Damage to the infill walls

Building A at SMP Negeri 1 Biromaru School (refer to Figure 7.24) is a 2-storey RC frame with brick masonry infill (see Figure 7.34). This sustained damage to columns at the rear side of the building that were supporting the balconied areas. The columns, which were founded on made ground, suffered failure at their foundation as this made ground was affected by the earthquake. This failure is not depicted well in Figure 7.34 – right, as the column failure was to the left of the picture taken. Nevertheless, Figure 7.34 does show the columns supporting the balcony, and some separation of the made ground with the school wall (brown crack).



Figure 7.34 - SMP Negeri 1 Biromaru School, Building A in Fig. 7.24a. Left – front entrance to the building. Right – the rear of the building showing columns that support the balcony sited on a 1m high “slab” of made ground covered in concrete screed.

7.3.2.3 Temporary Learning Centres

In the earthquake affected school compounds, several temporary learning centres (TLCs) have been established to continue the teaching and learning process. These have been built by local government or donated by NGOs. The construction types were observed to vary but were usually semi-permanent light-weight structures as shown in Figure 7.35.



(a) Light steel framed structure

(b) Light bamboo framed structure

Figure 7.35. - TLCs established in the school compounds by the government and NGOs.

7.4 Healthcare Facilities

7.4.1 Tadulako University Hospital

The university hospital comprises two large buildings composed of reinforced concrete frames with masonry infill. Both buildings sustained moderate level of damage (DET2). The buildings are sited perpendicular to each other, forming an L-shape in plan (as shown in Figure 7.18) separated by a narrow seismic gap but are operationally connected to each other at all levels.

The hospital had been open for only one month before the earthquake struck, and was not occupied or used at the time of the EEFIT mission, with no repairs yet started. The Dean of Engineering of the University told the EEFIT team that at the time of the main shock all hospital patients were on the ground floor of the hospital, where, as part of the hospital disaster management plan, they had been moved by the medical staff after foreshocks earlier in the day. No injuries were reported in the hospital due to the earthquake.

Building A has its long dimension in the N-S direction and is 3 storeys high (Figure 7.36). This building sustained heavy non-structural damage to masonry infills and partitions (Figure 7.367–Right and Figure 7.39 - Left), shattering of the glass cladding of the front entrance, falling of ceiling covering and light fittings (Figure 7.39 - Middle). However, no structural damage was observed. Approximate column dimensions are 500mm x 500mm and beam dimensions are 600mm x 500mm, with the beams being

reinforced with 6 x 20mm diameter steel reinforcing bars (as observed from its protrusion from the side of the building, see Figure 7.37 - Left).



Figure 7.36 - Tadulako University Hospital Building A. Left – Front view. Right – rear view, showing damage to gable.



Figure 7.37 - Tadulako University Hospital Building A. Left – Beam reinforcement detailing. Right – damage to brick masonry infills.

Building B, with long dimension spanning E-W, is 3 storeys high and sustained damage to masonry infill and partition walls (Figure 7.38 - Left). Buildings A and B are separated by a small spacing that is filled with masonry blocks. At the separation location the beams of Building B extend out from the frame to provide support for the internal floor that connects the buildings. Some localised pounding damage is seen where these have hit the structure of Building A during the ground shaking (Figure 7.38 –Right and Figure 7.39-Right).



Figure 7.38 - Tadulako University Hospital Building B. Left – Side view of Building B, showing out of plane failure of infill wall at second floor (n.b. plane of infill wall is E-W). Right – location of damage due to pounding between Buildings A and B.

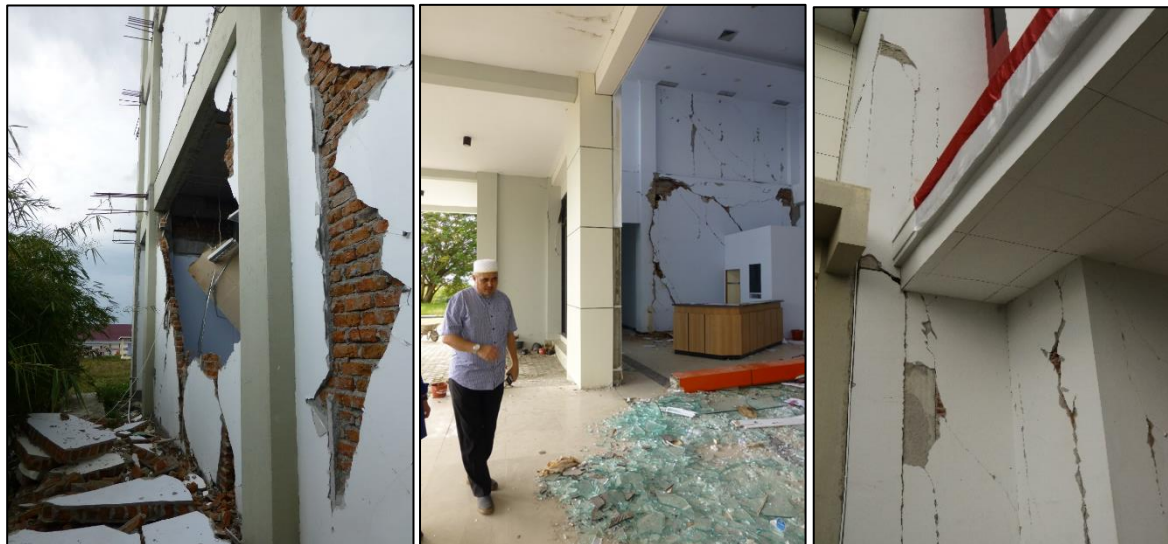


Figure 7.39 - Tadulako University Hospital Buildings: Left - Building A out-of-plane failure of infill walls (plane of walls is E-W). Middle - Damage to entrance and interior fittings of Building A. Right – Detail of damage due to pounding between Buildings A and B.

7.4.2 Anutapura Hospital

Anutapura Hospital is located in Palu city, near the toe of the Balaroa landslide. The hospital comprised one- and two- storey RC frame structures that were intact and fully operational, and two 4-storey RC frame structures that had sustained damage. One of the latter structures had undergone soft storey collapse of the ground level, which had been a car park. Figure 7.40a shows the collapsed structure (DET4) where it is evident that the ground and first-storey beams are significantly larger than the supporting columns. Much of the collapsed material (rubble) had been cleared at the time of the EEFIT-TDMRC visit, and this exposed the side of the remaining four-storey structure that had not collapsed as the car park (soft storey) did not extend across the full length of the building (Figure 7.40b).

This structure has similar sized columns and beams, with the beam depth slightly larger than the column width, but also having significant joint reinforcement (Figure 7.40c). Although still standing, this structure exhibited significant shear cracking and damage characterized as very heavy (DET3). Figure 7.40d shows the undamaged (DET0) low-rise structures on the site that remained operational.

Anecdotally, the death toll at Anutapura Hospital was, remarkably, just three people. It was reported verbally to the team that on feeling the foreshocks earlier in the day, the hospital was evacuated and all staff and patients were outside the building by the time of the main earthquake. The exception were three nurses who had returned inside the building to fetch items for treating patients outside. The decision to evacuate the Hospital as a result of the foreshocks clearly saved a significant number of lives.



Figure 7.40 - Damage at Anutapura Hospital a) soft story collapse of four story RC frame structure; b) RC frame of remaining structure visible following removal of collapsed debris; c) column=beam joint reinforcement exposed in collapsed structure; d) low-rise hospital structures were relatively undamaged and remained operational.

7.5 Hotel Buildings

At the time of the EEFIT-TDMRC mission, many of the buildings that were severely affected or collapsed by the tsunami, had been cleared from the area of Palu Beach. The Team therefore decided to survey those buildings still standing, with a particular focus on those of reinforced concrete construction.

The reinforced concrete hotel buildings surveyed by the TDMRC-EEFIT team, that were affected by both the earthquake ground shaking and the tsunami, were sited on the southern side of Palu bay.

Significant examples include the Grand Duta Hotel, Mercure Hotel and Swiss Belhotel (see Figure 7.41).

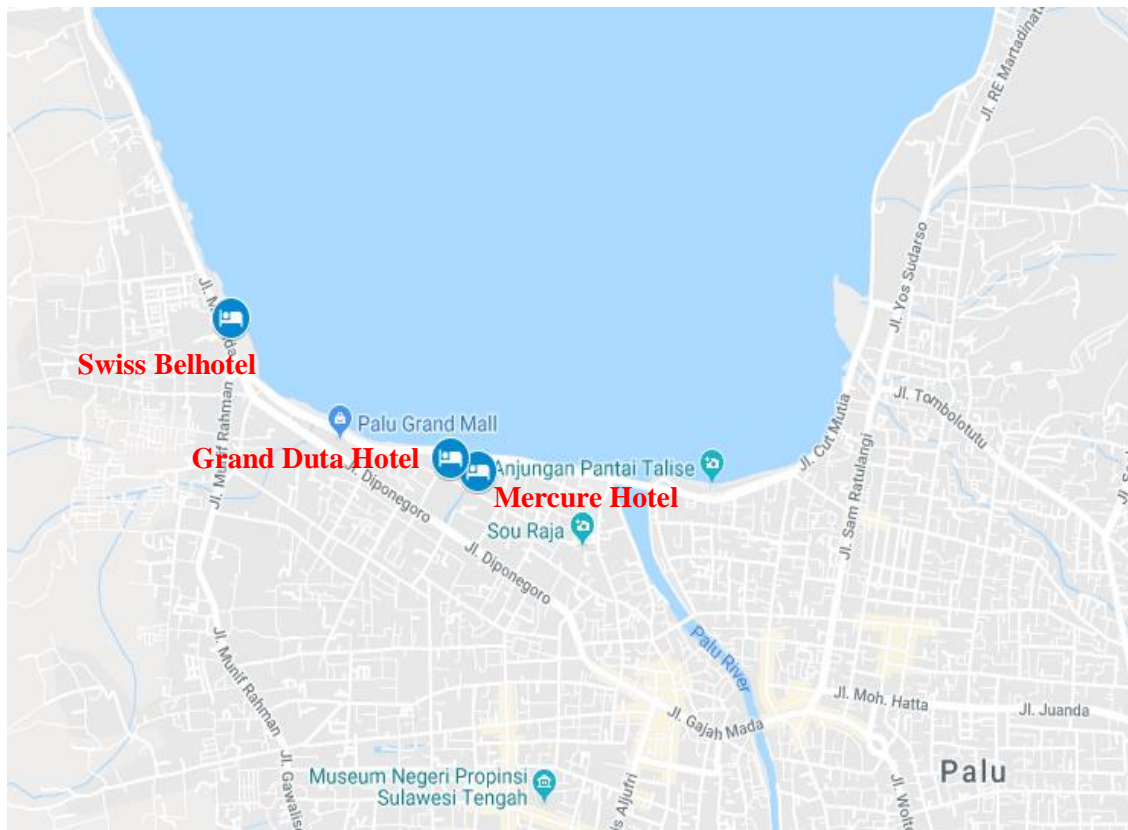


Figure 7.41 - Locations of hotels surveyed in Palu bay area during the EEFIT-TDMRC mission.

7.5.1 Grand Duta Hotel

The Grand Duta Hotel consists mainly of two reinforced concrete frame buildings (connected via an RC elevator shaft (Figure 7.42)). The three-storey building to the East of the elevator shaft had 3 bays of 3.5m span, whilst the four-storey structure to the West of the elevator had 7 bays of 3.5m span. The building did not suffer any damage due to the earthquake ground shaking, but did suffer damage to its ground floor windows, cladding and internal fittings due to the tsunami inundation. Damage to the main internal staircase’s railing at the ground floor was sustained due to its being impacted by a desk carried by the tsunami inundation (Figure 7.43). Inundation here was estimated at 1.5m above grade, as indicated by water marks.

No damage was observed to structural elements. Ground floor column sizes were 500mm x 400mm, whilst beams were 550mm deep by 400mm wide.



Figure 7.42 – Grand Duta Hotel, Palu Beach..



Figure 7.43 – Grand Duta Hotel, Left – image of intact column at ground floor. Right – Image of staircase inside the ground floor of the hotel. The staircase railing was damaged when it was hit by a large desk moved by the tsunami inundation.

Further west from the Grand Duta Hotel was another reinforced concrete building that also showed no structural damage, despite having been inundated by the tsunami. This structure, shown in Figure 7.44 was three-storeys high and is a moment resisting frame that presents large openings to the sea-front. The large openings at the ground floor offered little resistance to the tsunami inundation, and evidence of inundation included the blow out of infill walls at the back of the structure, as well as the presence of parts of sea defences evident inside the building ground floor. Tsunami inundation was limited to the ground storey, as evidenced by the glass in the 1st floor of the building still being intact.



Figure 7.44 – Three –storey RC building near the Grand Duta Hotel. This structure was inundated by the tsunami at its ground floor, but sustained no structural damage, just non-structural damage to sea front windows and to back walls and to fittings at ground-floor level.

7.5.2 Mercure Hotel

The Mercure Hotel consists of a series of buildings, with the main ones, shown in Figure 7.45 being three interconnected 5 storey reinforced concrete frame buildings, and a 3-storey reinforced concrete frame building. All the 5 storey buildings suffered soft-ground storey failure as shown in Figure 7.45, with the western wing also suffering the pancake failure of one of its bays. Details of the reinforced concrete elements are shown in Figure 7.46. Column sizes were approximately 350mm x 350mm and were reinforced with 8 x 25mm diameter reinforcing bars. Beams were large, of 650mm depth and 350mm width, to span the 8m bay widths. No shear reinforcement was observed in the exposed joints (see Figures 7.46 and 7.47). Like in the case of the collapsed RC frame building in Tadulako University, the remaining structure showed damage concentration at/near the joints, suggesting the soft-storey failure initiated at the joints and columns (rather than columns alone).

Little evidence of tsunami inundation was seen at the Mercure Hotel, which is therefore believed to have mainly been affected by the earthquake ground shaking.

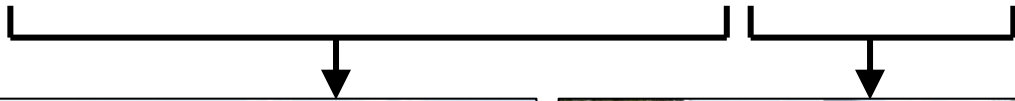


Figure 7.45 – Mercure Hotel, which suffered soft-storey failure of ground floor. Top – Image of the hotel before the earthquake, Source: Tripadvisor.com. Bottom – Pictures of the Hotel after the earthquake, showing the soft-storey failure of the ground storey of the structure.



Figure 7.46 – Mercure Hotel – Images of cover spalling in RC frame joints in the second storey of the structure



Figure 7.47 – Mercure Hotel – Detail of a joint within the first floor of the building (now at ground level following soft-storey collapse of ground floor).

7.5.3 Swiss Belhotel

The EEFIT-TDMRC mission visited this hotel just to the north-west of Palu city, coincidentally arriving when the owner and the building designers were on site. Whilst the front facade of the hotel looked unaffected, the rear terrace of the hotel facing the sea was washed away (Figure 7.48). A single storey confined masonry building on the seaward side had collapsed but the main reinforced concrete structure of the hotel did not sustain any visible structural damage. Non-structural damage was sustained to the ground floor of the hotel on its seaward side, with the tsunami inundation breaking 12 mm thick glass and damaging internal fittings (Figure 7.49).

Based on discussions with the building designers, the Swiss Belhotel was built in 2007 according to the National Building Standards of Indonesia. Both columns and beams have sections that are 600mm x 600mm. The concrete strength is 40MPa and the columns are reinforced with 12 x 16mm diameter deformed reinforcing bars. Shear reinforcement is provided via 10-12mm diameter stirrups, and in columns shear reinforcement spacing is 10cm near joints and 15cm near the column centres.

The hotel was evacuated after the earthquake ground shaking and there was no loss of life.



Figure 7.48 - Swiss Belhotel (Left) Undamaged front facade facing away from the bay (Right) Loss of confined masonry one-storey buildings to the shoreward side of the hotel



Figure 7.49 - Swiss Belhotel - damage to internal fittings at the ground storey of the shoreward side of the hotel. No structural damage observed in the main RC structure.

7.6 Palu Airport

Palu Airport was operational at the time of the EEFIT Mission (the team flew into this airport) however, it was reported to have sustained significant damage to its runways (large and deep cracks) due to ground movement during the earthquake (The Ministry of Transportation report in the website news on 3rd of October 2018 - <http://www.dephub.go.id/post/read/kemenhub-gencar-lakukan-perbaikan-runway-bandara-mutiara-sis-al-jufri>). The airport control tower sustained collapse of the roof of the control room, with the death of the controller reportedly due to his jumping out of the window of the control tower when he realised the roof was collapsing.

At the time of the EEFIT mission it was evident that the main airport building had also sustained significant non-structural damage with extensive cracks visible in external cladding and the falling of internal false ceiling panels (Figures 7.50 and 7.51). However, the main structure (reinforced concrete frame with light steel roof) presented no structural damage.



Figure 7.50 - View of Palu Airport passenger building from the runway. Damage to the infill walls at the ground floor is observed. A stack of fallen ceiling cladding can be seen in upper storey window.

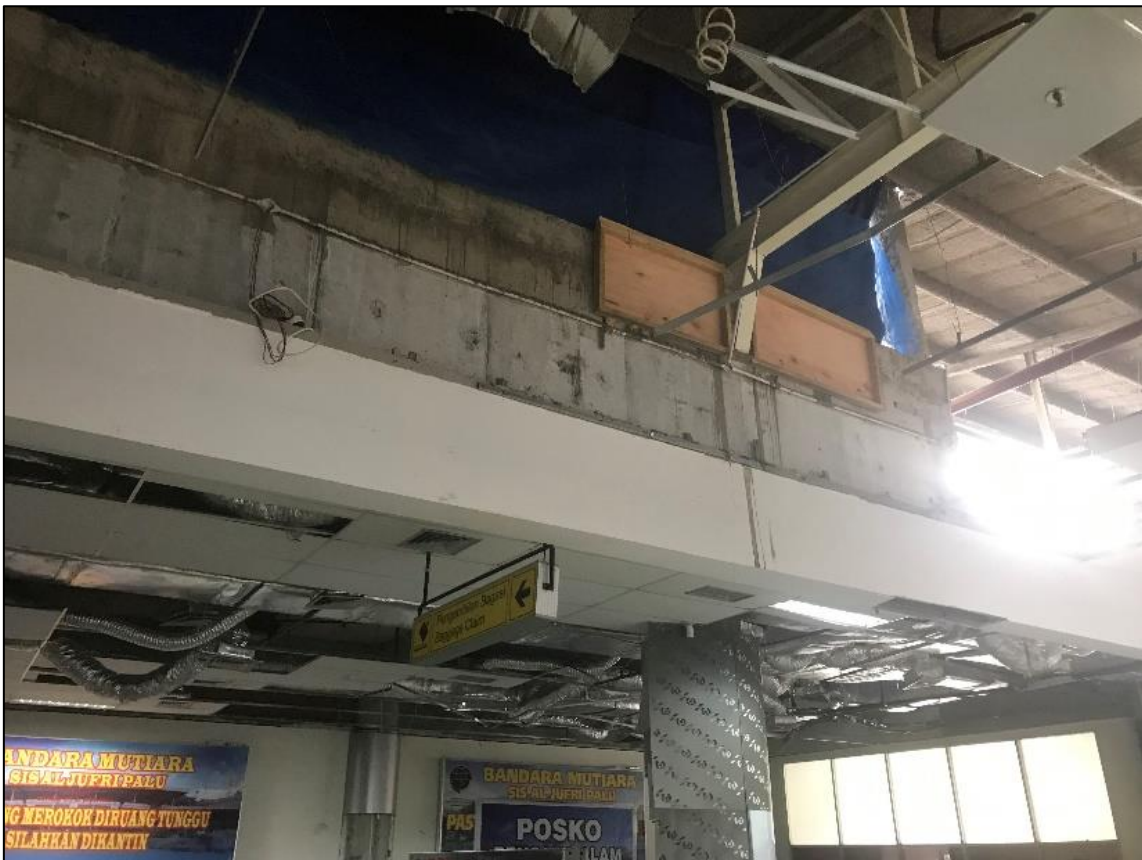


Figure 7.51 - Picture of missing ceiling cladding and damaged fixtures, inside Palu Airport passenger building.

7.7 Ponulele Bridge

This two span suspension bridge was a landmark in Palu. It had a length of 250m and crossed over Palu River's exit into the bay of Palu in the Talise Beach area, connecting west and east Palu. The bridge was characterised by the two steel arches that supported the bridge deck, and in turn were supported on reinforced concrete bridge piers (see Figure 7.52). Eye-witnesses report the bridge deck failed during the earthquake ground shaking, and hence that the bridge deck had already collapsed into the river when the tsunami arrived. Figure 7.53 shows the bridge after the earthquake and tsunami, whilst Figure 6.19 shows the bridge at the time of the TDMRC-EEFIT mission. At this time, the remnants of the steel arches had been removed, but the bridge deck was still lying across the river mouth.



Figure 7.52 - Images of Ponulele bridge before the earthquake and tsunami. The location of the liquefaction jet seen by the EEFIT-TDMRC Team is indicated by the red arrow in the picture on the right. Source for photos: Shutterstock.com.

On the west side of the river mouth, starting from the western bridge pier and going south, strong evidence of liquefaction was seen by the TDMRC-EEFIT team. A large liquefaction hole was observed very near the western bridge pier, at the location of the red arrow on Figure 7.52. Liquefaction was also confirmed by local residents who reported seeing “water spurting from the ground like a geyser”. It was reported to the Team that measurements made by the local authorities indicated the western bridge pier had sunk by 50cm.

It is therefore postulated that the bridge failure occurred due to a combination of ground shaking and liquefaction. It is also possible, as indicated in Section 6, that the collapsed bridge deck may have acted as a protective barrier, reducing the intensity of the tsunami flow up the river and reducing inundation.



Figure 7.53 - Picture of Ponulele bridge showing the failed deck. Source: Tripadvisor.

7.8 Damage to coastal defences

7.8.1 Rudimentary seawall

A rudimentary seawall was observed at north-west tip of the mouth of Palu Bay (Figure 7.54). The topography rose quite steeply from the shoreline and the site did not appear to be particularly exposed despite the damage to the seawall which seemed historical due to evidence of weathering of the structure.

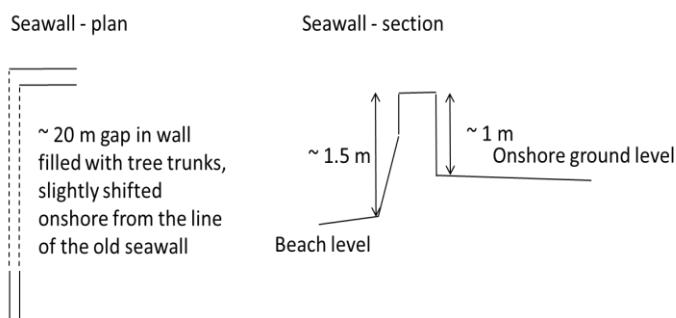


Figure 7.54 - Rudimentary seawall. Left - Sketch of layout and section. Right - Damaged sections with tree trunks closing the gap.

7.8.2 Mamboro seawall

This coastal defence structure had significant visible damage where the top of the wall was missing in many places, revealing ~1 cm rebar approximately every 0.5 m (Figure 7.55). These are presumed to connect to the recurve top of the wall which was still in place at some locations. The damaged seawall was apparently only one year old. Construction details comprised in-situ pouring of concrete of various thicknesses. Slightly further south (tens of metres) there was toppled recurve tops of the wall, but with no rebar connections between the recurve and lower section. The whole structure looked poured in phases from the rear. At the rear of the wall a fairly fast flowing stream was visible. Looking inland the stream could be seen to have flowed through a culvert under the road, but it was not clear how the stream was then routed through the seawall. There was a broken section of the wall, with a length of crest several metres long that could be seen in the sea, slightly to the south of the damage.



Figure 7.55 - Mamboro seawall showing loss of the crest of the structure

7.8.3 Revetment, south of Mamboro

A modern stepped revetment was observed further south from Mamboro as the sea-state was increasing in severity. The top ~0.5 m of the crest of the seawall was lost along most of the length (Figure 7.56).



Figure 7.56 - Stepped revetment South of Mamboro missing its crest.

7.8.4 Masonry seawall

Just to the south of Tasiburi was a damaged masonry seawall (Figure 7.57) that comprised a slender trapezoidal cross section with no apparent rebar.



Figure 7.57 - Damaged masonry seawall just to the south of Tasiburi

7.9 Quay walls

In a number of locations damage to piled quay walls was observed, with broken concrete cylinders strewn around (Figure 7.58). These were observed along Palu Beach, near the Swiss Belhotel and at the “Dolphin Park” at Donggala Koto Wisata.



Figure 7.58 - Collapse of quay wall at ‘Dolphin Park’ at Donggala Koto Wisata.

7.10 Port Structures

Palu bay is home to a number of modest-sized ports, most notably the one at Panoloan, not visited during the EEFIT mission.

7.10.1 Donggala Port structures

The old port of Donggala was observed to have suffered significant damage due to ground subsidence. The collapse, of old warehouses in the areas was observed by the EEFIT-TDMRC Team (Figure 7.59).



Figure 7.59 - Damage to old port of Donggala

7.10.2 Wani Port structures

The port comprised a number of structures including a jetty (Figure 7.60) and a revetment which was protected by cubic concrete armour of 0.8 m side length (Figure 7.61). The jetty seemed undamaged. The armour units appeared to be unreinforced but mostly intact. Two or three of the units had been moved inland by the waves.

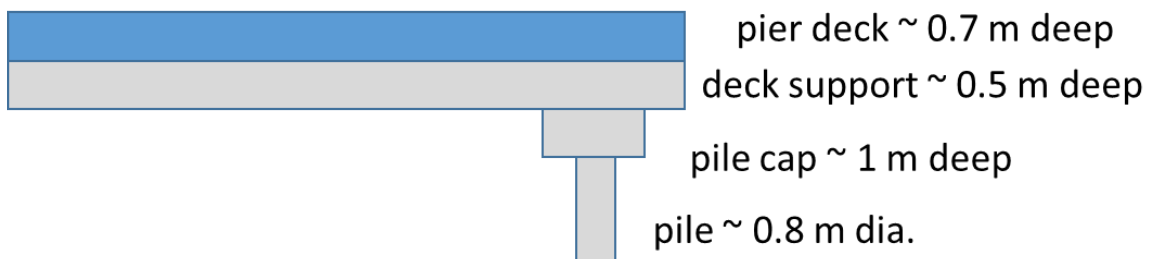


Figure 7.60 - Sketch of section through undamaged jetty at Wani port

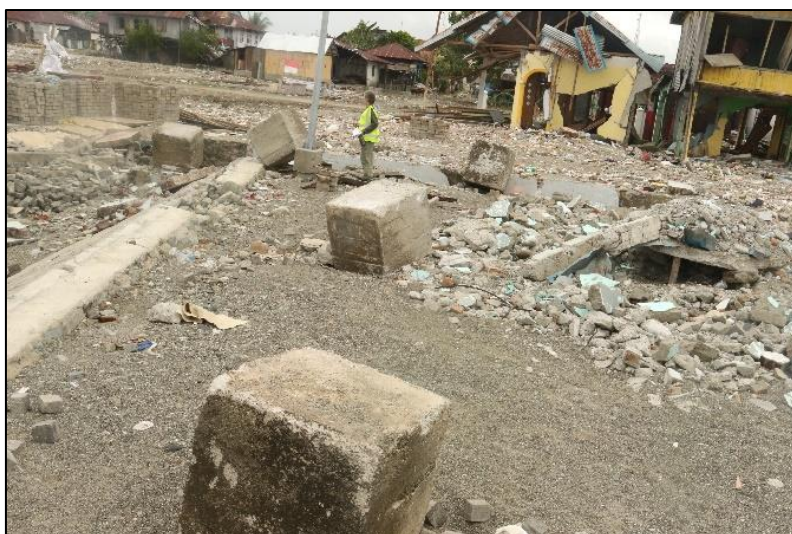


Figure 7.61 - Jetty structure and revetment at Wani port. Top – Jetty. Middle - Armoured revetment neighbouring the jetty. Bottom - Displaced armour units c. 0.8 m side lengths.

7.11 River walls

At Loli Tasiburi Banawa ('black sand') there is reclaimed land from the 1970s and an associated failure of river wall. The village leader said that ~ 30 m of land had disappeared and there was an associated increase in local water depth to 19 m.

At Lero the team visited a river mouth that showed quite extensive signs of subsidence with various properties standing in water (Figure 7.62) and not shown were open style beach shelters also standing in water. The south bank of the river has a large sandy gravel dyke with a crest about 1.5 m above the water level, a crest width of about 2.5 – 3 m and the river side face of the dyke being vertical. The north side of the river had very little protection, but again the sides were vertical and indicated the wave had cut it away (because of the abrupt angle).

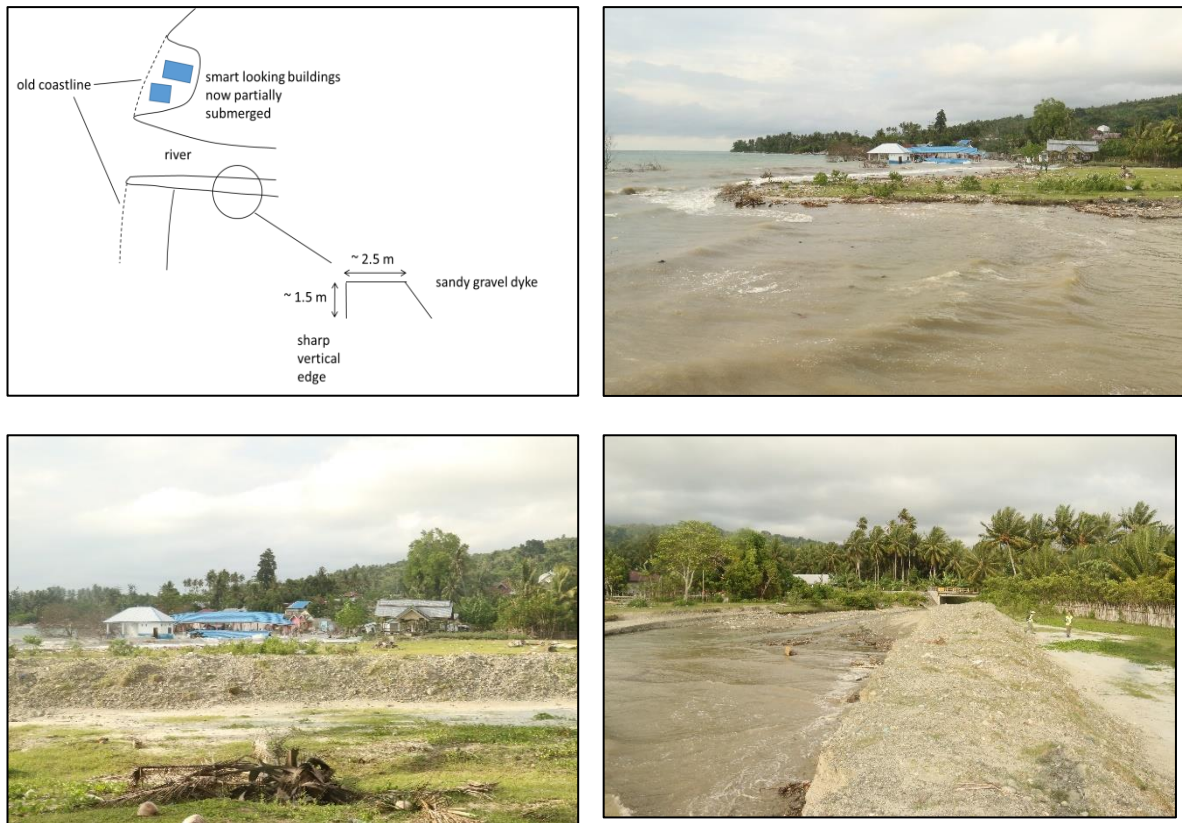


Figure 7.62 - River wall and surroundings at Lero. Top left - Schematic layout of site. Top right - River mouth. Bottom left - Landward side of river wall. Bottom right - Sheared face of river wall.

7.12 Vessels

At a number of locations e.g. Watusanpu naval base, Wani and Mamboro, the tsunami waves lifted vessels onto the land by a combination of buoyancy and onshore hydrodynamic forces, as shown in Figure 7.63. In some locations these caused damage but in others there were some reports of the protective effect e.g. at Mamboro.

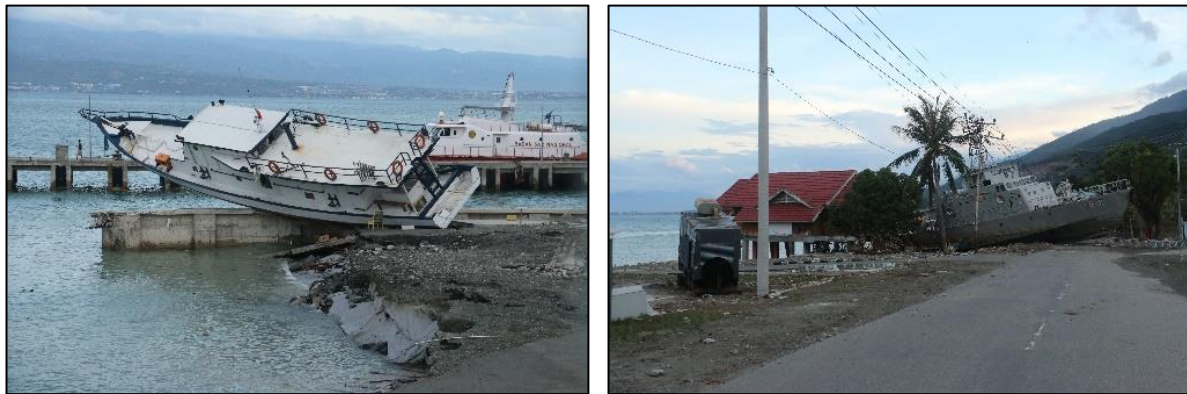


Figure 7.63 - Grounded vessels at Watusanpu Naval Base

7.12 Summary

The TDMRC-EEFIT Team conducted surveys of damage to buildings and infrastructure affected by the Sulawesi event, in Palu and Donggala regions. A new damage scale and survey form were developed and used to provide a consistent evaluation of the damage to buildings from both the earthquake and tsunami hazards. The damage scale is based on EMS-98 damage scale and those used in previous EEFIT missions. It has 5 damage states, referred to as DET0 to DET4, which range from no damage to collapse, and which are described for 4 different structural types.

Timber frame buildings and confined masonry (CM) structures formed most of the low-rise building construction in the area. These commonly collapsed when in the tsunami inundation zone, unless sheltered from the flow by other buildings. An exception to this were timber “stilt” houses, which performed well when the tsunami inundation depth was less than the height of the ground floor, (but collapsed otherwise). Earthquake damage to masonry infilled timber framed buildings was typically out-of-plane failure of the infill walls or separation between the infill and frame due to differential settlement. CM houses suffered out of plane failure of walls and shear damage in tie-columns, when affected by tsunami. Earthquake damage to these structures also included out-of-plane failure of walls, with wall and floor slab cracking and/or failure also observed when differential settlement affected these buildings. Guidelines for these types of housing exist in Indonesia, and were presented in Section 7.2.4. These are seen to present some earthquake resilient construction features, like requirements for secure tying of connections in timber-frame buildings and requiring masonry walls to be anchored to the confining columns in CM housing.

Most primary school complexes surveyed by the TDMRC-EEFIT team consisted of a number of 1 storey CM buildings and one reinforced concrete frame building, commonly 2 storeys in height. Earthquake damage to the CM school buildings included damage to poorly confined heavy gables and the out-of-plane damage/collapse of long and poorly confined CM walls. Like in the case of CM housing, wall and floor slab cracking and/or failure were observed when differential settlement affected these buildings. A number of construction defects and poor construction practices were identified, which should be considered in the reconstruction and strengthening of these buildings.

Both the University complex and all high school complexes consisted of several 3 to 4 storey RC frame buildings. It is noted that the university and high-schools visited were all outside of the inundation zone. Generally, the masonry infilled RC frame buildings in high schools were seen to perform fairly well under the earthquake ground shaking, with little or no damage to structural elements and limited damage to non-structural elements. This was also the case for most buildings in the Tadulako University Campus. However, some buildings did suffer significant damage and at least one building collapsed. In

the latter case failure occurred through the activation of a soft-storey type mechanism, due to plastic hinge formation in the beam-column joints.

Two hospitals were surveyed by the TDMRC-EEFIT Team. The University hospital was not operational after the earthquake due to extensive non-structural damage. The Anutapura Hospital was instead partially functional, but one of its buildings, a four-storey RC frame building, suffered soft-storey collapse over the portion of the building that had a car park at its ground floor. In the latter case, plastic hinge formation seemed to initiate at beam-column connections, similarly to what was observed in the collapsed structure in Tadulako university and in the Mercure Hotel. This failure mechanism, borne of similar sized beams and columns and weak slabs, has not been commonly seen in past EEFIT missions to other countries.

Palu Airport was functional at the time of the TDMRC-EEFIT mission, but was observed to have sustained significant non-structural damage. Significant damage to the runways and collapse of the control tower are also reported to have taken place due to the earthquake and subsequent ground movements.

At the time of the TDMRC-EEFIT mission, most of the collapsed buildings had been cleared from the inundated shoreline of Palu Beach. Three RC hotel structures, as well as several other multi-storey RC buildings, all of which had been inundated by the tsunami, were surveyed by the Team along Palu Beach. Except for the Mercure Hotel, that sustained a soft-storey collapse due to the earthquake, all the multi-storey RC frame buildings on Palu Beach surveyed by the Team had sustained varying degrees of non-structural damage but no structural damage due to the earthquake and tsunami. This is despite evidence of significant tsunami inundation depths at their sites.

Apart from buildings, several infrastructures were also surveyed by the Team. These included the Ponulele bridge, that is thought to have failed due to a combination of ground shaking and liquefaction. It is also possible, as indicated in Section 6, that the collapsed bridge deck may have acted as a protective barrier, reducing the intensity of the subsequent tsunami flow up the river and reducing inundation.

Several sea walls and quay walls were observed to have sustained significant damage from the tsunami inundation. Several port structures were also affected by the tsunami and by earthquake induced coastal ground subsidence. Vessels were also lifted and transported inland by the tsunami, acting as large debris in some cases.

8.0 Palu Contingency Plan (Meilianda, E.; Rezki-Hr, M.; Kumala, D.I.)

There are four phases in the Indonesian disaster risk management (DRM) framework, namely mitigation, preparedness (contingency), response and recovery (BNPB, 2011), see Figure 8.1. The pre-disaster mitigation and preparedness measures are seen as long-term strategies to reduce disaster risk and hence are embedded in the Indonesia National Development Plan and National Spatial Plan.



Figure 8.1 - Disaster Risk Management (DRM) Cycle in Indonesia and the Associated Plan. Modified from BNPB (2011).

All local governments in disaster prone area in Indonesia are required to have a contingency plan to deal with any potential disaster. This contingency plan contains the risk assessment, impact estimation based on the risk assessment, resource gap analysis to deal with the disaster, as well as the various strategies to be acted upon when the disaster strikes. In a pre-disaster context, this plan is used as the basis of emergency exercises and simulation.

When a disaster occurs, the contingency plan is activated and translated into an action plan, i.e. a protocol to be used during the response phase. During or after the response phase, the authority should conduct an assessment to develop a recovery plan. Figure 8.2 represents the timeline from earthquake to recovery for the case of Palu.

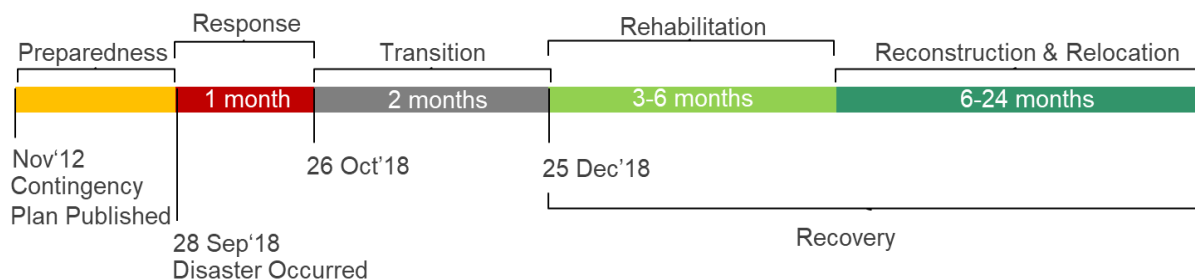


Figure 8.2 - Palu Disaster Management Phases

Due to limited time and data, this report only discusses the contingency plan by comparing the scenario and expected impact in the contingency plan with the actual event and impact. This discussion is important as contingency plans are a good indicator for assessing:

1. How well the authorities understand the potential hazard or disaster risk
2. How well the authorities have estimated the impact of potential hazards.

Palu city authorities published their contingency plan in November 2012. The following paragraphs are a direct translation of the scenario used in the Palu Contingency plan, together with the general impact of the expected hazard.

“On the early morning, 02.00 WITA (local time) while people are sleeping, suddenly an earthquake M7.4 strikes. The epicentre is on the ocean, 10 km depth, and it triggers 3.4m high of tsunami. Both earthquake and tsunami cause the mass destruction on the infrastructures of four districts within the Palu administrative area. The electricity and clean water infrastructures are suddenly cut off.

40% of the roads are expected damaged. 50% of the bridges on the west part of the national road in Palu are also predicted collapsed.” (Palu Contingency Plan, 2012: 25).

The contingency plan then estimates the potential damage in significant detail. However, it is difficult to compare that estimate to the actual impact of the 2018 earthquake and tsunami in Palu as available data from the Palu event are limited. For example, most of the available impact data are presented for the whole impacted area (i.e. aggregating the impact not only from Palu, but also from Sigi and Donggala regencies), while the contingency plan only estimates the impact in Palu administrative area. It is also not possible to collect comprehensive comparable data from the fieldwork as the time was very limited.

The following sections present the available comparable data collected from different sources.

8.1 Number of affected people

The contingency plan does not estimate how many fatalities will occur. Instead it mentions the number of “critically threatened” people as being 7,747. In reality, the number of fatalities as of 7th November 2018 is 4,438 with 1,373 further people missing (Pusat Krisis Kesehatan Kementerian Kesehatan, 2018). The other predicted impact in the contingency plan are the number of displaced and wounded people. Table 8.1 presents a comparison between the estimated number of affected people, and the actual number of people affected by the earthquake and tsunami. It can be seen from Table 8.1 that the number of people displaced and wounded in the Palu earthquake and tsunami are much higher than those estimated in the Contingency Plan. This is likely due to the occurrence of the massive landslides reported in Section 4.0, which were not considered in the Contingency Plan.

Table 8.1: Comparison between numbers of affected people estimated in the Contingency Plan (CP) for Palu versus those actually affected in the earthquake and tsunami.

	Estimated in CP	Actual Data as of 7 th November 2018 (Pusat Krisis Kesehatan Kementerian Kesehatan, 2018)
Critically threatened people	7,747	Total fatalities 4,438
Displaced people	35,692	173,552
Missing and Unidentified people	3,301	2,096 (unidentified dead), 1,373 (missing)
Wounded	18,399	83,122

8.2 Healthcare facilities

There are three types of health facility that are comparable based on the very limited available data: hospital, community health centre, and health centre. Table 8.2, presents the number of hospitals and health centres estimated by the Contingency Plan to be affected, and those reported as being actually affected by the Palu earthquake and tsunami, as reported by the Health Crisis Centre of the Health Ministry (Pusat Krisis Kesehatan Kementerian Kesehatan, 2018). Of the latter, the level of damage is further reported to be: 12 units heavily damaged, 20 units moderately damaged, and 42 minor damaged.

The Contingency Plan simply presents overall numbers, without identifying the healthcare facilities, but from Table 8.2, it is evident that the affected community health centres are severely underestimated by the Contingency Plan.

Table 8.2 - Damaged Health Facilities

Type of Health Facility	Estimation (unit)	Actual (unit) as of 26 th October 2018 (Pusat Krisis Kesehatan Kementerian Kesehatan, 2018)
Hospital (<i>Rumah Sakit</i>)	1	1*
Community Health Centre (<i>Puskesmas</i>)	5	50
Health Centre (<i>Puskesmas Pembantu</i>)	15	18
Village Health Centre (<i>Poskesdes</i>)		5

*It is noted that the University Hospital had only been open one month at the time of the earthquake and hence may not be included in the numbers shown in Table 8.2. i.e. the real number of affected hospitals is 2.

8.3 Ports

There are two major ports in Palu, namely Pantoloan and Feri Taipa. Both are estimated to suffer heavy damage in the contingency plan and this matches the damage sustained, as reported in AHA-Centre (2018b) and Beritatrans (2018).

8.4 Electricity Generators

The contingency plan estimates that the electricity main generators in Panau will be severely damaged, while the generator in Silae will be moderately damaged. This estimate coincides with what happened in the Palu event of the 28th September 2018. A report by Afriyadi (2018) shows that the Silae Generator returned to operation shortly after the event, as it needed some minor repairs due the damage by the earthquake. Instead, the Panau Generator was reported not to be in service at the time of the TDMRC-EEFIT mission, and was still under repair.

8.5 Institutional Arrangements

The Contingency Plan estimated that the local government would be able to deal with the disaster impact. However, after the Palu earthquake, disaster response and recovery is being managed by higher levels of government, both provincial and national, involving some of international donors.

8.6 Summary

This assessment reveals that the implementation of the Contingency Plan was challenging for Palu City administration in responding to the multiple hazards of earthquake, tsunami, landslides and liquefaction that occurred on 28 September 2018. However, beyond the scale and complexity of the disaster, it is believed that lack of regular updating of the plan, lack of repeated simulation, and lack of engagement of all stakeholders also contributed to the poor implementation of the Contingency Plan after the Sulawesi event.

According to the Ministry of National Development Planning (BAPPENAS), overall, the Central Sulawesi disaster has had a strong effect on economic growth, inflation, capital stock and investment. The economic growth post-disaster reveals a declining figure of merely 1.75% from the baseline of 6.24% in the pre-disaster condition. If the growth of economic activities can be maintained at an average of 25%, it is projected by BAPPENAS that the economic recovery will be reached after 4 years.

9.0 Conclusions

The 28th September 2018 magnitude 7.5 (USGS) Sulawesi earthquake, triggered a tsunami, massive landslides and liquefaction that severely affected people, housing and infrastructure in the Palu and Donggala regions. A TDMRC-EEFIT reconnaissance team visited the affected areas for 7 days in November 2018. A number of observations were made by the TDMRC-EEFIT Team on the nature of these hazards and their effects on the built environment during the mission. These have been described in detail in this report, with key observations summarised here.

Fault Rupture:

- The TDMRC-EEFIT Team successfully conducted a surface ground-trothing of the Palu-Koro fault trace that had been mapped using satellite imagery and co-seismic displacement analysis by others.
- Figure 3.9 shows the results of this ground-trothing and the Team demonstrated that the Palu-Koro Fault demonstrates step-over faulting, (which is typical of pull-apart basins), in the south of the Palu valley.
- It is postulated that either a similar step-over faulting might be present where the fault crosses Palu bay, or that a contractional bend and resultant thrust faulting might exist there. The latter would cause an uplift of the sea bed and might be a possible contributing cause of the tsunami. However, neither of these postulations were proven by any of the bathymetric survey data available to the EEFIT-TDMRC Team at the time of the mission.

Landslides:

- The three main landslides at Balaroa, Jono Oge and Petobo that occurred following the earthquake are considered to be low-angle liquefaction-induced debris flows that were extremely mobile due to significant water content.
- The causal factors are largely thought to be related to the hydrogeological regimes' interaction with the topography as well as possible anthropogenic factors.
- A man-made irrigation channel runs along the eastern side of the valley and appears to be the initiation point of the two largest landslides within evidence suggesting the underlying hydrogeological regime is significantly affected by its' presence, i.e. through the significant volume of additional water introduced into the ground.
- It is recommended that the role of the irrigation channel on the ground failure should be clarified.
- It is also recommended, as good practice, that enhanced drainage infrastructure be provided to reduce water saturation, and that the irrigation channel end be connected to the Palu river to reduce accumulation of water.

Liquefaction:

- Liquefaction was a factor in the landslide triggering.
- Only limited incidences of liquefaction were observed in Palu city itself, with ejecta and ground settlement observed.
- Shear wave velocity profiles were obtained for sites across Palu, and it is observed that sites of observed liquefaction correlated only with the soils identified to have a Vs lower than 200 m/s
- Liquefaction was observed frequently around the coastline of Palu Bay in the form of spreading and subsidence of material into the Bay. In the bay area, eye-witnesses provided helpful observations that substantiated liquefaction theories.

Tsunami:

- The tsunami generation mechanism is as yet unclear, with combinations of seismic and landslide sources (due to the steep bathymetric profiles of Palu Bay) being prevalent.
- Tsunami inundation heights of ~ 7m were evident at the head of Palu Bay and unusual reports of plunging type wave suggesting landslide generation.
- As expected, Tsunami inundation was observed to be affected by distance from shoreline, building type and sheltering effect of neighbouring buildings.
- Eye-witnesses described seeing both crest and trough-led waves. It needs to be borne in mind that some of the tsunami waves, as described by eye-witnesses, may have been generated very locally, immediately following liquefaction and subsidence of the shoreline. In the latter cases, to some extent the tsunami at these locations would have been a 'backwash', (i.e. water travelling seawards from the land), a characteristic not reported previously.
- No formal tsunami warnings were provided, but lives were saved due to self-evacuation. This was a critical factor to saving lives.

Surveying damage due to multiple hazards:

- The Sulawesi event induced damage in buildings and infrastructure from a number of different hazards.
- A new damage scale and survey form were thus developed and used to provide a consistent evaluation of the damage to buildings from both the earthquake and tsunami hazards.
- The damage scale is based on EMS-98 damage scale and those used in previous EEFIT missions. It has 5 damage states, referred to as DET0 to DET4, which range from no damage to collapse, and which are described for 4 different structural types.
- The damage scale and form were successfully tested by the Team in the field. However, further assessment and testing of these is required, with independent teams and the wider EEFIT expertise.

Damage to low-rise timber housing:

- Low-rise timber housing commonly collapsed when in the tsunami inundation zone, unless sheltered from the flow by other buildings.
- Traditional timber "stilt" houses, however, performed well when the tsunami inundation depth was less than the height of the ground floor, (but collapsed otherwise).
- Earthquake damage to masonry infilled timber framed buildings comprised the out-of-plane failure of the infill walls or separation between the infill and frame due to differential settlement.
- Indonesian guidelines for the construction of timber housing includes some resilient features for earthquakes, such as cross-bracing and enhanced connection details. Tsunami are not considered in these guidelines, most likely due to the rarity of these events.

Damage to low-rise confined masonry houses and school buildings:

- Both CM houses and school buildings suffered out of plane failure of walls and shear damage in tie-columns, when affected by tsunami.
- Earthquake damage to CM housing included out-of-plane failure of walls.
- Earthquake damage to CM school buildings included damage to poorly confined heavy gables and the out-of-plane damage/collapse of long and poorly confined CM walls. This was more pronounced in school buildings than in housing due to the relatively longer wall spans.

- Wall and floor slab cracking and/or failure were observed in CM houses and schools when differential settlement affected these buildings.
- A number of construction defects and poor construction practices were identified in CM schools that affected their earthquake performance. These include:
 - the use of poor material quality of brick units, mortar and concrete,
 - corrosion in reinforcement
 - poor reinforcement detailing in tie-elements
 - low confinement level of thin walls in both horizontal and vertical directions
 - large and poorly confined/unconfined gables.

It is recommended that when these buildings are re-built that such construction and design defects be addressed.

- Recommendations from the World Bank Global Program for Safer Schools (World Bank 2019) can be used to direct improved CM school design and detailing.

Damage to Reinforced Concrete Infilled frame mid-rise buildings (housing, hotels, high-school and university buildings):

- Generally, masonry infilled mid-rise (3-4 storey) RC frame buildings were seen to perform well under the sustained earthquake ground shaking, with little or no damage to structural elements and limited damage to non-structural elements.
- Significant non-structural damage was however seen to compromise functionality of the Palu airport buildings and of Tadulako University Hospital.
- Some cases of collapse of infilled RC buildings due to ground shaking were observed. In these cases, collapse was induced by soft-storey mechanisms initiated at the ground storey, often due to the presence of stiffness irregularities (e.g. lighter cladding or presence of car park). However, in these cases plastic hinge formation was consistently seen to initiate in the beam-column joints, rather than the ends of columns. This is considered to be due to the use of similarly sized beams and columns and the presence of weak floor slabs. Such a failure mechanism has not been commonly seen in past EEFIT missions.
- At the time of the TDMRC-EEFIT Mission most of the collapsed buildings had been cleared from the inundated shoreline of Palu Beach. Several RC buildings had not been cleared as they had survived the event. These were surveyed and observed to have sustained no structural damage, but substantial non-structural damage due to the tsunami inundation. This is despite the latter inundation depth being up to 6m in some of the locations visited.

Damage to Infrastructure:

- Ponulele bridge, an iconic bridge crossing the mouth of the Palu river, collapsed in the Sulawesi event. The TDMRC-EEFIT Team believe the bridge failed due to a combination of ground shaking and liquefaction. Liquefaction ejecta holes were observed in the vicinity of the western abutment and eye-witness reports confirm the deck of the bridge collapsed after the ground shaking and before the tsunami.
- It is also possible, as indicated in Section 6, that the collapsed bridge deck may have acted as a protective barrier, reducing the intensity of the subsequent tsunami flow up the river and reducing inundation.
- Several sea walls and quay walls were observed to have sustained significant damage from the tsunami inundation. Several port structures were also affected by the tsunami and by earthquake induced coastal ground subsidence.

Contingency Plan effectiveness:

- The scale and complexity of multiple hazards of this disaster were not considered in the Palu Contingency Plan.
- It is posited that lack of regular updating of the plan, lack of repeated simulation, and lack of engagement of all stakeholders also contributed to the poor implementation of the Contingency Plan after the Sulawesi event.
- There is evidence that people self-evacuated from their houses after the ground shaking, which appears to have been based on past experience rather than specific evacuation education.

The devastation caused by the 28th September 2018 earthquake and subsequent triggered hazards on communities in Palu and Dongalla was extensive. However, the TDMRC-EEFIT Team observed that local people and businesses were beginning to recover from the disaster. At the time of the mission, although many people were living in temporary accommodation, provisions were being made by the government and NGOs to provide more permanent shelter. Temporary school facilities had already been erected in some locations with students attending these.

10.0 Acknowledgements

The TDMRC-EEFIT Team would like to acknowledge the support of the European Research Council under the European Union's Seventh Framework Programme (FP7/20072013)/ERC grant agreement number 336084, who funded the participation of Prof. Tiziana Rossetto and Dr David Robinson on the Sulawesi Earthquake Mission. The Engineering and Physical Sciences Research Council Grant "Learning from Earthquakes: Building Resilient Communities Through Earthquake Reconnaissance, Response and Recovery" (EP/P025641/1) is also acknowledged for supporting the participation of Prof. Alison Raby, Dr Andrew Brennan and Mr Mohammed Rezki-Hr. Ove Arup Singapore is thanked for supporting the participation of Richard Lagesse. Syiah Kuala University in Banda Aceh, Sumatra, Indonesia, is also thanked for supporting the participation of Dr Ella Meilianda, Dr Yunita Idriss, Ibnu Rusydy and Intan Dewi Kumala in the reconnaissance mission. In addition, the TDMRC-EEFIT Team acknowledge the support of a large number of people, who provided logistical information, information on the events, helped with data collection and field surveys. These have been named in Section 1.2. The Team also thank Dr Sean Wilkinson of Newcastle University and Dr Joshua Macabuag of World Bank, who acted as base coordinators in the UK for the reconnaissance Team. Finally, the Team thank Matthew Free of Arup, Dr Joshau Macabuag of World Bank and Antonios Pomonis of Risk Management Solutions for reviewing the current report.

11.0 References

AHA-Center. (2018). Situation Update No. 10 M7.4 Earthquake & Tsunami Sulawesi, Indonesia. Published on 10 October 2018. Available at: https://ahacentre.org/wp-content/uploads/2018/10/AHA-Situation_Update-no10-Sulawesi-EQ.pdf

AHA-Center. 2018a. Situation Update No. 12 M7.4 Earthquake & Tsunami Sulawesi, Indonesia. Published on 15 October 2018. Available at: https://ahacentre.org/wp-content/uploads/2018/10/AHA-Situation_Update-no12-Sulawesi-EQ-rev.pdf

AHA-Center. 2018b. Situation Update No. 1 M7.4 Earthquake & Tsunami Sulawesi, Indonesia. Published on 29 September 2018. Available at: https://ahacentre.org/wp-content/uploads/2018/10/AHA-Situation_Update-no12-Sulawesi-EQ-rev.pdf

- Afriyadi, Achmad D. *Pasokan Listrik Sulteng Sudah Pulih 70% Pasca Gempa* (Electricity Supply in Centra Sulewaesi Have Been Recovered Post Earthquake). Available at: <https://finance.detik.com/energi/d-4247197/pasokan-listrik-sulteng-sudah-pulih-70-pasca-gempa>
- Andrus, R.D. & Stokoe, K.H. II (2000) Liquefaction resistance of soils from shear-wave velocity. *ASCE J. Geotech & Geoenv. Engg.* 126(11), 1015-1025.
- Battjes, J.A. (1974), "Surf similarity", *Proceedings 14th International Conference on Coastal Engineering*, pp. 466–480.
- Bellier, O., Se'Brier, T., Beaudouin, M., Villeneuve, R., Braucher, R., Bourles, L., . . . Pratomo, I. (2001). High slip rate for a low seismicity along the Palu-Koro active fault in central Sulawesi (Indonesia). *Terra Nova.* 13, 463-470.
- Bergman, S. C., Coffield, D. Q., Talbot, J. P., & Garrard, R. A. (1996). Tertiary Tectonic and magmatic evolution of western Sulawesi and the Makassar Strait, Indonesia: evidence for a Miocene continent-continent collision. In *Special Publication 106* (pp. 391-429). London: Geological Society of London.
- Beritatrans. (2018). *Gempa Dahsyat, Dirjen Budi: Pelabuhan Penyeberangan Taipa dan Terminal Mamboro Rusak Berat* (Massive Earthquake, General Director Budi: Taipa Port and Mamboro Bus Terminal are Heavily Damaged). Available at: <http://beritatrans.com/2018/09/29/gempa-dahsyat-dirjen-budi-pelabuhan-penyeberangan-taipa-dan-terminal-mamboro-rusak-berat/>
- Bird, M. I., Taylor, D., & Hunt, C. (2005). Palaeoenvironments of insular Southeast Asia during the Last Glacial Period: a savanna corridor in Sundaland. *Quaternary Science Reviews*, 24 (20-21), 2228-2242.
- BNPB. (2011). *Panduan Perencanaan Kontinjensi Menghadapi Bencana Edisi Kedua* (Guidance of Contingency Planning to Deal with Disaster Second Edition).
- Buldakov, E. (2013) Tsunami generation by paddle motion and its interaction with a beach: Lagrangian modelling and experiment. *Coastal Engineering.* 80, 83-94.
- Cipta, A., Robiana, R., Griffin, J. D., Horspool, M., Hidayati, S., & Cummins, P. (2016). Geohazards in Indonesia: Earth Science for Disaster Risk Reduction. In *Special Publication* (Vol. 441). London: Geological Society of London.
- Dall'Osso, F., M. Gonella, G. Gabbianelli, G. Withycombe, and D. Dominey-Howes (2009). A revised (PTVA) model for assessing the vulnerability of buildings to tsunami damage. *Natural Hazards and Earth System Sciences.* 9(5), 1557-1565.
- Davidson, J. W. (1991). The Geology and Prospectivity of Buton Island, S.E. Sulawesi, Indonesia. *Proceedings of the Indonesian Petroleum Association 20th Annual Convention*, (pp. 209-233).
- Department of Cipta Karya, (2006). *Pedoman Umum Rumah dan Bangunan Gedung Tahan Gempa* (The guidelines of the earthquake resistant residential houses and buildings), Jakarta
- EERI (2011). *Seismic Design Guide for Low-Rise Confined Masonry Buildings*, Earthquake Engineering Research Institute, Oakland, CA, USA.
- ERCC (2018) DG ECHO Daily Map 16/11/2018 Available online: <https://erccportal.jrc.ec.europa.eu/getdailymap/docId/2708> [Accessed 2 February 2019].
- European Commission. (2018). Mw 7.5 earthquake in Indonesia, 28 Sep 2018, JRC Emergency Reporting—Activation #021—UPDATE #1—01 Oct 2018.
- Fortuin, A. R., Smer, M. E., Hadiwasastra, S., Van Marle, I. J., Troelstra, S. R., & Tjokrosapoetro, S. (1991). Late Cenozoic Sedimentary and Tectonic History of South Buton, Indonesia. *Journal of Southeast Asian Earth Sciences*, 4, 107-124.

- Fraser, S., Raby, A., Pomonis, A., Goda, K., Chian, S.C., Macabuag, J., Offord, M., Saito, K. and Sammonds, P., 2013. Tsunami damage to coastal defences and buildings in the March 11th 2011 M w 9.0 Great East Japan earthquake and tsunami. *Bulletin of earthquake engineering*, 11(1), pp.205-239.
- Geological Research & Development Centre (1973). Preliminary Geological Map, Indonesia. 1:250,000 Scale. Sheet: Palu – 2015 & 2115.
- Grünthal, G. (ed.), Musson, R., Schwarz, J., and Stucchi, M.: 1998a, European Macroseismic Scale 1998, *Cahiers du Centre Européen de Géodynamique et de Sismologie*, Vol. 15, Luxembourg
- Hadi, Syafiul. (2018). *Jumlah Korban Tewas Terkini Gempa dan Tsunami Palu 2.113 Orang* (Palu Earthquake and Tsunami Update: 2,111 Died). Source: <https://nasional.tempo.co/read/1138400/jumlah-korban-tewas-terkini-gempa-dan-tsunami-palu-2-113-orang/full&view=ok>
- Hamilton, W. (1979). *Tectonics of the Indonesian Region*. Professional Paper 1078, 345 pp.
- Heidarzadeh, M., Muhari, A. and Wijanarto, A.B., 2019. Insights on the source of the 28 September 2018 Sulawesi tsunami, Indonesia based on spectral analyses and numerical simulations. *Pure and Applied Geophysics*, 176(1), pp.25-43.
- Jamelot, A., Gailler, A., Heinrich, P., Vallage, A. and Champenois, J., 2019. Tsunami simulations of the Sulawesi M w 7.5 event: Comparison of seismic sources issued from a tsunami warning context versus post-event finite source. *Pure and Applied Geophysics*, 176(8), pp.3351-3376.
- Japan Cabinet Office (2013) Residential disaster damage accreditation criteria operational guideline.pdf. Retrieved from <http://www.bousai.go.jp/taisaku/unyou.html>
- Kruyt. (1938). *Situatie Kaartvan de Vlake van Paloe*.
- Lauterjung, J., Letz, H. (Eds.) (2017): *10 Years Indonesian Tsunami Early Warning System: Experiences, Lessons Learned and Outlook*, Potsdam: GFZ German Research Centre for Geosciences.
- Leeuwen, T. (1981) *The Geology of Southwest Sulawesi with Special Reference to the Biru Area. The Geology and Tectonics of Eastern Indonesia At: Bandung Indonesia Volume: Geological Research and Development Centre, Special Publication 2*, pp. 277-304.
- Mansur, F. (2006). *Konservasi dan Revitalisasi Bangunan Lama di Kota Donggala (The conservation and revitalisation of the heritage buildings in Donggala city)*, MEKTEK Magazine. VIII (2), Palu
- Metcalfe, I (2009) *Late Palaeozoic and Mesozoic tectonic and palaeogeographical evolution of SE Asia*, Geological Society, London, Special Publications, 315, 7-23
- Moss, S. J.; Wilson, M. E. J. (1998) Biogeographic implications of the tertiary paleogeographic evolution of Sulawesi and Borneo. *Biogeography and Geological Evolution of SE Asia*, pp. 133-163.
- Muhari, A., Imamura, F., Arikawa, T., Hakim, A.R., Afriyanto, B. (2018). Solving the Puzzle of the September 2018 Palu, Indonesia, Tsunami Mystery: Clues from the Tsunami Waveform and the Initial Field Survey Data, *Journal of Disaster Research 13 (Scientific Communications) sc20181108*.
- Network, C. M. (2011). *Seismic design guide for low-rise confined masonry buildings*. World Housing Encyclopaedia, EERI & IAEE.
- Palu Contingency Plan. (2012).
- Parkinson, C. D. (1991). *The Petrology, Structure and Geologic History of the Metamorphic Rocks of Central Sulawesi*. London: University of London.
- Pedoman Teknis Rumah dan Bangunan Gedung Tahan Gempa, Kementrian Pekerjaan Umum dan Perumahan Rakyat, Indonesia, (2006). (Technical guidelines of earthquake resistant houses and buildings construction that published by the Indonesian ministry of public works and houses). Indonesian Ministry of Civil Works and Residential Houses

- Pelinovsky, E., Yuliadi, D., Prasetya, G., & Hidayat, R. (1997). The 1996 Sulawesi Tsunami. *Natural Hazards*, 16, 29-38.
- Pusat Krisis Kesehatan Kementerian Kesehatan (2018) Update Data Bencana Sulawesi Tengah. Available at: <https://bit.ly/2TWft4a>
- Response Update Brief (2019). Central Sulawesi Earthquake and Tsunami Response, Indonesia Response Update Brief: 22 March 2019. e-mail circular made available by Save The Children
- Rossetto, T., Peiris, N., Pomonis, A., Wilkinson, S.M., Del Re, D., Koo, R., Gallocher, S. (2007). The Indian Ocean Tsunami of December 26, 2004: Observations in Sri Lanka and Thailand. *Natural Hazards*. 42 (1). 105-124
- Sassa, S. & Takagawa, T. (2019) Liquefied gravity flow-induced tsunami: first evidence and comparison from the 2018 Indonesia Sulawesi earthquake and tsunami disasters. *Landslides* 16: 195-200. doi: 10.1007/s10346-018-1114-x
- Satyana, A. H., Muly, S. N., & Faulin, T. (2011). Tectonic Evolution of Sulawesi: Implications for Proven and Prospective Petroleum Plays. The 36th HAGI and 40th IAGI Annual Convention and Exhibition. Jakarta.
- Smith, R. B., & Silver, E. A. (1991). Geology of a Miocene Collision Complex. *Geological Society of America Bulletin*, 103, pp. 660-678.
- Socquet, A., Vigny, C., Chamot-Rooke, N., Simons, W., Rangin, C., & Ambrosius, B. (2006). India and Sunda plates motion and deformation along their boundary in Myanmar determined by GPS. *Journal of Geophysical Research*, 111.
- STEER (2019) StEER: Structural Extreme Event Reconnaissance Network Palu Earthquake and Tsunami, Sulawesi, Indonesia Field Investigation Team (FAT-1) Early Access Reconnaissance Report. Available online: <https://www.designsafe-ci.org/data/browser/public/designsafe.storage.published/PRJ-2128> [Accessed 2 February 2019].
- Stevens, C. R., McCaffrey, Y., Bock, Y., Genrich, J., Endang, C., Subrya, S., . . . Vigny, C. (1999). Rapid rotations about a vertical axis in a collisional setting revealed by the Palu Fault, Sulawesi, Indonesia. *Geophysical Research Letters*, 26, 2677-2680.
- Stone, H., Putrino, V., & D'Ayala, D. (2018). Earthquake damage data collection using omnidirectional imagery. *Frontiers in Built Environment*, 4(51).
- Sukanto. (1975). The structure of Sulawesi in the light of plate tectonics. Regional conference on the geology and mineral resources of southeast Asia organised by association of Indonesian geologists. Jakarta.
- Supartoyo, C. S., & Sulaiman, C. (2014). Kelas tektonik sesar Palu Koro, Sulawesi Tengah Tectonic class of Palu Koro Fault, Central Sulawesi. *Jurnal Lingkungan dan Bencana Geologi*, 111-128.
- Suppasri A, Mas E, Charvet I, Gunasekera R, Imai K., Fukutani Y, Abe Y, and Imamura F. (2013). Building damage characteristics based on surveyed data and fragility curves of the 2011 Great East Japan tsunami. *Natural Hazards*. 66 (2): 319-341.
- Takagi, H., Pratama, M.B., Kurobe, S., Esteban, M., Aránguiz, R. and Ke, B., 2019. Analysis of generation and arrival time of landslide tsunami to Palu City due to the 2018 Sulawesi Earthquake. *Landslides*, 16(5), pp.983-991.
- Thein, P.S., Pamumijoyo, S., Brotopuspito, K.S., Kiyono, J., Wilopo, W., Furukawa, A. and Setianto, A. (2014) Estimation of seismic ground motion and shaking parameters based on microtremor measurements at Palu City, Central Sulawesi Province, Indonesia. *World Academy of Science, Engineering and Technology International Journal of Geological and Environmental Engineering* 8(5): 308-319.

Ulrich, T., Vater, S., Madden, E.H., Behrens, J., van Dinther, Y., van Zelst, I., Fielding, E.J., Liang, C. and Gabriel, A.A., 2019. Coupled, physics-based modeling reveals earthquake displacements are critical to the 2018 Palu, Sulawesi Tsunami. *Pure and Applied Geophysics*, pp.1-41.

UNDRR and UNESCO-IOC (2019), *Limitations and Challenges of Early Warning Systems: A Case Study of the 2018 Palu-Donggala Tsunami*. United Nations Office for Disaster Risk Reduction (UNDRR), Regional Office for Asia and the Pacific, and the Intergovernmental Oceanographic Commission of United Nations Educational, Scientific and Cultural Organization. (IOC Technical Series N° 150)

Valkaniotis, S., Tsironi, V., Ganas, A., & Barberopoulou, A. (2018). A preliminary report on the M7.5 Palu earthquake co-seismic ruptures and landslides using image correlation techniques on optical satellite data. Unpublished.

Van Leeuwen, T. M. (1981). The Geology of Southwest Sulawesi with Special Reference to the Biru Area. In A. J. Barber, & S. Wiryosujono, *Geology and Tectonic of Eastern Indonesia* (Special Publication 2 ed., pp. 277-304). Bandung: Geological Research and Development Centre.

Walpersdorf, A. C., Vigny, C., Subarya, C., & Manurung, P. (1998c). Monitoring of the Palu-Koro Fault (Sulawesi) by GPS. *Geophysical Research Letters*, 2313-2316.

Wells, D. L., & Coppersmith, K. J. (1994). New empirical relationships among magnitude, rupture length, rupture width, rupture area, and surface displacement. *Bulletin of the Seismological Society of America*, 974-1002.

Widiyanto, W., Santoso, P.B., Hsiao, S.C. & Imananta, R.T. (2019) Post-event field survey of 28 September 2018 Sulawesi Earthquake and Tsunami. *Nat. Hazards Earth Syst. Sci, Discuss.* doi: 10.5194/nhess-2019-91.

World Bank (2019) *Global Library of School Infrastructure (GLOSI)*, Global Program for Safer Schools (GPSS). Available online at: <https://gps.worldbank.org/en/glosi>

Zare, M., Haghshenas, E., Kalantari, A. (2018). Earthquake of 30 September 2009, Mw7.6, Padang, Sumatra, Indonesia: A Preliminary Reconnaissance Report. International Institute of Earthquake Engineering and Seismology (IIEES), Tehran, Iran.

EEFIT

Earthquake Engineering Field Investigation Team

EEFIT is a UK based group of earthquake engineers, architects and scientists who seek to collaborate with colleagues in earthquake prone countries in the task of improving the seismic resistance of both traditional and engineered structures. It was formed in 1982 as a joint venture between universities and industry, it has the support of the Institution of Structural Engineers and of the Institution of Civil Engineers through its associated society SECED (the British national section of the International Association for Earthquake Engineering).

EEFIT exists to facilitate the formation of investigation teams which are able to undertake, at short notice, field studies following major damaging earthquakes. The main objectives are to collect data and make observations leading to improvements in design methods and techniques for strengthening and retrofit, and where appropriate to initiate longer term studies. EEFIT also provides an opportunity for field training for engineers who are involved with earthquake-resistant design in practice and research.

EEFIT is an unincorporated association with a constitution and an elected management committee that is responsible for running its activities. EEFIT is financed solely by membership subscriptions from its individual members and corporate members. Its secretariat is generously provided by the Institution of Structural Engineers and this long-standing relationship means that EEFIT is now considered part of the Institution.

© All material is copyright of the Earthquake Engineering Field Investigation Team (EEFIT) and any use of the material must be referenced to EEFIT, UK. No material is to be reproduced for resale.

This report can be downloaded from www.eefit.org.uk

EEFIT

c/o The Institution of Structural Engineers,

47 – 58 Bastwick St, London EC1V 3PS

Tel: +44 (0)20 7235 4535

Fax: +44 (0)20 7235 4294

Email: mail@eefit.org.uk

Website: www.eefit.org.uk